Role of Versican in

Epithelial Ovarian Carcinoma

BY

MARK DESJARDINS
B.S., UNIVERSITY OF WISCONSIN RIVER FALLS, 2006

THESIS

Submitted as partial fulfillment of the requirements
for the degree of Master of Science in Biopharmaceutical Science
in the Graduate College of the
University of Illinois at Chicago, 2012

Chicago, Illinois

Defense Committee:

Maria Barbolina, Chair and Advisor
Debra Tonetti
Steven Swanson, Medicinal Chemistry and Pharmacognosy

ACKNOWLEDGEMENTS

I would to thank my thesis advisor Dr. Maria Barbolina for her constant encouragement, guidance, and support throughout the whole period of my studies. Also, I want to thank the members of my thesis committee, Dr. Debra Tonetti and Dr. Hyatt Onyuksel for their time and advice. Additionally, I am grateful for all the faculty members who have shared their knowledge with me and helped me build a solid scientific foundation.

Lastly, I would like to thank my wonderful wife who throughout this whole process constantly encouraged and supported me. Without her this accomplishment would not have been possible.

TABLE OF CONTENTS

LIST OF TABLES

LIST OF FIGURES

FIGURE **PAGE**

LIST OF FIGURES (continued)

FIGURE **PAGE**

SUMMARY

Epithelial ovarian cancer is currently the most deadly gynecological malignancy in the United States with approximately 14,000 women dying annually. The major obstacle in the clinical management of the disease is that the majority of women present with advanced staged carcinoma having already metastasized. Data from numerous groups have implicated the Wnt-Signaling pathway in the formation of cancer including ovarian carcinoma. Our lab has previously established that there is downregulation of several secreted Wnt signaling inhibitors, which led to the upregulation of a number of genes including one that encodes for the protein Versican (VCAN). Versican is a extracellular matrix protein, which has been linked to various types of cancers and more recently ovarian cancer. Additionally, recent data has suggested that the formation of multicellular aggregates known as spheroids may play a huge role in the resistance to the traditional therapies.

The role of the extracellular matrix in the formation cancer is well established with it contributing to the regulation of proliferation, adhesion, differentiation, and migration. With that in mind we tested the effect of versican expression on cellular migration, adhesion, spheroid formation, and spheroid disaggregation. Versican expression levels were measured using quantitative real time polymerase chain reaction. Interestingly, we found that the downregulation of versican using siRNA and shRNA slowed the migration rate in the scratch wound healing assay in Skov-3 and Dov-13 cell lines. In addition, we found that when versican expression was silenced there was a decrease in single cell adhesion as well as spheroid adhesion to extracellular matrix components. This led to our lab examining the effects of cellular adhesion on the mesothelial monolayer LP-3, which coincided with our results on extracellular matrix components that found that decreased versican expression resulted in decreased adhesion.

SUMMARY (continued)

Moreover, we found that versican expression positively affected the overall size of the spheroid as well as the number of spheroids that were formed during the assays. Based upon literature, the increase in spheroid size and formation could lead to an increase in therapeutic resistance. Lastly, when spheroids were allowed to disaggregate on extracellular matrix components as well as on a mesothelial monolayer we found that disaggregation was incomplete and decreased in cells expressing lower levels of versican.

In conclusion, these current studies provide a better understanding of how versican may play a role in the metastatic spread of epithelial ovarian cancer. Finally, it may potentially serve as a potential target for successful therapy.

1. INTRODUCTION

1.1 Ovarian Cancer

1.1.1 Introduction to Ovarian Cancer

Ovarian cancer represents the most deadly gynecological malignancy, and is responsible for the death of approximately 14,000 women annually in the United States.[1] Nearly 70% of women present with advanced stage ovarian carcinoma, which has already metastasized into the peritoneal cavity.[2] As a result of late diagnosis, and the highly metastatic nature of ovarian cancer the current 5 year survival ranges from 20-90% depending upon the stage.[3] The poor prognosis is a direct result of relatively few advances in treatment options as well as late stage diagnosis. Also, the high mortality rate can be attributed to a high rate of relapse and resistance even in the early stages of tumor progression.[4-5] Current lifetime risk of developing ovarian cancer in the United States is roughly 1 in 80 women, which has remain largely unchanged for the past two decades.[3] Thus far, there have been no biomarkers capable of predicting the presence of early ovarian cancer. CA-125, was at one time hailed as a potential biomarker, but has since proven to not have the sensitivity required to be reliably used.[6-7]

1.1.2 Types of Ovarian Cancer

There are three types of ovarian carcinoma: epithelial, germ cell, and stromal cell carcinoma. Nearly 90% of all ovarian cancer cases are epithelial in origin, while 5-8% of the remaining cases are classified as stromal tumors.[8] Germ cell tumors represent only 3-5% of all reported cases, but represent highly malignant tumors usually seen in younger females.[8]

Epithelial ovarian cancer (EOC) can be further subdivided into three groups: Serous, mucinous, and endometriod. Serous carcinoma represents 50% of all ovarian cancer incidences, 25% are endometriod, and 20% are mucinous.[1,9] EOC when diagnosed in the early stages has a

very favorable prognosis with a 85% 5-year survival rate.[3] The major challenge in attempting to create a more favorable prognosis is developing a means to detect the cancer at an earlier stage, where current therapeutic regimens are effective.

1.1.3 The Risk Factors for Ovarian Cancer

Important risk factors for ovarian cancer include age, family history of breast cancer, family history of ovarian cancer, genetic mutations, prolonged estrogen replacement therapy, early menarche, late menopause, high fat diet, and low parity.[10-12] Many of these factors are associated with increased ovulation, resulting in damage to the surface of the ovary that increases the opportunities for genetic insult to the tissue. The repeated rupturing of the follicle requires repair to the epithelial cells, which creates opportunities for damage to the genes possibly leading to mutations.[13-15]

Factors that are associated with a decrease incidence of ovarian cancer include: oral contraceptive use, early menopause, hysterectomy, multiparity, late menarche, low fat diet, and breast feeding.[10-12] These factors unlike those above are mainly associated with decreased ovulatory rupturing decreasing the number of opportunities for damage to the cells to occur.[10-15]

Based upon epidemiological data it appears that age has the greatest influence on the incidence of developing ovarian cancer since over 90% of cases are diagnosed in women over 50 years of age.[16-17] The second most important risk factor is a family history of ovarian cancer or breast cancer. Women with a family history of either disease have a 12% chance of developing ovarian cancer.[18] However, the hereditary risk is greatly increased in those women with a BRCA1 or BRCA2 mutation.[18-20] Additionally, individuals with Lynch II Syndrome have higher than normal incidence of ovarian cancer.[20]

1.1.4 Treatments for Ovarian Cancer

The treatment administered will be determined by the stage, histologic type, and the patient's overall condition. If detected early enough in Stage I, the first line therapy is surgery, in which the fallopian tubes and ovaries are removed.[18,20] Subsequently, the regional lymph nodes are biopsied, and if the laboratory results are negative no further treatment is required. However, for women diagnosed in Stage II conventional therapy involves surgery (hysterectomy, bilateral oophorectomy, debulking, and lymph node biopsies) combined with chemotherapy with or without radiation therapy.[18,20] The chemotherapy regimen is traditionally a combination of paclitaxel and a platinum containing compound such as cisplatin or carboplatin.[18,20] Treatment for Stage III and Stage IV cases are virtually similar to the treatment received by women diagnosed with stage II ovarian cancer with the potential for experimental treatment.[18,20]

In recent years, researchers have experimented with delivering chemotherapy directly into the peritoneal cavity in attempts to reach higher local concentrations of drug. To date there has been conflicting results regarding the use of intraperitoneal use of cisplatin and paclitaxel versus the intravenous use of the two drugs.[21-26] Initial trials showed a significant survival benefit, while other randomized trials have showed only a modest benefit in mean survival.[21-26] An additional factor confounding the results, is that due to the toxicity associated with intraperitoneal administration a significant proportion of patients were unable to finish the chemotherapy regimen.[21-26]

Treatment of advanced stage ovarian cancer has also been confounded by resistance to platinum-based chemotherapeutic agents. This remains a key obstacle since platinum agents tend to be the most successful in killing the cancer cells at early stages, but becomes rapidly useless in many advanced stage cases where platinum resistance is widespread.

Alternatively, immunotherapy has become an attractive treatment option as more protein surface markers have become identified and targetable by synthetic antibodies. One such marker has been the mucin protein, which has been targeted with the monoclonal antibody HMFG1.[27-28] Initial results were impressive with a 10 year survival of 78%, as compared to the 10-year overall survival rate of 35-40% for normal therapies.[27-28] However, the initial success has not been repeated as successive trials have shown only a modest improvement in survival as compared to standard therapy. With moderate increases in mean survival from the likes of Provenge for advanced prostate cancer, researchers are optimistic concerning the success of immunotherapy in the future for ovarian cancer patients.

1.1.5 Ovarian Cancer Metastasis

As previously stated, metastatic ovarian cancer is highly lethal as evident by the poor 5-year survival rate. The mechanism of metastatic spread of ovarian cancer is unique in that malignant cells are believed to be shed off the ovary and then are transported by the intraperitoneal fluid to the peritoneum (Figure 1).[29-30] After adhesion to the peritoneum, the cancer cells then proceed to migrate through the peritoneum and into other organs. This is in direct contrast to other cancer types where metastatic cells are carried by the blood and lymphatic ducts to their site of implantation. It is not clear whether ovarian cancer cells spread intra-peritoneally due to anatomical proximity or whether other factors responsible for the microenvironment such as extracellular matrix proteins are the key to intra-peritoneal implantation.[29-30] When malignant cells disseminate off the surface of the ovary they can exist as single cells or multicellular aggregates often referred to as spheroids. This process of metastatic spread is depicted below in Figure 1 (adapted from [30]). Once the single cells have attached to the

lining of the peritoneal cavity they undergo changes in cell-cell and cell-matrix interactions that allow them to disaggregate, migrate, and become invasive.[30-31]

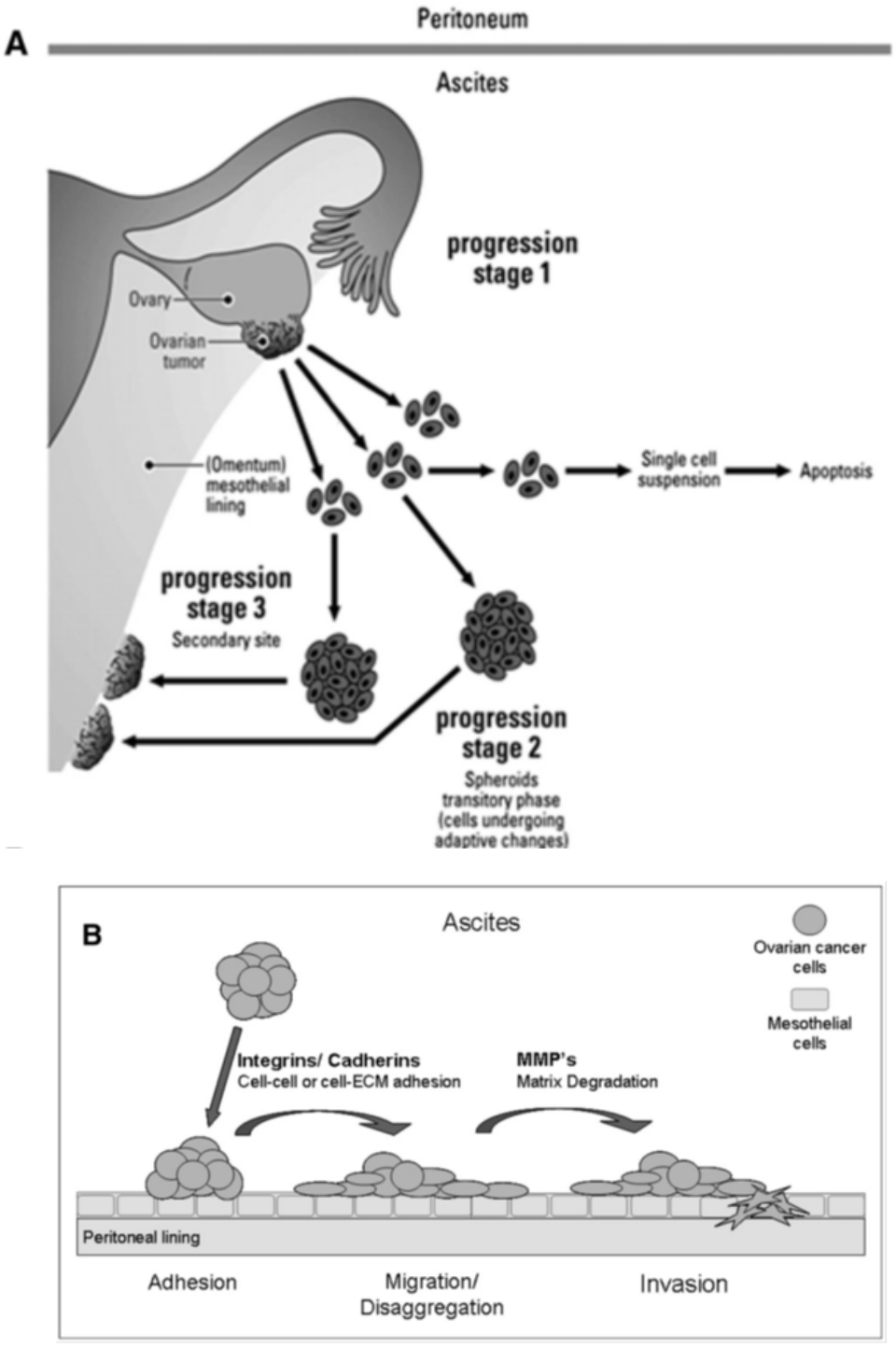

Figure 1. Epithelial Ovarian Carcinoma Metastatic Progression.
Adapted from: Multicellular spheroids in ovarian cancer metastases: Biology and pathology.Kristy Shield, M. Leigh Ackland, Nuzhat Ahmed, Gregory E. Rice Gynecol Oncol. 2009 April; 113(1): 143–148.

1.1.6 Ovarian Cancer Spheroids

Formation of spheroids is extremely problematic in the treatment of ovarian cancer for a number of reasons. The characteristics of spheroids that make them especially troublesome are that they are able to escape cell death quite easily allowing them to form distant metastatic sites. They are able to do so by their ability to survive in an anchorage independent fashion as well as in vascular-independent conditions that would not support the survival of the majority of single cancer cells.[29,32,33]

The compaction of the cells into a spheroid occurs as a result of changes in expression of cell-cell adhesion molecules (CAMs), which allows the cells to form tight cell-cell junctions that maintain integrity of the cells preventing cell death from stressors in the environment.[32-36] In order to get spheroid formation it has been observed that there is change in cadherin expression, specifically a change in the ratio of E-cadherin and N-cadherin expression.[32,34,36,37]

Secondly, spheroids have been found to harbor innate resistance to many chemotherapeutic agents.[38-46] Part of their ability to withstand chemotherapy is that spheroids are slow cycling and mostly in a quiescent state, and thus are relatively unaffected by drugs that target proliferating cells.[43-44] Furthermore, the chemotherapeutic agents must be able to travel into the center of the spheroids to kill the inner core cells, which is currently a barrier due to the degree of compaction that spheroids undergo.[38-46]

Their resistance to radiation is derived from their enhanced ability to accumulate and repair radiation damage that would normally be lethal to single cells or monolayer of cells.[47-50] The proposed mechanisms of radiation resistance include enhanced intercellular communication between spheroidal cells that causes a subsequent shift in gene expression of DNA repair proteins that allow for more efficient repair of damage.[50] Furthermore in the larger spheroids the

cells at the center eventually become hypoxic, which is a stimulus for angiogenesis. This stimulus has also been shown to cause the upregulation and expression of the transcription factor hypoxia-inducible factor 1 α as well as hypoxia-inducible factor 2 α.[52-54] These two inducible hypoxic factors proceed to elevate levels of VEGF and basic fibroblast growth factor (bFGF), which causes increased resistance to radiation damage and promotes cell survival.[52-54] However, the resistance to radiation and some chemotherapeutic agents appear to be size dependent as it has been found that smaller spheroids can actually be more sensitive to these treatments, which could potentially represent a target for therapy.[55-56]

1.2 Versican

1.2.1 Role of Extracellular Matrix in Ovarian Cancer

The extracellular matrix (ECM) is a key player in controlling and regulating cellular functions such as proliferation, adhesion, differentiation, and migration. Additionally, the extracellular matrix serves as a barrier that ovarian cancer cells must adhere to, invade, and degrade in order to form a distant metastatic site (Figure 1). Thus, it is no surprise that tumor cells have been shown to remodel the extracellular matrix through mechanisms that involve degradation of the existing ECM, and by alteration of the synthesis of extracellular matrix proteins.[57-69] In some cases this altered expression involves proteins that may not be expressed in the normal tissue or are expressed at higher levels.[68]

Proteoglycans are a major component of the extracellular matrix. There is evidence of altered expression of proteoglycans such as hyaluronan, versican, CD44, and hyaluronidase in tumors and transformed cells.[70] Altered expression of these ECM constituents all contribute to changes in migration, proliferation, and growth associated with tumor progression.[71,72] Abundant amounts of hyaluronan has been correlated with invasive tumor cell types, as well as a poor prognosis in patients with breast cancer, non-small-cell lung cancer, colon cancer, prostate cancer and ovarian cancer.[73-76] Elevated levels of CD44 has been associated with increased activity of signaling pathways that are thought to cause increased motility, adhesion, and invasion of tumor cells.[77-78] The activation of the pathways occurs by the binding of CD44 to hyaluronan.[76-78] The proteoglycan versican is an hyaluronan binding protein which has been correlated with prostate, melanoma, breast, brain, colon, pancreas, endometrium, and ovarian cancer.[79-82]

1.2.2 Structure and Function of Versican

Versican is a large chondroitin sulfate proteoglycan composed of glycosaminoglycans (GAG) chains, that belongs to the hyalectin family.[83-84] The versican gene is composed of 15 exons, which to date has been found to produce five splice variants designated V0, V1, V2, V3, and V4 which is not shown (Figure 2).[85-88] Each of the five isoforms are structurally different with varying functions, however V0, V1, and V2 differ only in the core region as seen in figure 2. V0 is the largest isoform and contains two GAG chains, GAG-α and GAG-β, which is where the chondroitin sulfate chains are linked to. In contrast, V2 contains only the GAG-α, while the V1 isoform consists of the GAG-β domain at its core. V3 is uniquely different from the other 3 isoforms in that it is completely devoid of the GAG domains and chondroitin sulfate side chains.[85-88] All versican isoforms are similar at their C-terminus domain (G3) and their N-terminus domain (G1). The N-terminus is primarily associated with HA binding, while the C-terminus domain has functional groups that bind epidermal growth factors. It should be noted that a fifth splice variant, Versican V4 has only been isolated in breast tissue.[89] Structure wise, V4 is nearly identical to V3 with the addition of a cryptic splice site responsible for exon 8.[89]

Functional assays, assessing the effect of versican on cells include alteration of proliferation, growth, migration, and adhesion.[90-99] Results of these studies have produced mixed conclusions, as the different isoforms have been shown to produce opposing effects.[98-100] For instance, the expression of V1 has been tied to increase proliferation, while expression of V2 inhibits the rate of proliferation.[101-102]

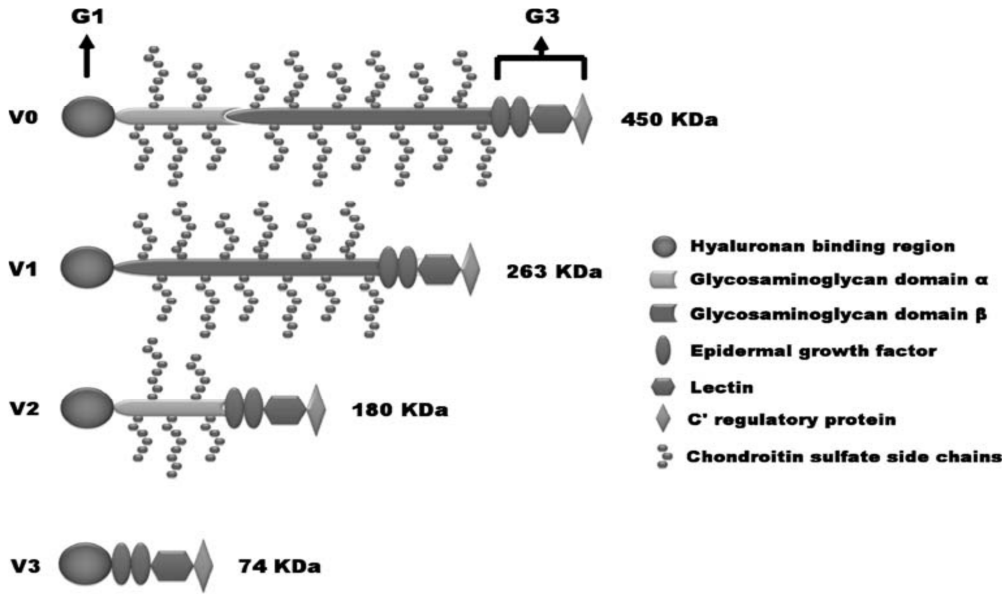

Figure 2. Structure and domains of versican splice variants. Adapted from [88]

1.2.3 Biological Role of Versican in Cancer

The ability of versican to regulate cellular activities such as adhesion, proliferation, apoptosis, migration, and invasion is a result of the highly negatively charged chondroitin sulfate side chains and through interactions of the G1 and G3 domains with other proteins.[103-105] There is contradictory information in regards to function of each isoform, and is more than likely a result of its ability to bind a wide variety of cell surface markers that include CD44, integrins, EGFR, chemokines, collagen, and selectins. In previous experiments, versican has been demonstrated to be a downstream target of Wnt signaling, with increased activity of which has been linked to various cancers including EOC.[106]

The correlation between elevated levels of versican found at distant metastases and progression of the cancer indicates that versican is involved in cancer cell motility and invasion. This is evident by the functional studies establishing that versican can increase cell motility, proliferation, and metastasis.[90-99] Individual isoforms have been found to have different effects

that have been elucidated on various types of cancer cells, and as previously noted have produced mixed results.

An additional factor that has led to difficulty in understanding the roles of versican and its splice variants is derived from the fact that it is enzymatically cleaved by ADAMTS and MMPs.[107-108] Upon cleavage the two main cleavage products are the G1 and G3 domains, of which the G1 product has been the predominant product found in cancerous tissue. The mechanisms responsible for regulating the breakdown of versican into cleavage products are poorly understood and have yet to be studied. [109-110]

For instance, V0 which is normally present only during embryogenesis and cancer, and has been shown to promote motility in prostate cancer cells.[111] This increased motility was accompanied by an overall decrease in cell attachment to ECM components. Interestingly, the recombinant G1 cleavage product alone has been shown to be capable of stimulating increased motility upon binding to its targets in glioma and lung cancer cells.[109,112] This begs the question of whether it is the merely the G1 domain that is responsible for the change in motility, or is it the full length V1 isoform responsible for the migration.

Cell proliferation of NIH-3T3 cells is stimulated by V1, whereas it is inhibited by presence of elevated V2.[100] The changes in proliferation was further evident when siRNA was used to knockdown expression in lung cancer cells, and the result was an overall decrease in tumor growth in vivo.[100] The mechanism responsible for the shift in proliferation is hypothesized to be that versican is acting as a mitogen through its binding to the epidermal growth factor receptor.[113] Activation of the EGFR pathway also has been demonstrated to increase cell survival and inhibit apoptosis through the up-regulation of integrins and CAMs.[100] There was also down-regulation of Fas death receptor mRNA when V1 induced NIH-3T3 tumors

in nude mice, contributing to a reduction in apoptosis.[114] Overexpression of the isoform V3 as well as the G1 and G3 products have induced a metastatic phenotype capable of forming secondary metastases at a higher rate than the control group in both lung cancer cells as well as in prostate cancer cells further strengthening the evidence of versican's involvement in tumor progression.[91,95,99]

1.2.4 Role of Versican in Ovarian Cancer

Elevated levels of versican in stromal tissue has been correlated with a poor prognosis for endometrial cancer patients as well as epithelial ovarian cancer patients.[65] This overexpression of stromal versican has been further associated with ovarian carcinoma patients with a high FIGO stage, and lymph node metastases.[115] The degree of epithelial versican staining was not nearly as high as stromal versican, but was significantly higher in patients with metastases in their lymph nodes and in higher FIGO stages.[115] However, in patients with a low FIGO stage only weak epithelial versican staining was present, perhaps indicating that the presence of versican is associated with progression of tumor growth and metastasis. This coincides with previous studies demonstrating the ability of versican to promote a phenotypic change associated with increased metastasis in melanoma cells.[91] Additionally, it has been shown that a pericellular matrix is a requirement for the proliferation and migration of mesenchymal cells, of which both hyaluronan and versican are instrumental in the formation of this matrix.

In functional studies recombinant V1 was able to increase the invasiveness and motility of ovarian carcinoma cell lines OVCAR-5 and SKOV-3 cells.[96] Furthermore the authors of the paper were able to reverse the enhanced motility and invasiveness by administering hyaluronan

oligosaccharides. These oligomers are hypothesized to block the CD44-HA interaction which is made possible by versican binding the hyaluronan in a manner that allows it to interact with CD44.[116]

1.2.5 Wnt-signaling in Ovarian Cancer and Regulation of Versican levels

The Wnt pathway is comprised of a large family of secreted proteins that act in a local manner and are responsible for the regulation of many physiologic events, especially early on in embryogenesis.[117-118] Wnt signaling has also proven to be vital in regulating proliferation, differentiation, migration, and apoptosis in adult tissues as well.[117-128] When inappropriately activated the Wnt pathway has been implicated in the promotion of tumorigenesis in lung, breast, colon, and ovarian tissues.[117-128]

Two main pathways for activation of the Wnt pathway exist, the canonical Wnt/B-catenin and the non-canonical Beta-catenin independent pathway. Thus far the canonical pathway has proven to be the pathway most implicated in the progression of ovarian carcinoma. The main effector of the canonical Wnt/B-catenin pathway is beta-catenin, which in the absence of a Wnt ligand is localized to the cytoplasm or phosphorylated and degraded rapidly.[117] Upon binding to the surface proteins LRP and Frizzled, the signaling protein Dishevelled becomes activated, in turn inactivating GSK 3β preventing β-catenin from being phosphorylated and degraded. The accumulation of undegraded β-catenin in the cytoplasm eventually leads to the translocation of β-catenin into the nucleus. Inside the nucleus the free β-catenin in an unknown mechanism displaces the co-repressor Groucho, and binds the LEF-1/TCF regulatory complex, and then in turn acts as co-activator inducing the transcription of a number of downstream target genes.[117] This sequence of events is summarized in Figure 3 (adapted from [129]).

It has been assumed that abberant Wnt-signaling only played a key role in endometroid cancer and not the epithelial ovarian cancer subtype.[130,131] This was thought to be true as few researchers had found mutations in Wnt-signaling pathway in EOC tissue samples, while there have been numerous mutations found in tissues of patients diagnosed with endometriod cancer.[130,131] However, in recent years there has been mounting evidence suggesting that Wnt signaling may in fact be a large contributor to the development of ovarian cancer, without the presence of mutations.[132-134] This hypothesis has been further strengthened by Wnt-signaling activation independent of gene mutations in breast, lung, and prostate cancer.[135-140] The mechanism of mutation independent activation is thought to occur through a few proposed mechanisms: 1) repression of wnt anatagonists, 2)overexpression of wnt ligands or 3)a combination of repression of antagonists combined with the overexpression of wnt ligands.[106] PYGO, a protein that plays a role in the B-catenin/TCF transcription complex, believed to be a co-activator has been found to be overexpressed in six EOC cell lines as well as in over 82% of patients sampled in the study.[132]

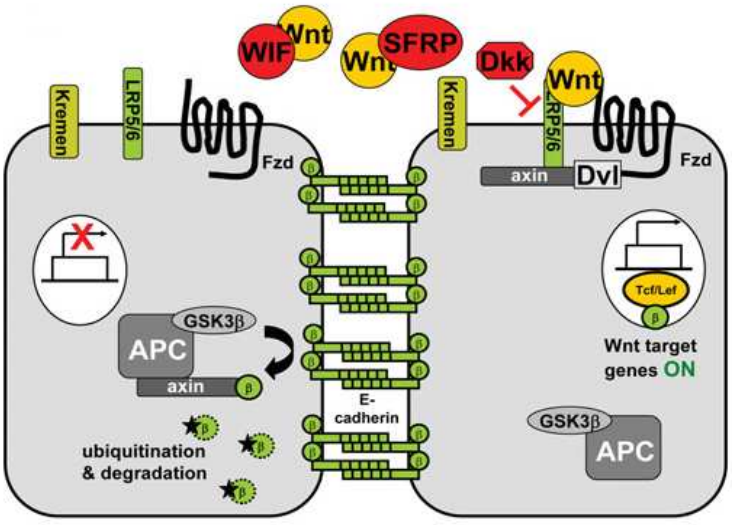

Figure 3. Canonical Wnt-Signaling. (A) Wnt signaling off (B) Wnt pathway activated. (adapted from [129]).

Several Wnt signaling inhibitors, Dickkopf-1 (DKK1) and Connective Tissue Growth Factor (CTGF) were downregulated in EOC cell lines.[106] Downregulation of these inhibitors causes nuclear translocation of beta-catenin and activation of Wnt signaling resulting in the upregulation of target genes Versican, HIF1α, and HIF2α in EOC cell lines in the absence of mutations in the Wnt signaling pathway.[106] Other target genes of Wnt activation identified in ovarian cancer include Fibroblast Growth Factor-9, Follistatin, Wnt-5, MSX2, COX2, c-Myc, RARG (Retinoic acid receptor), BIRC5 (survivin), and Cyclin D1.[106,141-143] In many cases the upregulation of the previously listed genes results in promotion and progression of tumorigenesis through increased proliferation, migration, adhesion, and differentiation.[106,117,118]

2. MATERIALS AND METHODS

2.1 Cell Culture

The human ovarian cancer cell lines SKOV-3 and Dov-13 were grown in Minimum Essential Media (Sigma-Aldrich) supplemented with 10% fetal bovine serum (FBS), 2mM of glutamine, 5 mL of 100mM sodium pyruvate, 5 mL of 10 mM non-essential amino acids, 26.2 nM sodium bicarbonate, and maintained in the presence of penicillin, streptomycin, and amphotericin in a humidified incubator with 5% CO2 at 37°C. The human ovarian cancer cell lines OVCA429 and OVCA 433 were maintained in complete growth media consisting of 50% media 199 (Sigma-Aldrich) and 50% MCDB105 supplemented with 10% fetal bovine serum, 2mM glutamine, 5 mL of non-essential amino acids, 2.2 grams sodium bicarbonate, 5mL of pencillin strep, and 1mL F-amphotericin in a humidified incubator with 5% CO2 at 37°C. The human ovarian cancer cell line IGROV-1 was maintained in the complete growth media RPMI-1640 supplemented with 2.2 grams of sodium bicarbonate, 2mM glutamine, 10% fetal bovine serum, 5 mL of Penicillin-streptomycin, and 1 mL of F-amphotericin in a 37°C humidified incubator in the presence of 5% CO2. Mesothelial cell strains LP-3 and LP-9 were cultured in a 1:1 mixture of medium 199 (Sigma-Aldrich) and MCDB 105 (Sigma-Aldrich) supplemented with 15% fetal bovine serum, 10ng/mL Epidermal growth factor, 0.4 µg/mL hydrocortisone, 10 mL/L sodium pyruvate, 5mL/L nonessential amino acids, and 2mM glutamine in a humidified incubator with 5% CO2 at 37°C. Skov-3 vcan shRNA cells were maintained in the same conditions as the skov-3 cells with the addition of 3 ng/mL of puromycin to maintain positive selection for clones. Prior to experiments cells were incubated in serum free media for 24-36 hours.

2.2 RNA Extraction

Following treatment, total RNA was isolated from the ovarian cancer cell lines using RNAzol RT (Molecular Research Center, Inc). Briefly, cells were lysed by directly adding 1mL of RNAzol reagent and then homogenate followed by the addition of 0.4 mL of RNase free water to precipitate out the DNA and proteins. After 5-15 minutes the mixture was centrifuged at 12,000g for 15 minutes. The supernatant (~1mL) was transferred to a clean RNase free centrifuge tube, followed by the addition of 0.4 mL 75% ethanol to precipitate the RNA. The samples were stored for 10 minutes and centrifuged at 12,000g for 8 minutes. Supernatant was removed and the RNA pellet was washed with 75% ethanol followed by centrifugation at 8,000g for 3 minutes. This last step is repeated twice. Finally, the RNA pellet was dissolved in 0.25 mL of water. The concentration of RNA extracted was determined with a NanoDrop ND-1000 Spectrophotometer (NanoDrop Technologies, Inc), and the ratio of absorbance at 260 nm over 280 nm was within the range of 1.9 to 2.1 to ensure the purity of RNA samples.

2.3 Quantitative RT-PCR

Total RNA was reversed transcribed to generate complementary deoxyribonucleic (cDNA) using RT^2 First Strand Kit from Origene (Rockford, MD) according to manufacturer's protocol. Amplification reactions were performed using qPCR kit for Sybr Green (Promega) according to manufacturer's protocol. Fluorescent PCR analysis was performed using a BIO-RAD iCycler (BIO-RAD, Hercules, CA). The following PCR conditions were used: 10 minutes at 95°C, 45 cycles of 30 seconds at 95°C, followed by annealing at appropriate temperature. Housekeeping gene EEF1A1 was used for normalization of the versican expression data. The

primers used for quantification of versican expression were synthesized by Integrated DNA Technologies (Coralville, Iowa) based upon literature sequences for the isoforms.* Relative quantification was performed using standard curves generated through a dilution series, and subsequently adjusted with the normalization factor. The target gene amount was divided by the housekeeping gene amount to obtain a normalized target value. The sequences of the synthesized primers are listed in Table 1. P-values were calculated by one-way ANOVA.

Table 1. Primer Sequences for qRT PCR

Gene	Sequence size (bp)
V0 Forward	5' CCAGCAAGCACAAAATTTCA 3' (162)
V0 Reverse	5' TGCACTGGATCTGTTTCTTCA 3'
V1 Forward	5' CCCAGTGTGGAGGTGGTCTAC 3' (124)
V1 Reverse	5' CGCTCAAATCACTCATTCGACGTT 3'
V2 Forward	5' TCAGAGAAAATAAGACAGGACCTGATC 3' (135)
V2 Reverse	5' CATACGTAGGAAGTTTCAGTAGGATAACA 3'
V3 Forward	5' CCCTCCCCCTGATAGCAGAT 3' (71)
V3 Reverse	5' GGCACGGGGTTCATTTTGC 3'
V4 Forward	5' CAGTACCACTGTTGAGGAAAAAGAAAA 3'
V4 Reverse	5' CGTTAAGGCACGGGTTCATT 3'
EEF1A1 Forward	5' CTGGCAAGGTCACCAAGTCT 3' (99)
EEF1A1 Reverse	5' CCGTTCTTCCACCACTGATT 3'

2.4 RNA Interference

Short interfering RNA (siRNA) targeting versican (Santa Cruz Biotechnologies) and control siRNA (Santa Cruz Biotechnologies) and DharmaFect (Dharmacon) were used in the transfection of ovarian cancer cell lines. Cells were grown to 80% confluency, and then treated with Solution A for the treatment group or Solution B for the control group. Solution A consists of 8 µL of versican siRNA and 6 µL of Dharmafect in 200 µL of serum-free media. Solution A is allowed to incubate for 20 minutes on ice before addition to cells. Prior to adding solution A,

the cells are rinsed with serum free media, and then incubated in A for 6 hours. After the 6 hours have passed, 1 mL of complete media is added and allowed to incubate overnight. Following overnight incubation an additional 1 mL of complete media is added and placed back in incubator overnight. For controls, Solution B was substituted for Solution A, which consisted of 2 µL of control siRNA and 6 µL of Dharmafect in 200 µL of serum free media.

Hush shRNA plasmid (29-mer) construct against versican (VCAN) as well as a HuSH shRNA 29-mer Non-effective Scrambled vector were purchased from Origene (Rockville, MD). From each of the four vials containing the VCAN constructs, 1 µg was taken and combined with 12 µL of Dharmafect in 200 µL of serum free media, and incubated for 30 minutes at room temperature. Following incubation the mixture was added to an 80% confluent monolayer of Skov-3 cells with 4 mL of serum free media following a rinse of the cells with serum free media. To create a control cell line HuSH shRNA scrambled vector was reconstituted to a concentration of 1 µg/µL. Subsequently, 1 µL of the vector was combined with 8 µL of Dharmafect in 200 µL of serum free media and incubated for 30 minutes at room temperature. Following, incubation the scrambled vector mixture was added to an 80% confluent monolayer of Skov-3 cells. At 100% confluency, the transfected cells are passed and maintained in growth media containing 1-2 µg/mL puromycin to maintain selection pressure.

2.5 Scratch Migration Assay

The spreading and migration abilities of Skov-3, Dov13, OVCA 429, and OVCA 433 were assessed using the scratch wound healing assay. Cells were seeded into six well tissue culture plates and grown to 100% confluency. Prior to wounding with a P100 pipette tip, cells were incubated overnight with serum free media. After wounding, cellular debris was removed by washing with PBS, and then incubated in 2.5% fetal bovine serum. Wound closure was

monitored at 5, 10, and 24 hours and calculated using AxioVision software on the Axio Observer D1 inverted microscope. The wound closure area that was used for measurements was carefully marked, so as to be identifiable at every time point. The difference between the width of the scratch at any given time period divided by the original width times 100 represents the percent of wound closure. A total of 6-8 measurements were taken per field of image (see figure 4 below), and the mean average percent closure was used in statistical analysis. The experiments were repeated in duplicate wells and repeated a minimum of three times with a minimum of four fields of measurements per well. To account for differences in the width of the initial wound, data was normalized to represent wound closure of equal width. This was done by using the amount of migration from initial borders rather than by using wound width alone, as a wider wound could skew data.

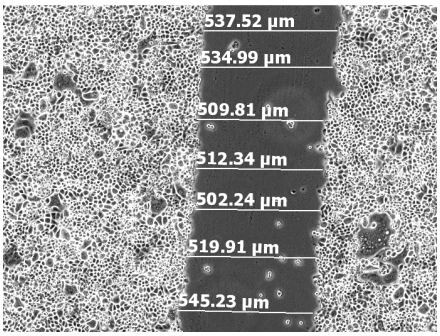

Figure 4. Wound Healing Analysis. An average of 6-8 measurements were made using the AxioVision software, and the average was used to determine the percent wound closure for that field.

2.6 Spheroid Culture

Spheroids were generated using a liquid agarose overlay technique described by Burleson et al.* Agarose was melted in complete media to a concentration of 0.5% (25mg in 5mL), and then 2 mL of agarose was poured into six well tissue culture plates to prohibit cell adhesion to the tissue culture plate and allowed to cool for a minimum of thirty minutes. Following cooling OVCA-429, OVCA-433, Dov-13, and Skov-3 cells grown in monolayer were released with 1%

trypsin and resuspended in 2% serum containing media at 125,000 cells/mL. Then 2 mL containing 250,000 cells were added to the solidified agarose, and then supplemented by the addition of 1 mL of 2% serum containing media. The tissue culture plates were incubated for 48 hours at 37°C. Following 48 hours of incubation, the spheroids were gently removed from the surface of the solidified agarose, and separated from single cells by centrifugation at 100 x g for 2 minutes before use in experiments. Spheroids were defined as having a diameter between 30-275 µm.

2.7 Fluorescent Labeling

In adhesion assays in order to differentiate between mesothelial cells and OVCA-429, OVCA-433, Dov-13, and Skov-3 cells, Vybrant DiO (Invitrogen, Grand Island, NY) was used to label the membrane of ovarian cancer cells. Cells were lysed and resuspended at a density of 1 x 10^6 cells/mL in serum free media, and 8 µL of Vybrant DiO was added per mL of cell suspension. The suspension was gently mixed by pipetting, and incubated at 37°C for 30-35 minutes. After the incubation period the cell suspension was centrifuged at 1500 rpm for 2 minutes. The supernatant was removed and cells were resuspended in serum free medium, and centrifuged again followed by resuspension in appropriate medium depending upon use.

2.8 Spheroid Adhesion Assays

Six well plates were coated with either 25 µg/mL collagen in PBS or matrigel (1:100 concentration) in PBS and incubated at 37°C for 4 hours. The six well plates were then blocked with 2% BSA in PBS overnight in the 37°C incubator. Additionally, spheroids were allowed to adhere to the tissue culture plate. Approximately 50-75 spheroids of OVCA-429, OVCA-433,

Dov-13, and Skov-3 were suspended in 4 mL of serum free media and added to the six well plates and allowed to adhere for 24 hours in the 37°C incubator. The total number of spheroids added to each well was counted manually. Nonadherent spheroids were gently removed with PBS, and remaining adherent spheroids were counted under a light microscope. Percent adhesion was determined by dividing the number of adherent spheroids by the total number of spheroids seeded. The percent adhesion was calculated at 1,2,5, and 24 hours.

To evaluate OVCA-429, OVCA-433, Dov-13, and Skov-3 spheroid adhesion to mesothelial cell monolayers LP-3 and LP-9 were grown to confluence in six well tissue culture plates. Prior to culturing of spheroids, the ovarian cancer cell lines were fluorescently labeled with Vybrant DiO. The fluorescently labeled spheroids were allowed to adhere to the mesothelial cell lines for 24 hours. The percent adhesion was determined in the same manner described above. Adherent spheroids were counted under a fluorescent microscope.

The experiments were performed in triplicate and a minimum of four times for statistical analysis. Spheroids smaller than 30 µm or larger than 275 µm were not used in statistical analysis.

2.9 Spheroid Disaggregation Assay

Six-well plates were coated with 25 µg/mL Collagen, and Matrigel (1:100) in PBS and incubated overnight at 37°C. The wells were then blocked with 2% BSA for 3 hours, and rinsed 2x with PBS. OVCA-429, OVCA-433, Dov-13, and Skov-3 spheroids were suspended in 2% serum containing medium and 25-40 spheroids were added to each well. The spheroids were allowed to disaggregate for a period of 24 hours. Spheroids were digitally photographed after one hour, this time was previously determined to be the time required for spheroid adhesion to

initiate. After 24 hours the spheroids were again digitally photographed, and the total area encompassed by the cells was determined using the AxioVision software by outlining the area of disaggregated spheroid plus any single cells that may have come from the spheroid. Disaggregation is represented as fold change in the pixel area of the spheroids from time 0 hours to 24 hours. To accurately track the separate spheroids and correlate the images at 1 hour and 24 hours the six well plates were divided into 27 individual square grids.

The experiments were performed in triplicate and a minimum of four times for statistical analysis. Spheroids smaller than 30 µm or larger than 275 µm were not used in statistical analysis.

2.10 Spheroid Disaggregation on Mesothelial Monolayers

To evaluate disaggregation on a system closer to what is experienced in vivo, LP3 mesothelial cells were grown to confluence in P35 dishes. Prior to culturing of spheroids, single cell suspensions were fluorescently labeled with Vybrant DiO (Invitrogen) as described earlier. Spheroids were then resuspended in 2% serum containing media, and then gently added to the mesothelial monolayer and incubated at 37°C. Approximately, 15-30 spheroids of the four EOC cell lines were added to their respective dish. Spheroids were imaged at 1 hour and at 24 hours to assess disaggregation under a fluorescent microscope. Disaggregation was calculated by dividing the pixel area at time 0 by the pixel area at 24 hours. The P35 dishes were divided into 20 individual square grids for accurate tracking of spheroids.

Inhibition of spheroid disaggregation on LP-3 mesothelial cells was evaluated by incubating with the EOC spheroids with monoclonal antibodies against the CD44 protein for 30 minutes at 37°C, followed by addition to the LP-3 monolayer for a 24 hour period. Inhibition of

adhesion was also assessed by the addition of soluble hyaluronan to the LP-3 monolayer prior to spheroids being added. The experiments were performed in triplicate and a minimum of four times for statistical analysis. Spheroids smaller than 30 µm or larger than 275 µm were not used in statistical analysis.

2.11 Statistical Analysis

All analyses were performed using SPSS 17.0. Student's t-test, and one-way ANOVA test was used to determine statistical significance between treatment and control groups. Statistical significance is determined by P-values <0.05. All experiments were performed in triplicate and repeated at least three times.

2.12 Single Cell Adhesion Assay

OVCA-429, OVCA-433, Dov-13, and Skov-3 single cells were suspended in 2% serum containing media. Approximately 10,000-12,000 cells were added to six well plates that were coated with 25 µg/mL collagen, matrigel (1:100), or left uncoated. The degree of adhesion was represented by percent of adhering cells, which was determined by taking the number of adherent cells divided by the number of cells seeded initially. The percent of adhesion was calculated at 2 hours, 5 hours, and 24 hours. Non-adherent cells were removed by gently rinsing with PBS, and remaining cells were fixed and stained with Diff-Quik (Dade Behring, Inc., Newark, DE). The six well plates were divided into 20 individual grids to enable manual counting of adherent cells by light microscope. The plates were counted twice and the average was used for statistical analysis.

Additional experiments were performed to evaluate the degree of adhesion to a monolayer of LP-3 mesothelial cells in six well plates. The EOC cell lines were fluorescently labeled with Vybrant DiO prior to adding to the LP-3 monolayer. To the LP-3 cells were added 10,000-12,000 fluorescently labeled EOC cells. The percent of adhesion was examined at 2 hours, 5 hours, and 24 hours by gently removing non-adhering with a PBS rinse.

For inhibition assays, a monoclonal antibody against CD-44 or soluble hyaluronan was incubated with the fluorescently labeled EOC cells for 30 minutes prior to being added to the LP-3 monolayer. Percent adhesion was examined at the same times points, and calculated in the same fashion as above.

2.13 Downregulation of Versican Expression and Functional Assays

To examine the effects of versican on cellular adhesion, migration, spheroid formation, and spheroid disaggregation siRNA constructs targeting versican were used to downregulate its expression in the four EOC cell lines. Additionally, the verscian shRNA Skov-3 cells were used to reinforce results obtained from siRNA cells. All experiments described in methods section were repeated using the siRNA cells as well as the VCAN shRNA cells. Upon completion of experiments, total RNA was extracted from the cells and levels of versican were assessed using quantitative real-time polymerase chain reaction to ensure downregulation of versican expression was maintained for the duration of the experiments.

2.14 Modified Transwell Migration Assay

Corning 24-well plate inserts with an 8 micron diameter pore size had their bottom surfaces coated with matrigel (1:100). This was accomplished by adding 500µL of a 1:100

matrigel solution in PBS to 24 well tissue culture plates, and addition of inserts to the well. The inserts were incubated for 6 hours at 37°C. After incubation the inserts were washed with PBS twice, and placed in 4°C refrigerator.

To each well 500µL of serum free media was added and then the modified insert placed back into the well. Then cell suspensions of 100,000 cells/mL of OVCA-429, OVCA-433, Dov-13, and Skov-3 were prepared, and 10,000 cells were transferred into the inner chamber of the transwell insert. The plates are incubated for 6 hours in 5% CO2 at 37°C. As a control, the same aliquot used to transfer 10,000 cells into the inner chamber of the transwell, is pipetted into a clean well and manually counted to ensure that 10,000 cells were actually pipetted into the transwell chamber.

After 6 hours, the insert is removed and the media from the inner chamber removed by vacuum suction, being especially careful to not puncture the delicate membrane. Then using a cotton swap the inner chamber was swabbed to remove any cells that had not migrated. Inserts are submerged in Diff Quik fixative for 45 seconds, followed by submersion in Diff Quik Solution 1, then submersion in Diff Quik Solution 2 for 45 seconds. Between each solution the inner chamber can be vacuumed suctioned out. Following staining with solution 2, the inserts are washed in water to remove any residual stain. Finally, cells with migratory abilities were that able to navigate into the matrigel under layer were counted under a light microscope. The membranes were carefully divided into a numbered grid to aid in manually counting.

2.15 Spheroid Size Assay

In order to assess the effect versican has on spheroid formation, we observed its effect on overall spheroid size. To do this spheroids were generated as previously outlined in the spheroid

culture subsection. The 250,000 cells were transferred to a P60 plate and allowed to incubate for 48-72 hours, and then were isolated from single cells. The isolated spheroids were then transferred to a P100 dish, which was divided into a grid of 35 squares for manually counting. For counting purposes 20 of the 35 square grids were chosen to be counted (grey grids counted), and are represented below in Figure 5. For statistical purposes, spheroid size is graphically represented as diameter with units in micrometers. Spheroids smaller than 30 µm or larger than 275 µm were not used in statistical analysis. Additionally, to ensure there was no bias in transferring spheroids from their original P60 dish to the P100 dish, the original P60 dishes were divided into 20 square grids and manually counted in a fashion similar to what is represented in figure 5.

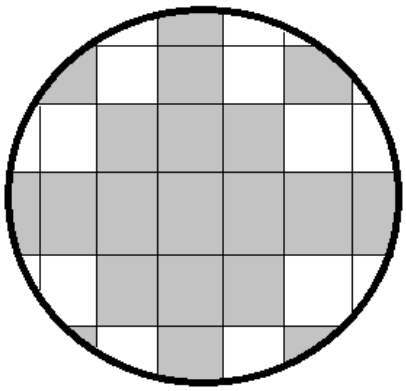

Figure 5. Spheroid grid template. The grid above represents the template used to randomly count the spheroids. Spheroids in the grey zones were counted.

2.16 Spheroid Formation Assay

OVCA-429, OVCA-433, Dov-13, and Skov-3 were allowed to form spheroids for 48-72 hours. Spheroid culture conditions were the same as described above, and after formation the isolated spheroids were transferred to a P100 dish divided into a 35 square grid as represented in figure 5. The same 20 squares used to assess the spheroid size were used to determine the

number of spheroids formed. To ensure there was no bias in transferring spheroids from their original P60 dish to the P100 dish as in the size assay, the original P60 dishes were divided into 20 square grids and the number of spheroids were manually counted and compared to median value from the transferred spheroids. Spheroids smaller than 30 µm or larger than 275 µm were not used in statistical analysis. Data was represented as fold change in the number of spheroids formed as compared to the control group, which received no treatment.

2.17 Protein Extraction

After assays were performed, cells were lysed in RIPA Lysis and Extraction Buffer (25mM Tris-HCl (pH 7.6), 150mM NaCl, 1% NP-40, 1% sodium deoxycholate, 0.1% SDS) (Thermo Scientific, Rockford, IL) supplemented with Roche Protease Inhibitor Cocktail tablets (Roche, Indiananoplis, IN) accorrding to manufacturer's guidelines. Prior to lysis cells were washed twice with PBS, and the pelleted by centrifugation. To the pellet was added 1 mL of RIPA buffer per $5x10^6$ cells, and then mixed by pipetting. The mixture was then placed on ice for 15 minutes followed by centrifugation at 14000g for 10 minutes at 4°C. Supernatants were collected and stored at -80°C. Protein concentrations were quanitified using BioRad Protein assay reagent (Bio-Rad Laboratories, Hercules, CA).

2.18 Western Blot

Proteins were mixed with sodium dodecyl sulfate (SDS) sample buffer, denatured by boiling at 95°C for 3-5 minutes. Equal amounts of protein (25-35 µg) were loaded per lane and separated on 7% SD-polyacrylamide gels. A Prestained Molecular Weight Marker (Sigma-Aldrich) was loaded onto the gel for correlation of protein masses. Following electrophoresis,

proteins were transferrred to PVDF membranes by a wet-transfer apparatus (Bio-Rad) overnight at 4°C for 90 minutes using a current of 350 mA. Membranes were blocked in 1X TBST buffer (20mM Tris, pH 7.6, 137mM NaCl, and 0.1% Tween-20) containing 5% BSA, and incubated for one hour at 4°C. Then the membranes were washed (3X) in 1X TBST for 5 minutes while being agitated on a shaker. Following washing, membranes were incubated overnight at 4°C in their respective primary antibodies diluted in 1X TBST containing 3% BSA. After incubation with primary antibodies, membranes were rinsed with 1X TBST (3X) for 5 minutes with agitation. Following rinsing, membranes are incubated with their appropriate secondary antibodies diluted in 1X TBST and 3% BSA and incubated for 2 hours at room temperature. Prior to chemiluminescent imaging, Pierce (Thermo Scientific) Fast Western Blot Kits were utilized according to manufacturer's protocl. Imaging was performed using a Chemidoc Gel Documentation System, equipped with Quantity One Software (Bio-Rad Laboratories).

The antibody against versican 12C 5 was purchased from the Developmental Studies Hybridoma Bank (DSHB, Iowa City, Iowa). The antibody against beta-tubulin (E7) was also purchased from the DSHB. The goat anti-mouse IgG-HRP linked antibody was purchased from Santa Cruz (Santa Cruz, CA).

3. RESULTS

3.1 Versican Expression Effects Migration

In previous studies, it has been shown that versican is a prerequisite in the formation of a pericelluar matrix, which is critical for the proliferation and migration of mesenchymal cells.[144] The increased migratory ability has been accredited to the anti-adhesive properties of its G1 domain.[92] Recombinant versican expression in prostate cancer cells was able to induce increased motility compared to cells receiving the empty vector.[96] Additionally, a recombinant vector overexpressing versican V1 isoform was able to promote increased motility in OVCAR-5 and Skov-3 ovarian cancer cells.[116] The researchers were also able to demonstrate that HA oligomers could be used to inhibit the increased motility by competing for the hyaluronan binding site on versican.[116] These previous results combined with our lab's observation that DKK1 is inhibited in ovarian cancer resulting in increased levels of versican led us to question what happens when versican is downregulated in EOC cell lines. Thus to address this question, we performed scratch wound healing assays as well as modified boyden chamber assays to assess migration in OVCA-429, OVCA-433, Dov-13, IGROV-1, and Skov-3 cells. The role of versican in the migration of these cell lines were examined by downregulating versican expression through siRNA (Santa Cruz, Inc). Additionally, HuSH 29mer shRNA construct (Origene) was used to create stable Skov-3 clones with versican downregulated.

OVCA-429, OVCA-433, Dov-13, IGROV-1, and Skov-3 cells were grown to confluency and subjected to wounding with a P100 pipette tip followed by incubation in 2% serum containing medium over a 24 hour period. Wound closure was monitored under a light microscope at 0, 5, 10, and 24 hours (Figures 6-9). The percent wound closure was calculated as described in the methods section. This procedure was repeated using siRNA targeting the

versican gene. The results are represented in Figures 10-14**.** We found that upon treatment with VCAN siRNA, migration of cells was significantly inhibited in the SKOV-3 and Dov-13 cell lines. At 24 hours, VCAN siRNA treated Skov-3 cells achieved 60-65% wound closure, whereas control cells had been able to close 87-90% of the wound gap. This correlated to a 27 % decrease in migration when versican expression was altered in Skov-3 cells. Loss of versican in Dov-13 cells corresponded to a 25% decrease in wound closure. In contrast, wound closure was only decreased 8-9% in OVCA-433 and OVCA-429 VCAN siRNA treated cells, however this difference was determined not to be significant. To verify the results seen in the Skov-3 cells, VCAN shRNA was used to create a stable line with VCAN downregulated. We observed similar results with VCAN siRNA and VCAN shRNA cells, which was roughly a 20-27% decrease in wound closure. In the case of IGROV-1 cells, we expected to see very little if any change in migratory abilities since VCAN was not found to be expressed in quantities measurable by our qRT-PCR analysis**.** We also observed noticeable changes in morphology in DOV-13 and SKOV-3 cells treated with VCAN siRNA, as they took on a fibroblastic shape (Figures 6-7). This is compared to the more epithelial morphology observed in the control groups.

With the results from the scratch wound healing assay, we decided to investigate changes in migration abilities resulting from silencing of versican by using modified boyden (transwell) chambers. The bottom of the transwell inserts were coated with matrigel to trap migrating cells as described in the methods section. The principle behind this assay is that more motile cells will be able to migrate through the filter pores into the matrigel layer. Thus based upon previous literature that recombinant versican can enhance motility in prostate cancer cells, we expected to see an observable decrease in the number of migratory cells.[96] Unsurprisingly, we observed

similar results in the modified boyden chambers as the scratch wound healing assay, with noticeable decreases in the number of migratory cells in Dov-13 and Skov-3 cells treated with VCAN siRNA (Figure 10-11). Altered versican expression through siRNA caused a 20-35% decrease in the number of Skov-3 migratory cells. Silencing of versican in Dov-13 cells coincided with 29% decrease in the average number of migratory cells. Despite a 15-19% decrease in the number of migratory cells in siRNA treated OVCA-429 and OVCA-433 cells (Figure 12-13), analysis by student t-test showed no statistical difference between treatment and control groups. Once again IGROV-1 served as our negative control, and demonstrated no real observable difference in the number of migratory cells between control and treatment groups (VCAN siRNA). These results combined with the scratch wound healing assay indicate that versican plays a role in cellular migration in ovarian cancer cells.

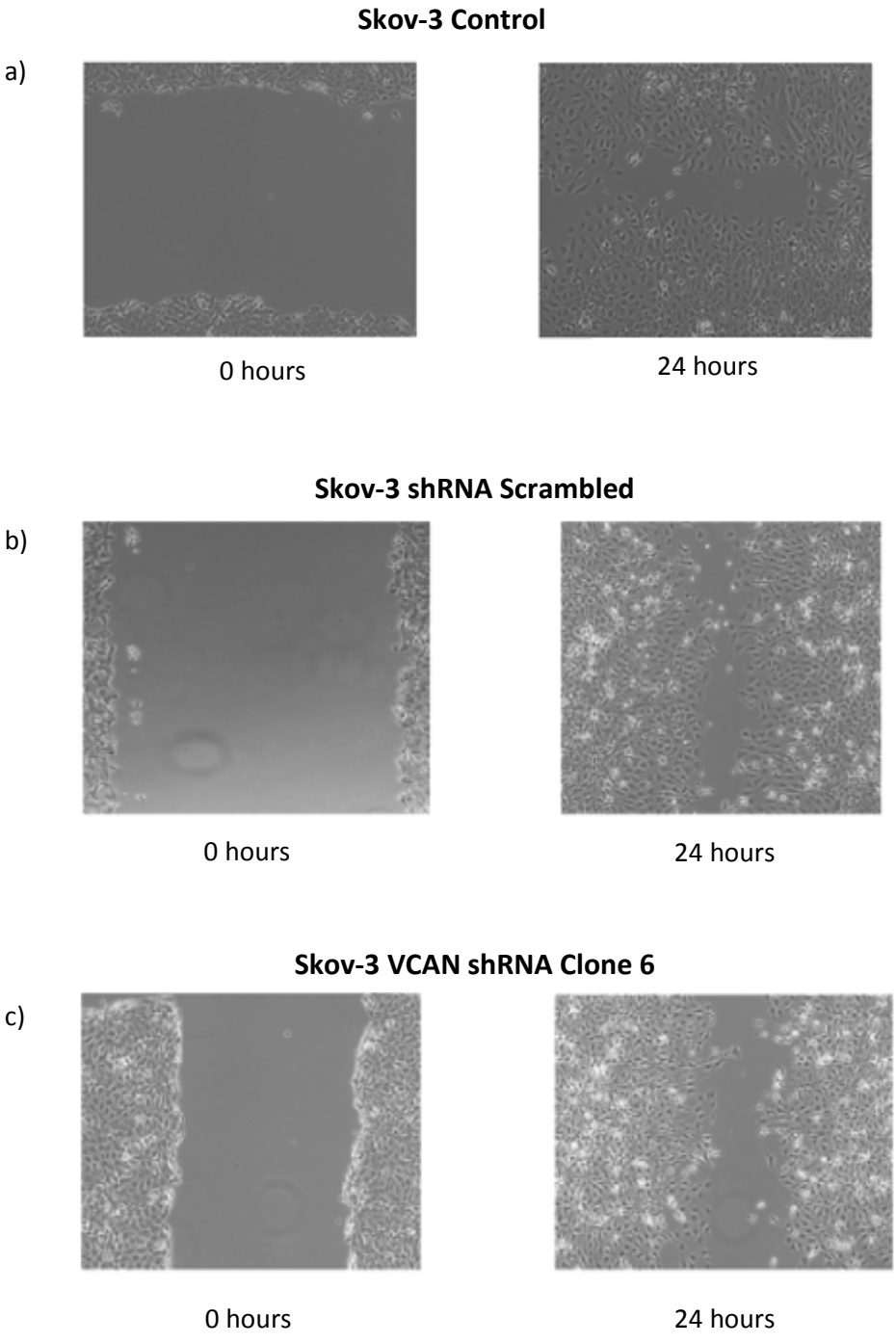

Figure 6. Monolayers of Skov-3, SKov-3 VCAN shRNA, and Skov-3 scrambled shRNA were cultured to confluency and subjected to wounding by a pipet tip. Wound closure was monitored over a 24 hour period under a light microscope. Digital photographs show wounding at time 0 as well as at 24 hours. Based on observations it is clear that versican expression causes an increase in motility.

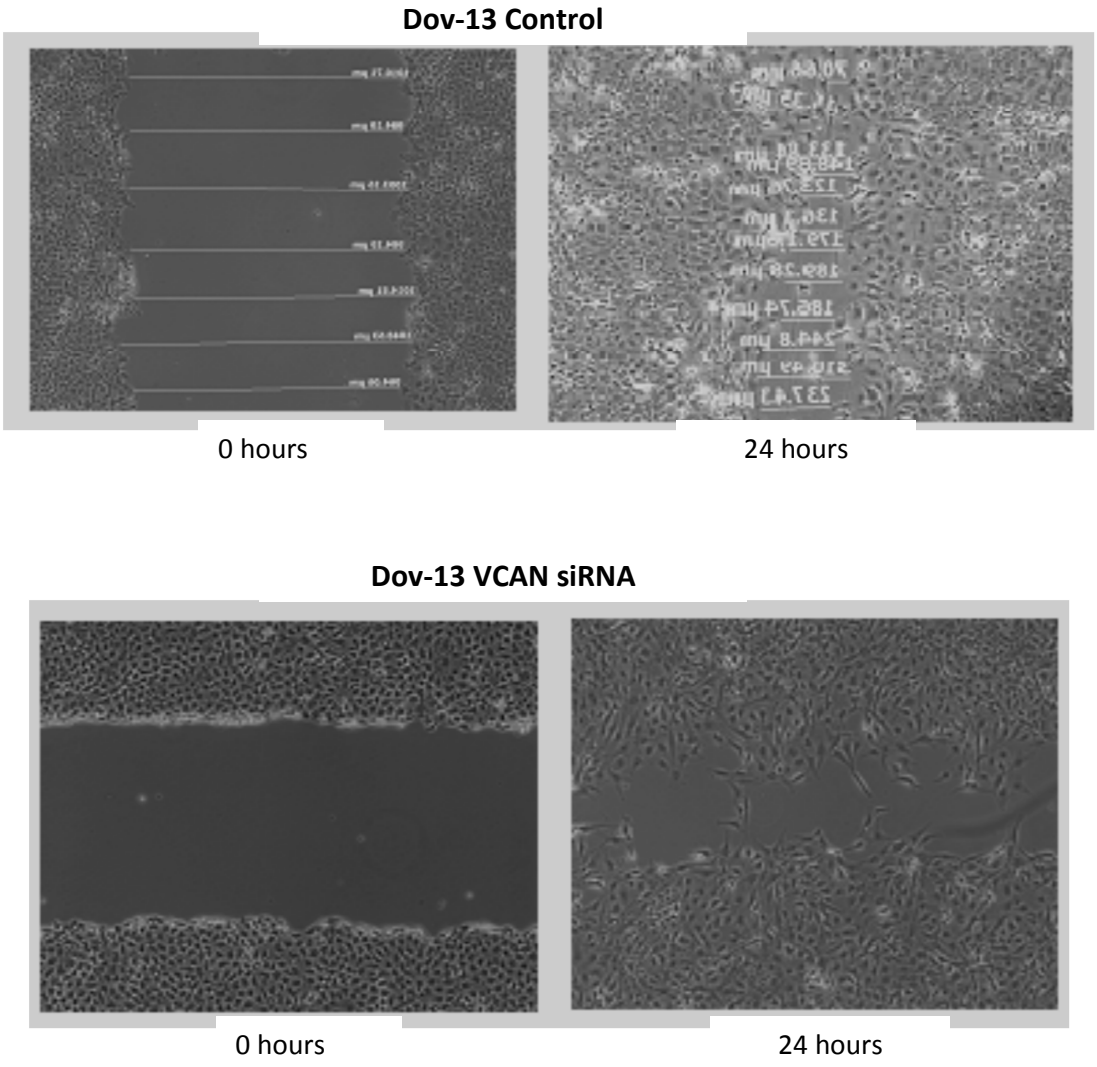

Figure 7. Versican mediated migration in Dov-13 cells was investigated by performing a scratch wound healing assay on control cells and on VCAN siRNA transfected cells.

IGROV-1 VCAN siRNA

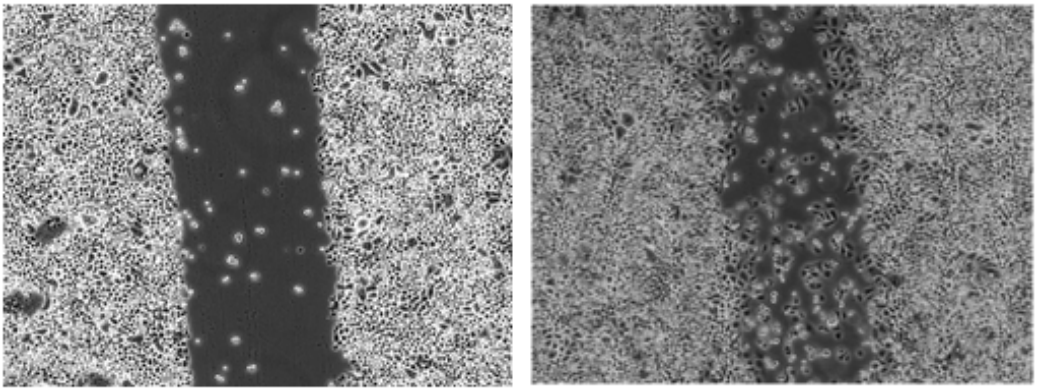

0 hours 24 hours

IGROV-1 Control

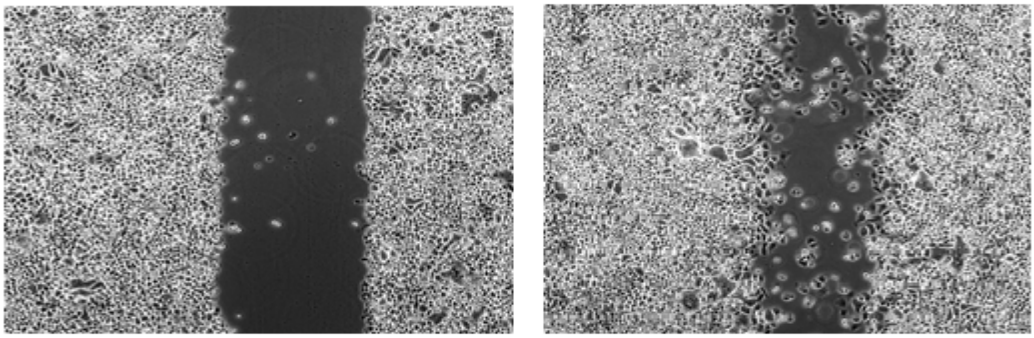

0 hours 24 hours

Figure 8. Migration of IGROV-1 cells was assessed by conducting a scratch wound healing assay. To assess migration mediated by versican, experiments were repeated using VCAN siRNA transfected cells.

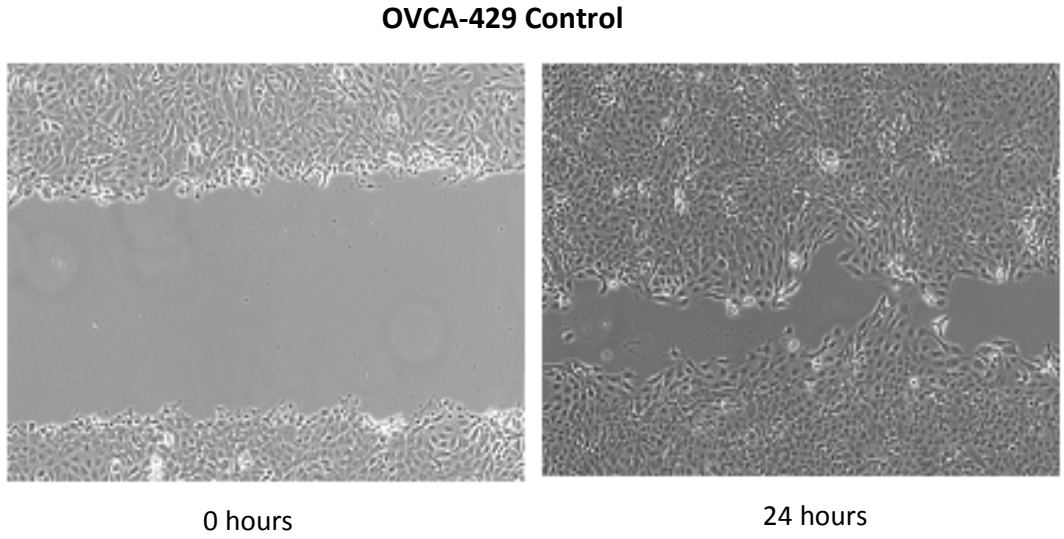

Figure 9. OVCA-429 cells grown to confluency were wounded and treated with 2% serum containing media, and monitored over a period of 24 hours. The experiment was repeated using VCAN siRNA transfected cells.

a)

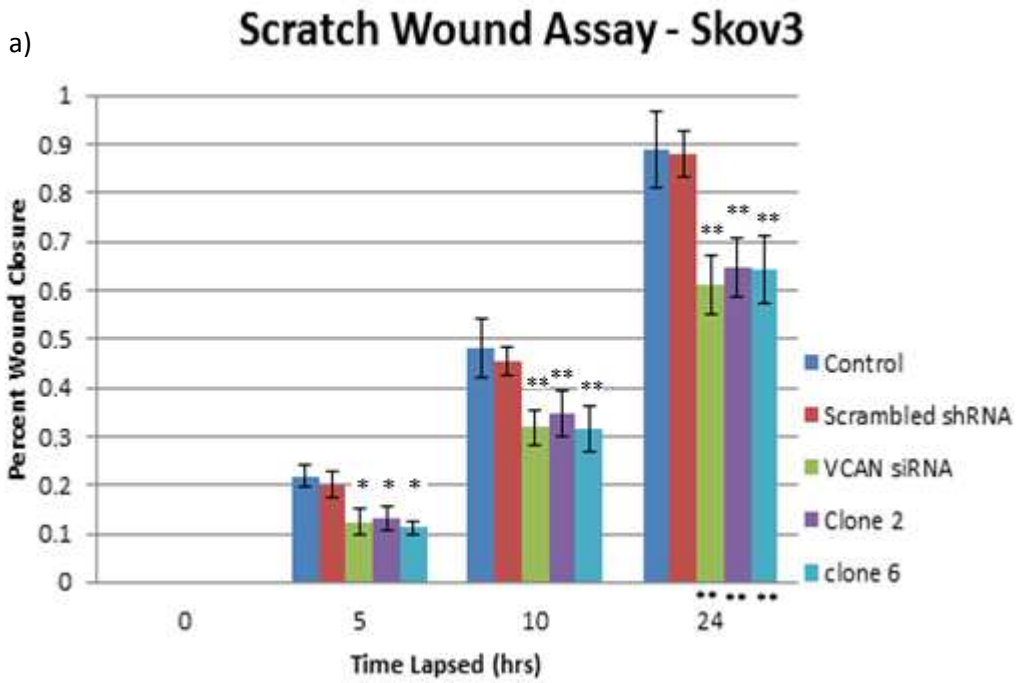

b)

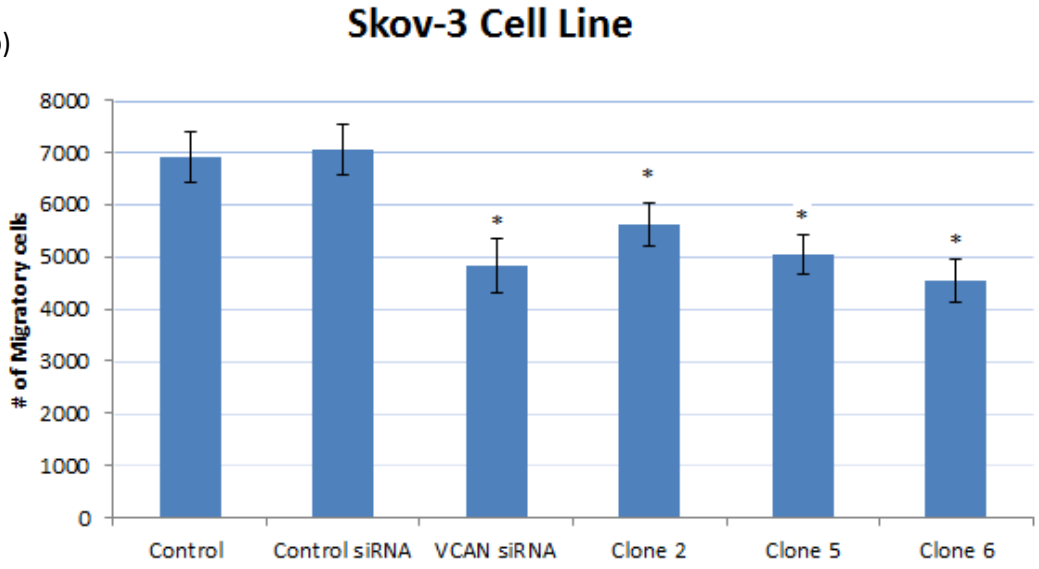

Figure 10. Versican mediates migration in Skov-3 cells. (a) Quantitative migration of Skov-3 control, scrambled shRNA, VCAN siRNA, VCAN shRNA clone 2 and clone 6 is represented as percent wound closure. Percent wound closure was calculated by measuring the distance of the wound at time 24 hrs and comparing it to time 0. (b) Migration was also assessed using modified boyden chambers. P-values were calculated using the student t-test.

*, $p < 0.05$
**, $p < 0.005$

a)

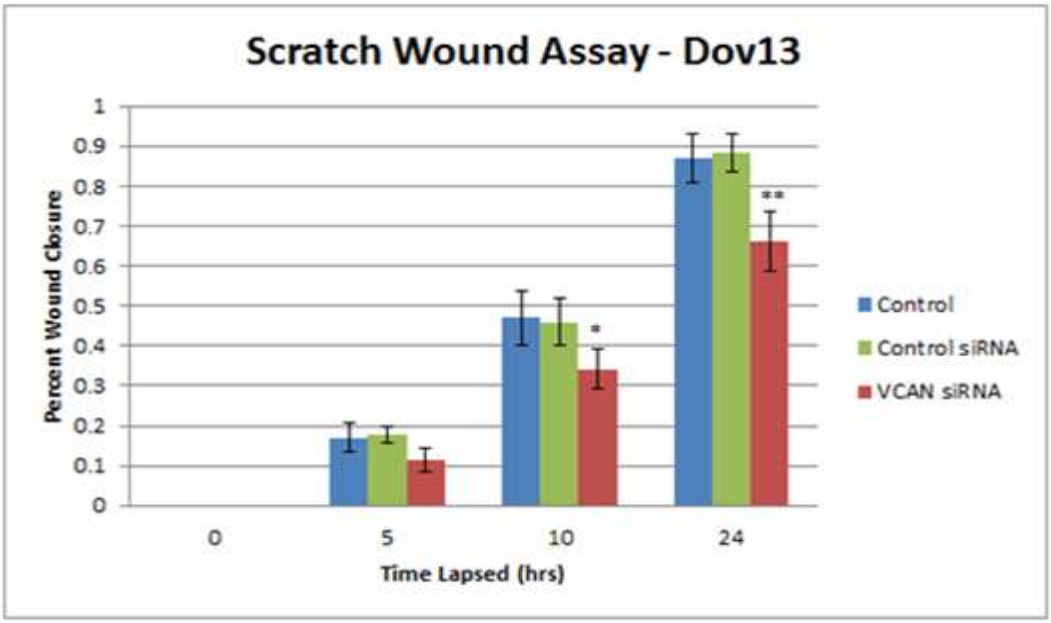

b)

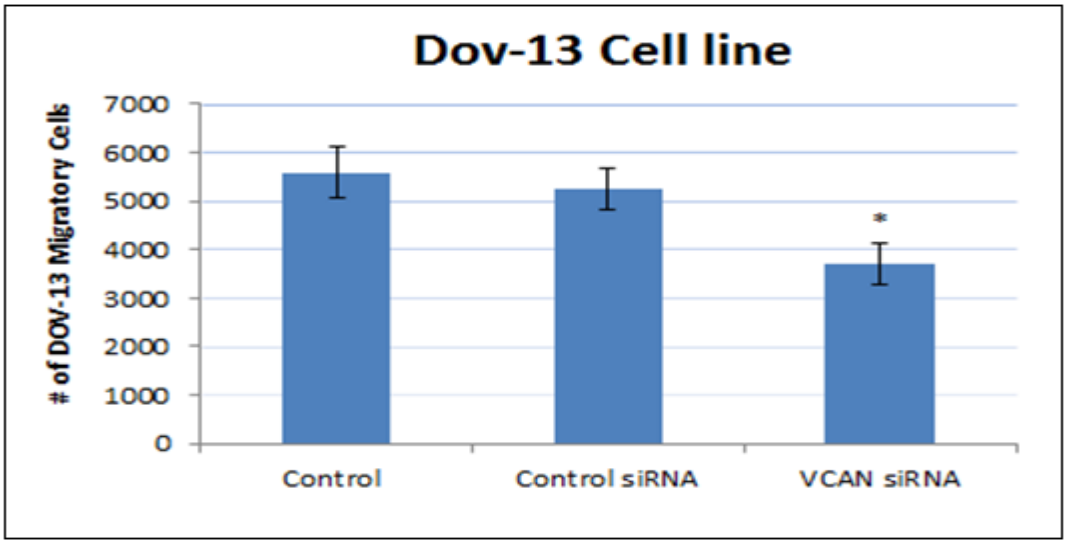

Figure 11. Effect of Versican on Dov-13 cell migration. (a) Analysis of migration of control, control siRNA, and VCAN siRNA cells was conducted by a scratch wound healing assay. Observations are represented Percent wound closure, which was assessed at 0, 5, 10, and 24 hours. (b) The migratory abilities have the control, control siRNA, and VCAN siRNA cells were further analyzed by performing a modified boyden chamber assay. Approximately 10,000 cells were transferred to the chamber and allowed to migrate for a duration of 6 hours. P-values were calculated by student t-test

*, $p < 0.05$
**, $p < 0.005$

a)

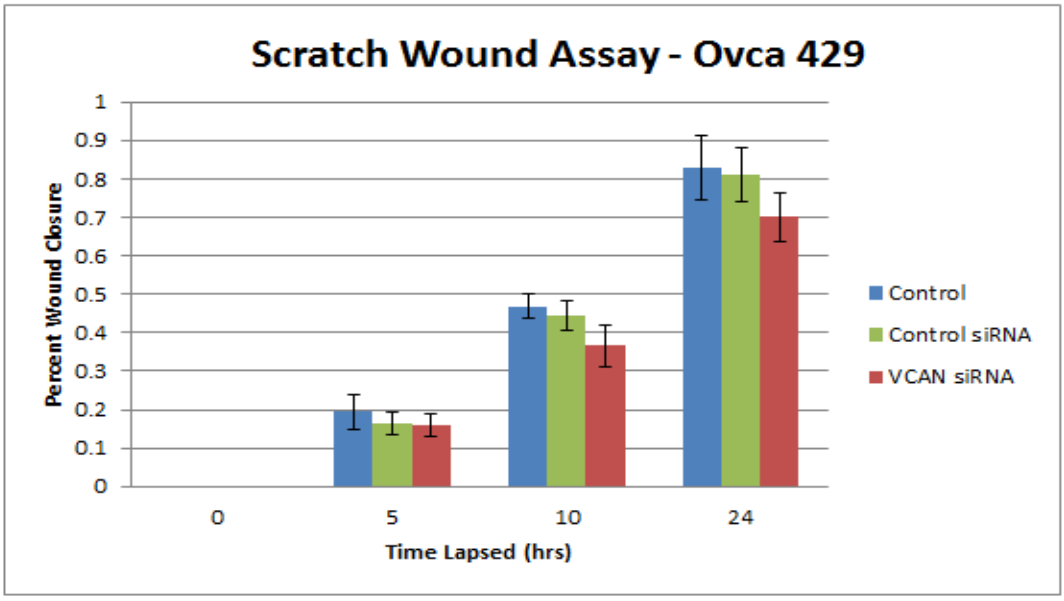

b)

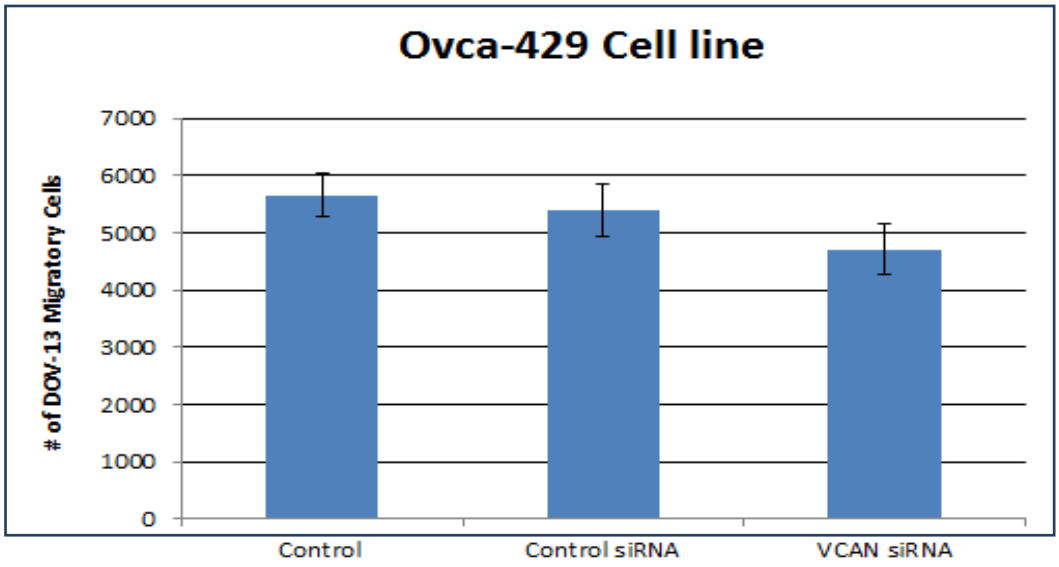

Figure 12. Downregulation of Versican and its impact on migration of OVCA-429 cells. (a) The ability of OVCA-429 cells to migrate was evaluated by scratch wound healing assay. Percent wound closure was examined at 0, 5, 10, and 24 hours. The experiment was repeated using control siRNA and VCAN siRNA cells to investigate the ability of versican to regulate migration. (b) To further assess the capacity of OVCA-429 cells to migrate, a modified boyden chamber assay was conducted using control, control siRNA, and VCAN siRNA cells.

*, $p < 0.05$
**, $p < 0.005$

a)

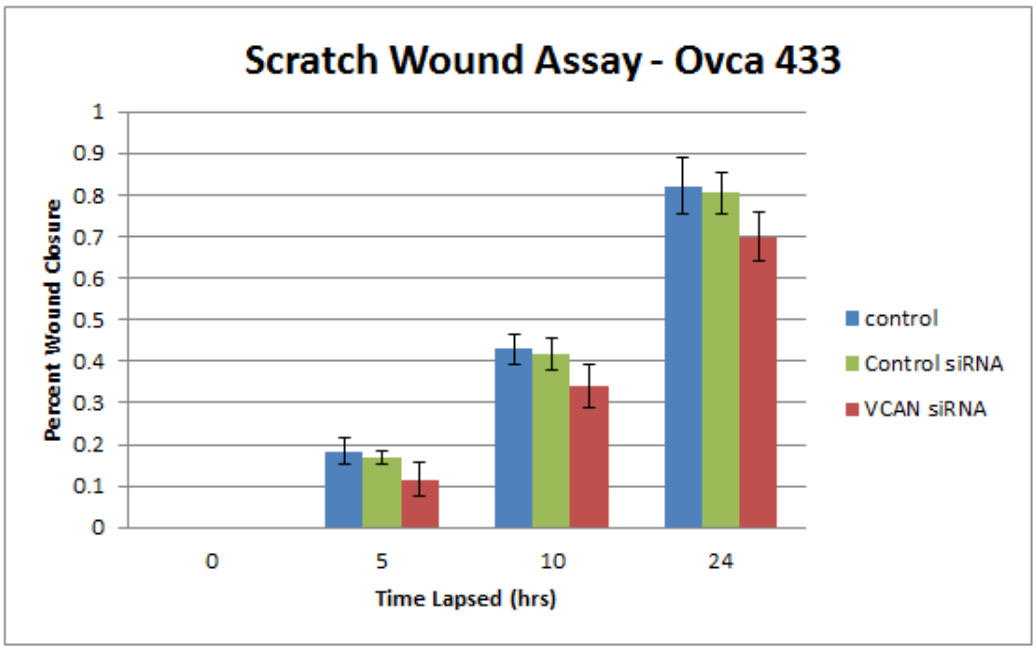

b)

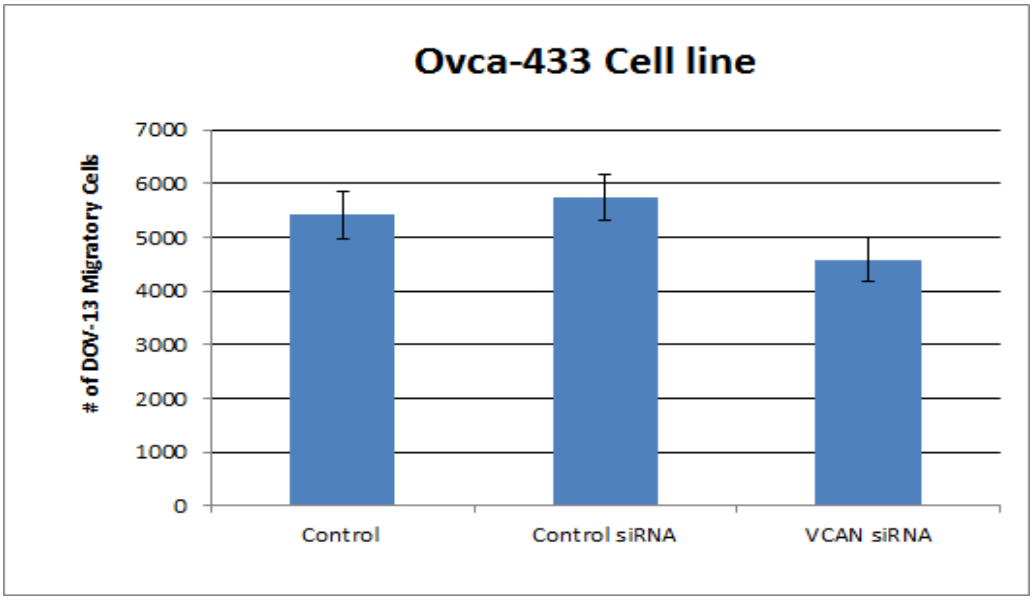

Figure 13. OVCA-433 migration and Versican Silencing (a) Migration of OVCA-433 cells was examined by monitoring the closure of a wound generated by a pipette tip over a 24 hour period. Percent wound closure was calculated at 5, 10, and 24 hours using software on the microscope. (b) The ability of versican to induce migration was additional assessed through a modified boyden chamber by silencing versican expression with VCAN siRNA.

*, $p < 0.05$
**, $p < 0.005$

a)

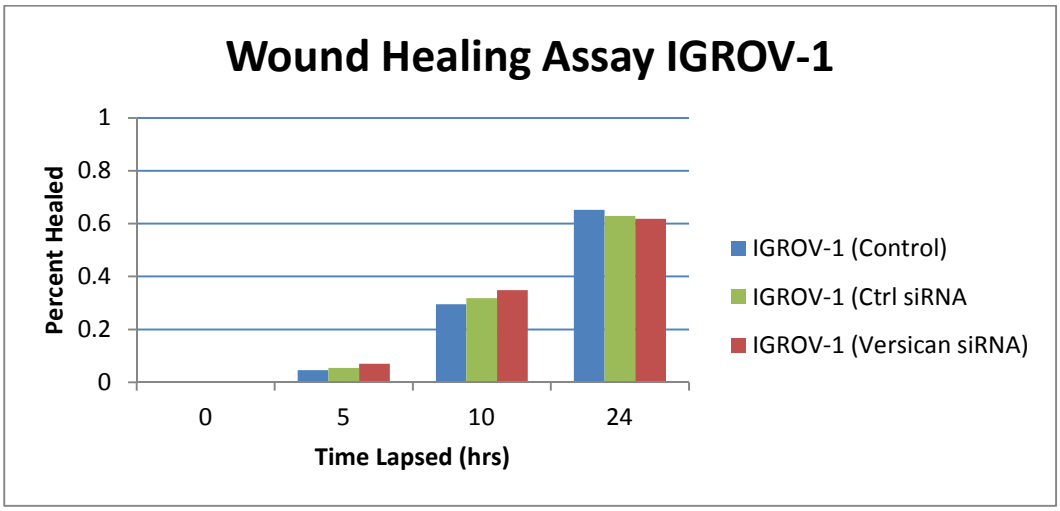

b)

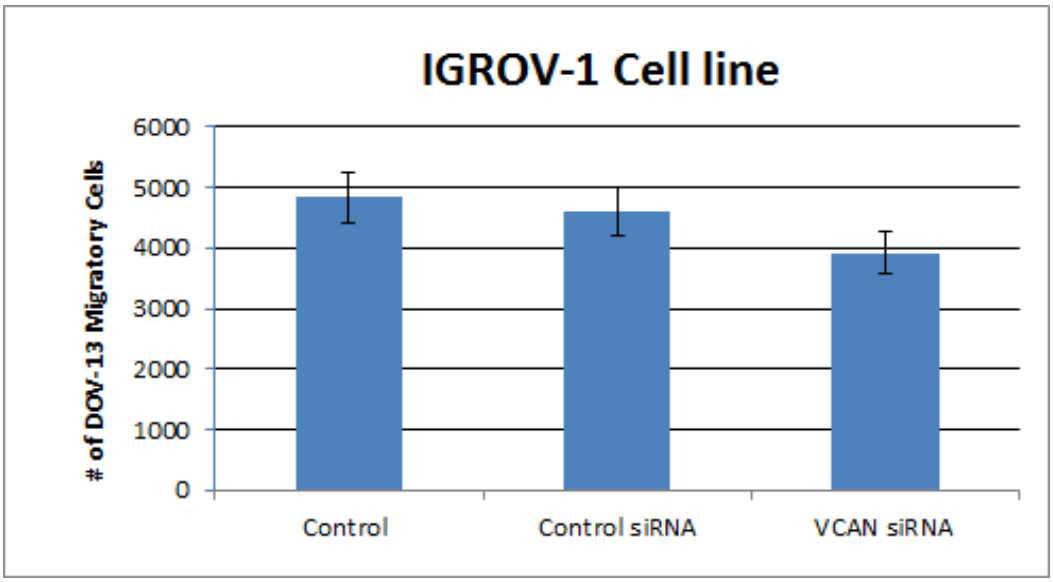

Figure 14. Downregulation of Versican in IGROV-1 cells does not affect migration. (a) Quantitative analysis of migration was assessed by conductingscratch wound healing assays on IGROV-1 monolayers incubated in 2% serum containing media. Assays were repeated using control siRNA and VCAN siRNA. Data is represented as percent wound closure. (b) Motility of IGROV-1 and siRNA transfected cells was investigated using the modified boyden chamber assay described in the methods section.

*, $p < 0.05$
**, $p < 0.005$

3.2 Versican's Effect on single cell adhesion

Cellular adhesion is an important phenomenon in normal tissue development, but when this tightly regulated function goes awry, pathologic states such as cancer can form. It is well established that the extracellular matrix secreted by the cells interacts directly with other cells and indirectly through other cell adhesion molecules. Due to the large and negatively charged side chains of versican it is no surprise that it has been found to be involved in cellular adhesion. There have been multiple studies looking at the effects of versican on cellular adhesion. Versican has been shown in some experiments to increase cellular adhesion in epithelial ovarian cancer cells, while in other studies it has been shown to have limited to no effect on cellular adhesion in EOC cells. In prostate cancer cells versican has been found to increase motility by causing decreased adhesion.[96] With conflicting information having been reported in regards to the effect of versican on adhesion, we decided to investigate what effects downregulating the expression of versican would have on cellular adhesion. Based on our lab's initial data and on evidence of increased versican expression having been found in EOC metastatic sites we hypothesized that versican silencing should decrease cellular adhesion.

We analyzed the effect of versican on the adhesion of EOC single cells to tissue culture plates coated with collagen, matrigel, and no treatment as well. Furthermore, we wanted to know whether the effect we saw on ECM components would be the same as on the mesothelial cell line LP-3. There has also been evidence to support the role of versican in mediating the attachment of ovarian carcinoma cells to the mesothelial layer lining the peritoneal cavity.[88,116] The role of versican in promoting cell adhesion has been downplayed though, as the protein CD 44 has been hypothesized by some to be the main mediator of cellular adhesion through its interaction with hyaluronan.[88] Yet, the exact mechanism of how CD44 initiates adhesion is

unknown, as functional assays by other groups using monoclonal antibodies against CD44 have failed to inhibit cellular adhesion. In some instances, the mAb against CD44 even caused an increase in adhesion. These conflicting results surrounding the role of versican and CD44, led us to investigate silencing of versican in single EOC cells combined with monoclonal antibodies against CD44 in attempts to elucidate the role of versican.

In the functional assays assessing the adhesion of EOC single cells to the extracellular matrix components collagen (25 µg/mL), matrigel (1:100), and to the poly-lysine coated tissue culture plates we plated 15,000 cells and observed adhesion over a 24 hour period. Non-adhering cells were gently removed by a PBS rinse at 1,2,5, and 24 hours. Adherent cells were fixed at their corresponding time points and manually counted as previously described. The results are summarized in figures 15-22. We observed a decrease in cellular adhesion in the OVCA-429, OVCA-433, Dov-13, and Skov-3 single cells on all three different components. As can be seen in the data figures, the greatest difference in adhesion was observed at 5 hours. Loss of versican in Dov-13 cells corresponded to a 23-35% (varies for the 3 plate coatings) decrease in adhesion after 5 hours. VCAN siRNA Skov-3 cells saw reduction in adhesion to matrigel, collagen, and poly-lysine in the range of 20-26%. In OVCA-429 and OVCA-433 cells there was a 14-18% reduction in the number of adhering cells at 5 hours, when cells were treated with VCAN siRNA. At 24 hours the decrease in adhesion from silencing of versican was diminished. This result was expected since mechanical forces from physically seeding the cells on the plate would promote adhesion given enough time.

With these results, we looked at how versican expression changed adhesion to the mesothelial monlayer composed of LP-3 cells. What we observed were similar results to those seen in the adhesion to the extracellular matrix components (Figures 15-22). Also as expected

from our expression data gathered by qRT-PCR, we saw that versican silencing had less of an effect on adhesion in the cell lines expressing lower amounts of verican such as OVCA-429 and OVCA-433 cells. In those cell lines the reduction in adhesion from downregulating versican was calculated to be roughly 15%. The loss of versican in Dov-13 and Skov-3 who express versican in higher amounts saw a 32% and 30% decrease in the number of adhering cells respectively. Furthermore, the addition of the monoclonal antibody against CD44 to the cells before addition to the LP-3 monolayer resulted in a decrease in adhesion to mesothelial monolayer. Administration of 1 ug/mL of CD44 mAb caused a 11% reduction in adhesion for the Skov-3 control cells. In VCAN siRNA and VCAN shRNA transfected cells the addition of the CD44 mAb corresponded to a nonsignificant 3-4% reduction in adhesion. When the concentration of mAb was doubled to 2 µg/mL there was only a slight further decrease in adhesion. This evidence suggests that CD44 does play a role in mediating adhesion, but that there are numerous other cell receptors capable of forming cell-cell or cell-matrix connections. To fully investigate this role we decided to test whether the addition of hyaluronan would increase adhesion, since versican is proposed to promote adhesion through its interaction with hyaluronan. The results, indicate that hyaluronan only marginally increased adhesion to the LP-3 monolayer. These results were somewhat surprising considering that there is literature supporting the role of hyaluronan in cellular adhesion. Our results suggest that hyaluronan, CD44, and versican each play a role in promoting adhesion that may be independent of each other.

a)

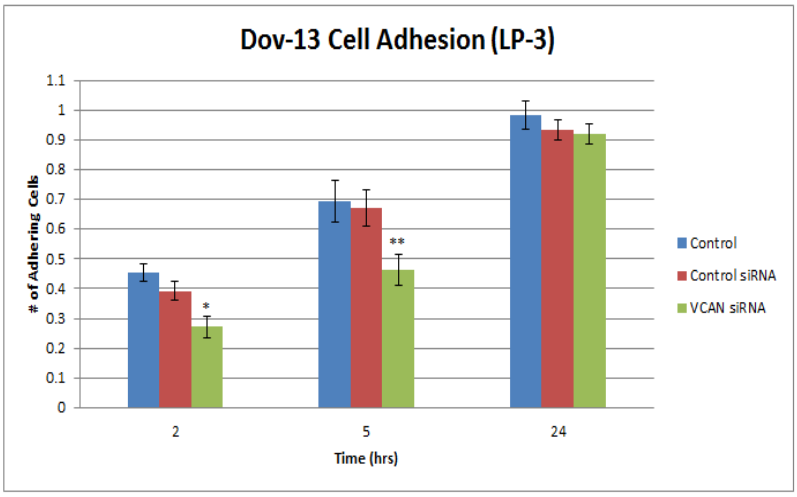

b)

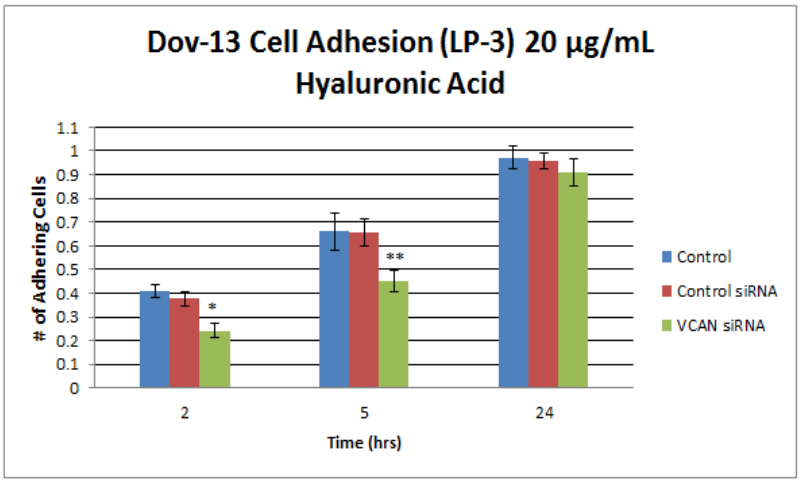

c)

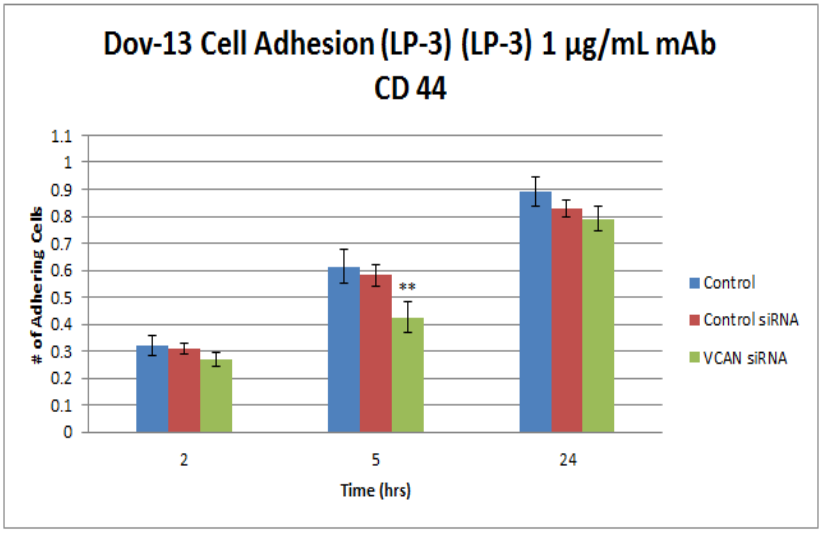

Figure 15. We tested the effect of versican on cell adhesion on the mesothelial cell line LP-3 under different conditions. (A) Downregulation of versican in Dov-13 led to a destabilization and ultimately a decrease in cell adhesion. (B) Addition of hyaluronan had no impact on the number of adhering cells in the control group or the VCAN siRNA treated cells. (C) Administration of a CD44 mAb intended to block the interaction of HA-Versican-CD44 complex led to a reduction in cell adhesion in all groups.

*, $p < 0.05$
**, $p < 0.005$

a)

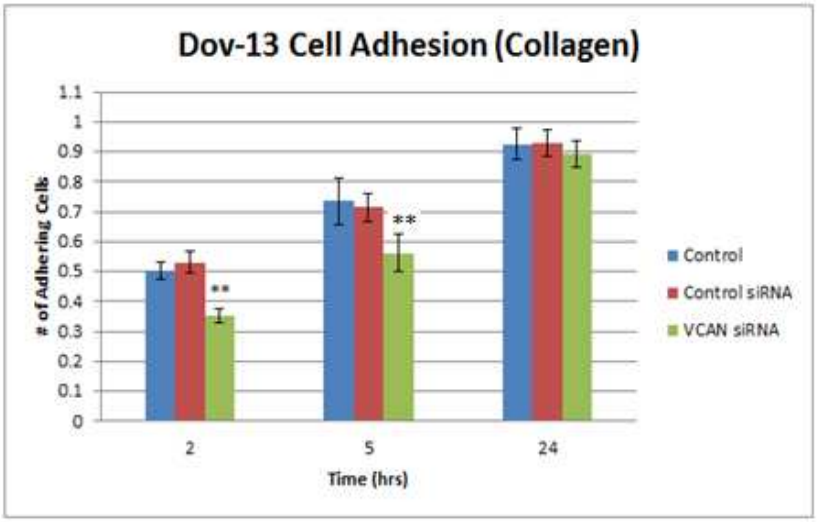

b)

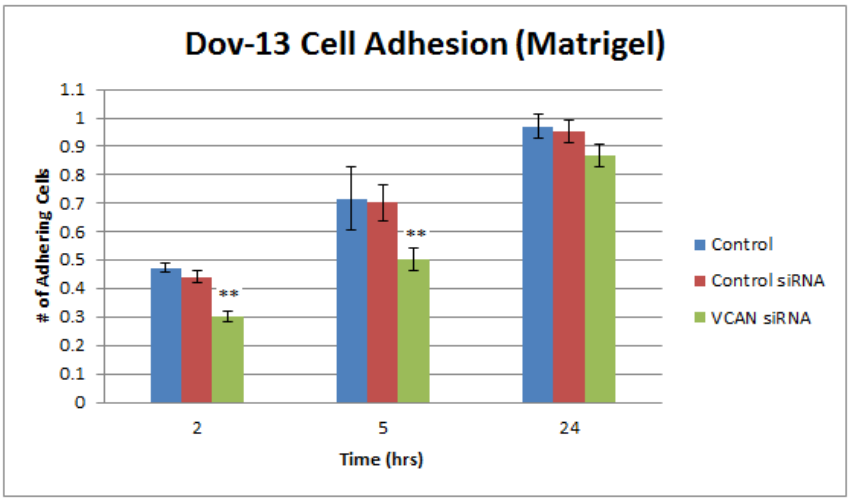

c)

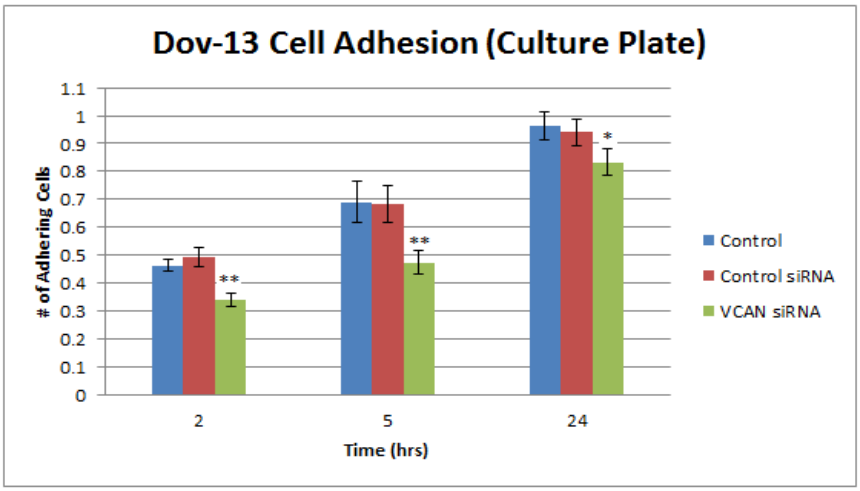

Figure 16. Single cell adhesion was tested on extracellular matrix components collagen type I (25µg/mL) and matrigel in addition to non-treated tissue culture plates. Similar adhesion was observed on all 3 coatings. Greatest difference in cell adhesion between the control and VCAN treated cells was at 5 hours.

*, $p < 0.05$
**, $p < 0.005$

a)

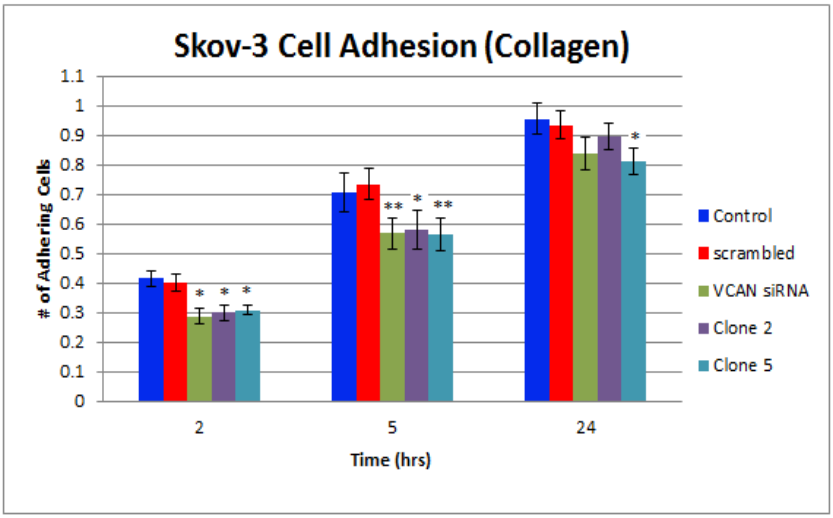

b)

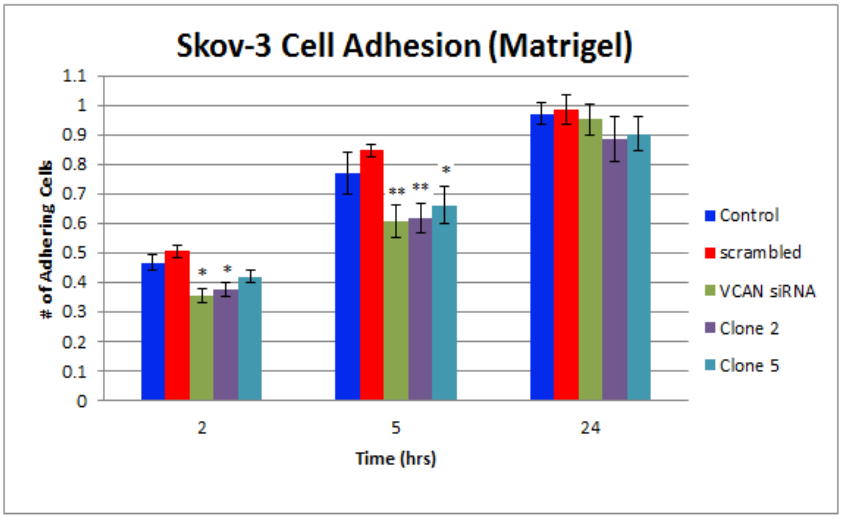

c)

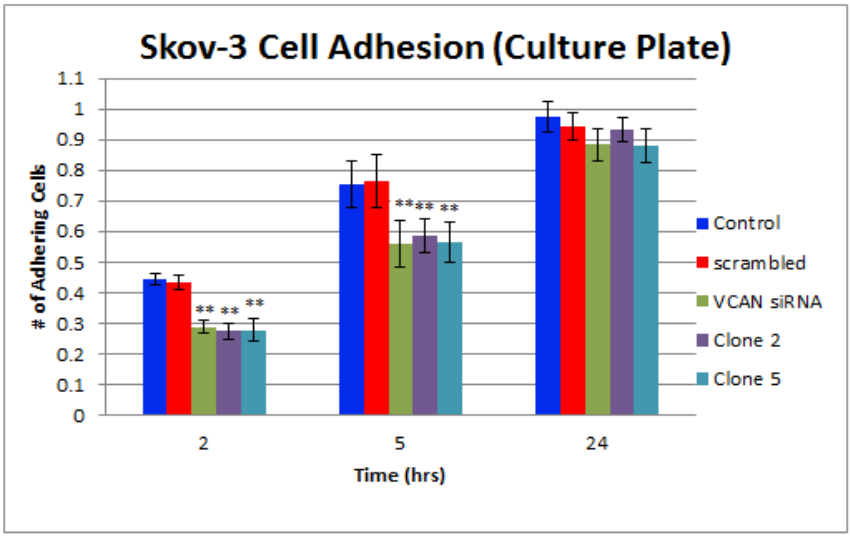

Figure 17. Roughly 15,000 Skov-3 cells were seeded onto untreated, collagen type I coated, and matrigel coated tissue culture plates. The decrease in adhesion from downregulation of versican at 5 hours on collagen, matrigel, and culture plate was 21% (a), 20% (b), and 25% (c) respectively.

*, $p < 0.05$
**, $p < 0.005$

a)

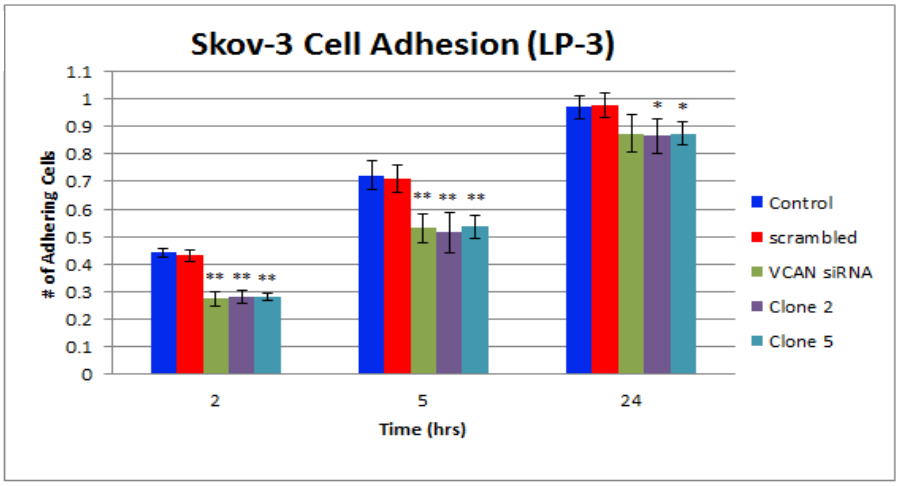

b)

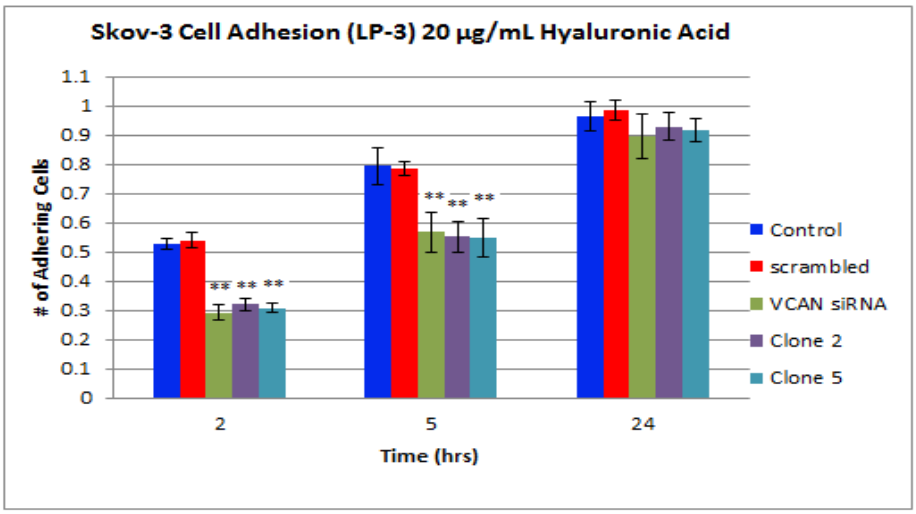

c)

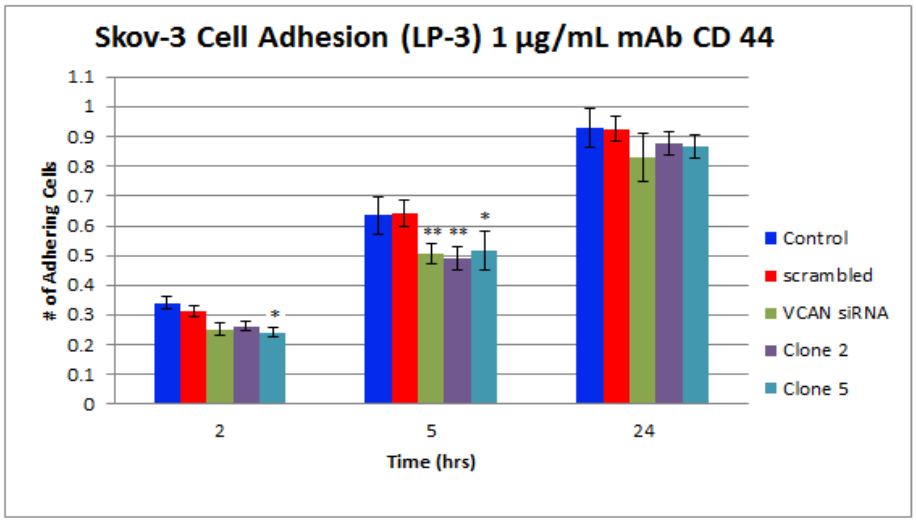

Figure 18. Single cell adhesion was assessed on the mesothelial cell monolayer, LP-3. For inhibition analysis a mAb against CD44 was added to the cell suspsension prior to addition to the LP-3 monolayer. (a) Transfected cells with VCAN siRNA or VCAN shRNA corresponded to a 29% decrease in the number of adhering cells when compared to the control. (b) Addition of hyaluronan saw an overall increase in cell adhesion in all groups. (c) Inhibition assays targeting CD44 with an mAb had a larger impact on non-transfected cells.

*, $p < 0.05$
**, $p < 0.005$

a)

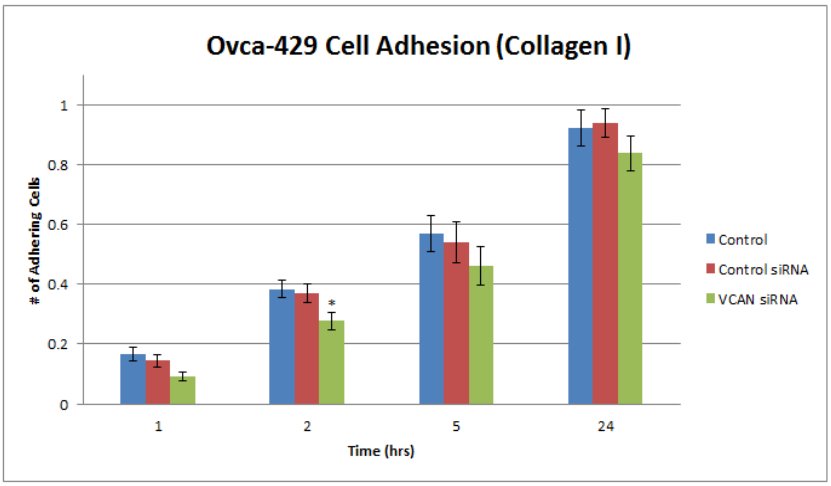

b)

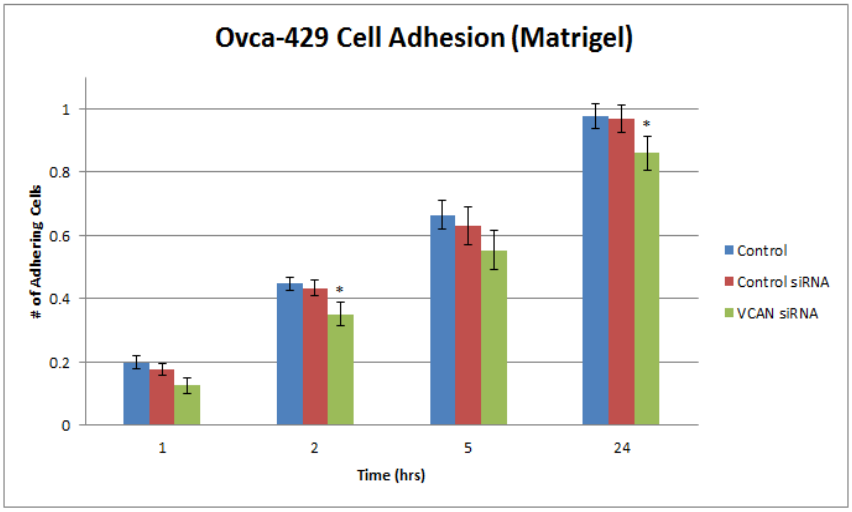

c)

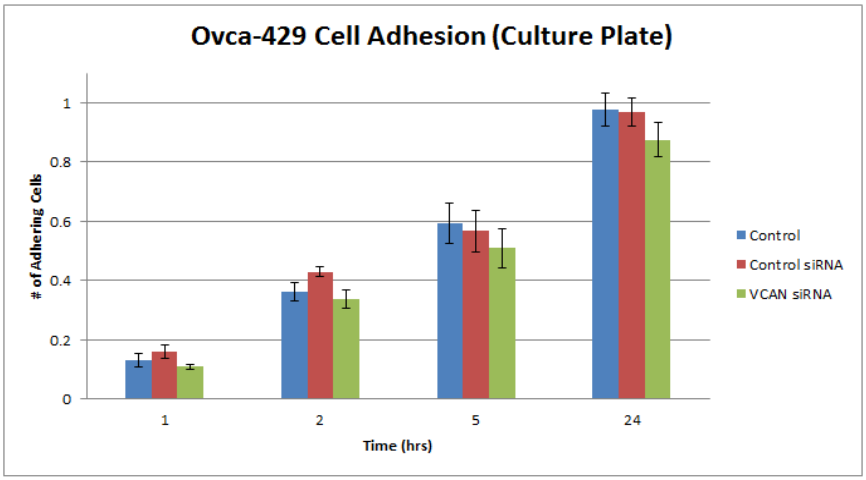

Figure 19. OVCA-429 cells express lower levels of versican than Dov-13 and Skov-3 cells, thus versican silencing had a marginal impact on adhesion on ECM components. On collagen type I the number of adherent transfected cells at 5 hours was reduced by 14% (a). On matrigel there were 17% more adherent cells at 5 hours when compared to cells with downregulated versican expression (b). There was roughly a 12% decrease in single cell adhesion of transfected cells on an untreated culture plate after 5 hours (c).

*, $p < 0.05$
**, $p < 0.005$

a)

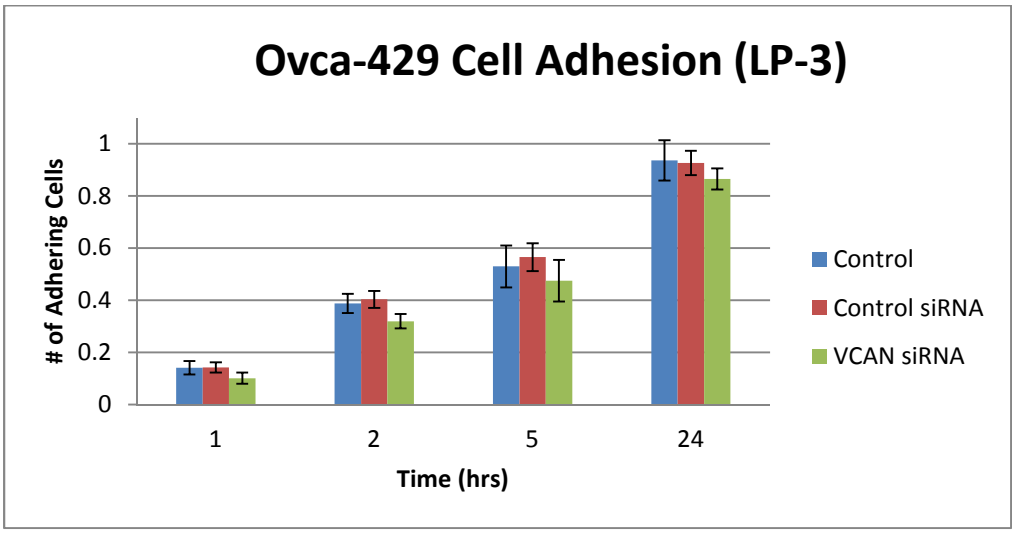

b)

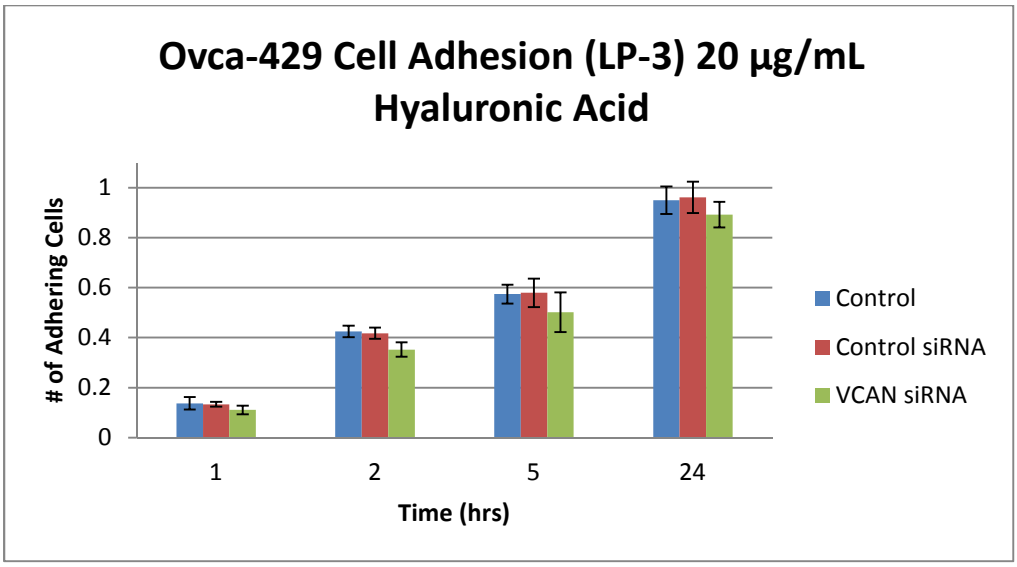

Figure 20. Single cell adhesion on the mesothelial monolayer LP-3 was allowed to proceed for 24 hours (a). We repeated this experiment with the addition of hyaluronan (b). Loss of versican expression resulted in 13% less cells adhering to the LP-3 monolayer. Addition of hyaluronan resulted in only a marginal increase in adhesion (b) in the 3 groups.

a)

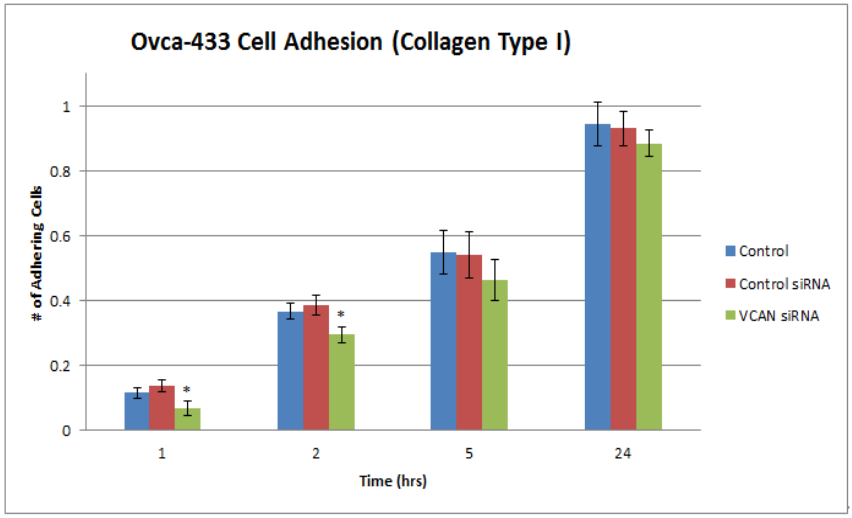

b)

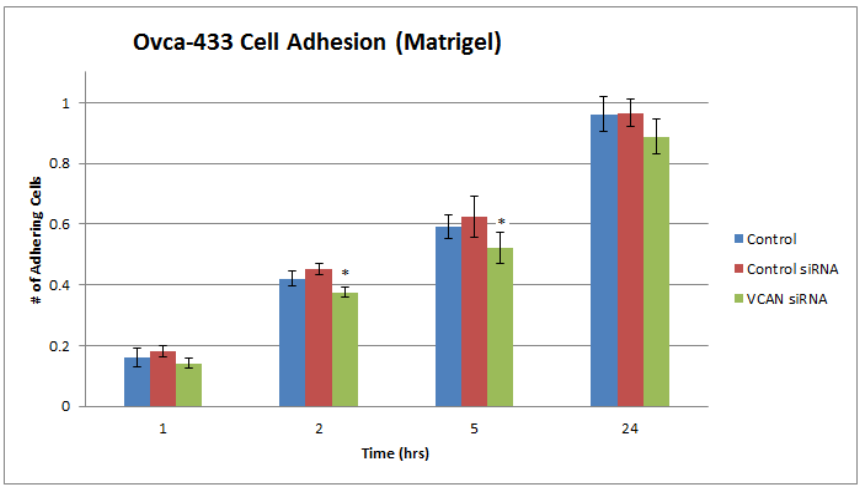

c)

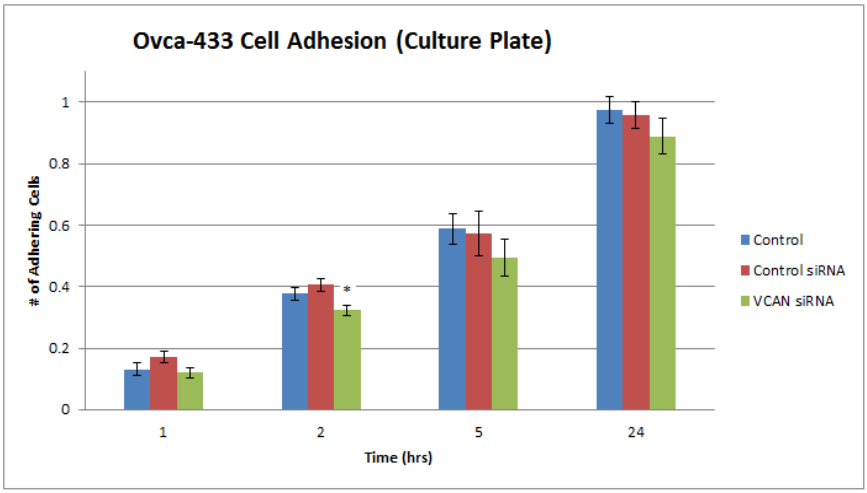

Figure 21. OVCA-433 similar to OVCA-429 cells express very low levels of versican. To assess the role of versican on single cell OVCA-433 adhesion on ECM components we seeded 15,000 cells and quantified the number of adherent cells at 1,2,5, and 24 hours. On all 3 surfaces the greatest difference in cell adhesion between control cells and transfected cells occurred at 2 and 5 hours (a-c).

*, $p < 0.05$
**, $p < 0.005$

a)

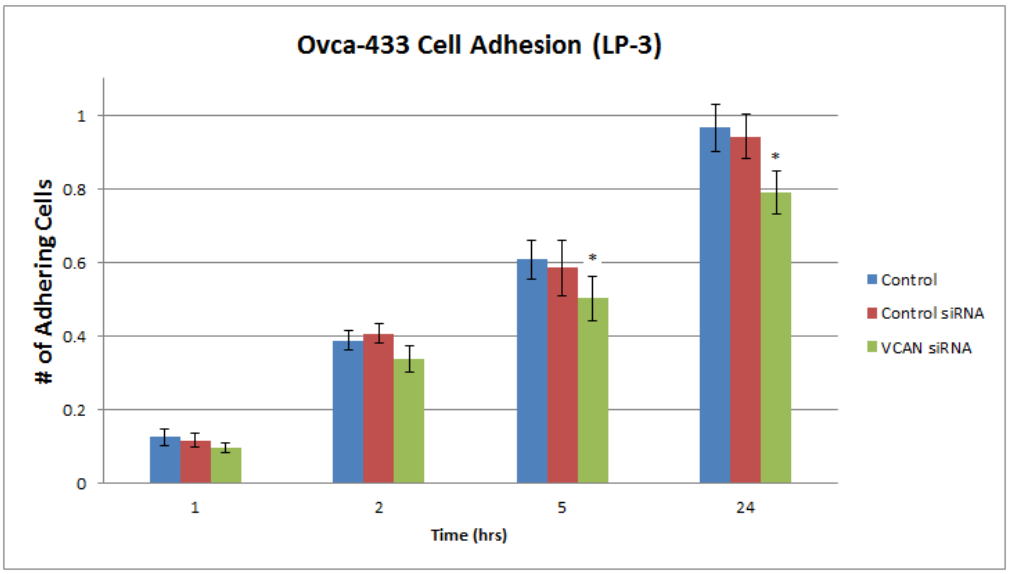

b)

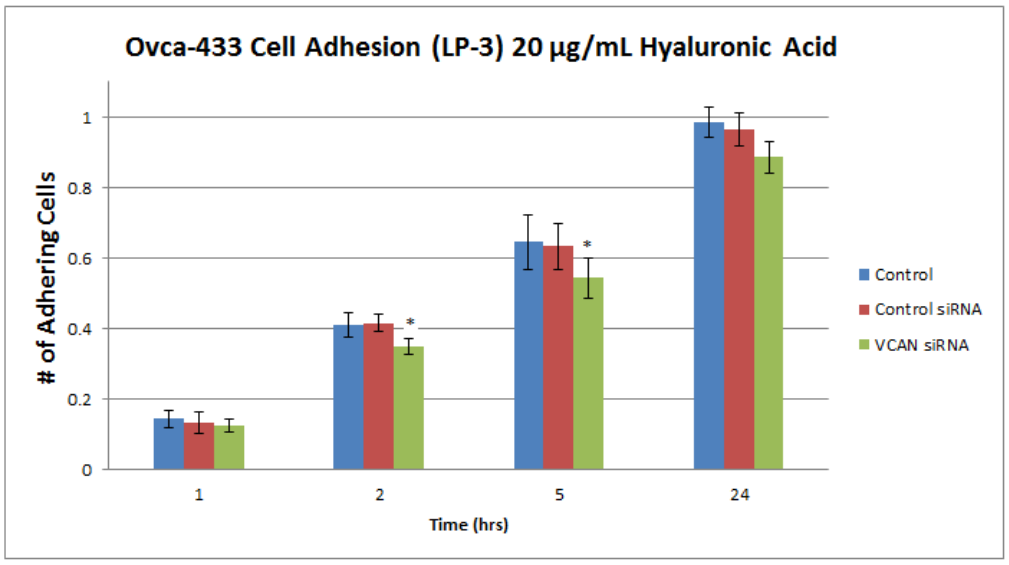

Figure 22. OVCA-433 single cell adhesion was further examined on a mesothelial monolayer made up of LP-3 cells. After being allowed to adhere for a period of 2 hours and 5 hours, cells with downregulated VCAN expression experienced a 14% and 16% decrease in adhesion respectively (a). With the addition of versican's binding partner, hyaluronan we found an increase in the number of adherent cells (b). In the control cells the addition of hyaluronan correlated to a 9% gain in the number of adherent cells after 5 hours. We observed in the transfected cells a 9% increase in the of adherent cells after a period of 5 hours.

3.3 Effect of Versican on Spheroid Size and Number

The lack of understanding on spheroid formation, and their potential contribution to widespread resistance to common antineoplastic agents led us to investigate the spheroid model. Altered extracellular matrix composition has been implicated in the formation of glioma cell spheroids.[145,146] Increased expression of integrins are believed to mediate attachment to the extracellular matrix, which may cause the initial aggregation of spheroid cells.[147-149] Of particular interest is the fact that beta-integrin has been shown to be a vital component in spheroid formation, and happens to be a binding partner of versican.[150,151] The binding of beta 1-integrin to versican demonstrated activation of focal adhesion kinase increasing the expression of integrins and promoting cellular adhesion. Thus, we decided to investigate what effects versican has on spheroid size and number.

Eight ovarian cancer cell lines were examined on their ability to form spheroids: Skov-3, Dov-13, OVCA-429, OVCA-433, A2780, OVCA-3, and OVCAR-5. Of these eight cell lines only Skov-3, Dov-13, OVCA-429, and OVCA-433 were observed to form spheroids. It should be noted the OVCAR-5 and OVCA-3 did demonstrate the ability to form loose spheroids, but took an extended formation time (3-8 days) and was unpredictable. The cell lines A2780 and IGROV-1 failed to undergo adequate compaction to form spheroids, and only formed loose aggregates. A2780 aggregates were easily broken apart upon gentle pipetting, but the IGROV-1 aggregates sustained mild agitation. However, the IGROV-1 aggregates never underwent the compaction that is associated with spheroids. Spheroid size (µm) and numbers were analyzed according to the protocol outlined in the methods section. The results are summarized in table 2 and Figure 23. Despite being a binding partner of beta 1-integrin, we found that downregulation of versican expression by siRNA did not affect the cells ability to form spheroids.

However, what we did find was that altered versican expression resulted in a decrease in spheroid size in the Skov-3, Dov-13, OVCA-429, and OVCA-433 treated cell lines. As can be seen in figure 23, the difference in sizes observed in the Skov-3 and Dov-13 cells was found to be statistically significant. The size change seen in the OVCA-429 and OVCA-433 on the other hand was not determined to be significant according to the student t-test. One explanation for this observation, may be that versican is only marginally expressed in these two cell lines as compared to Dov-13 and Skov-3 cells and consequently would be expected to have less of an effect. Downregulation of versican in Skov-3 cells corresponded to a 15% decrease in spheroids diameters, and was statistically significant with a P-value <0.05. Treating Dov-13 cells prior to spheroid formation with VCAN siRNA resulted in a diameter that was 10% smaller. Although there was an observable decrease in the diameter of the OVCA-429 and OVCA-433 spheroids, the difference was determined to not be statistically significant. The effects of versican on Skov-3 spheroids can be seen in Figure 24.

While monitoring the effect versican has on spheroid size, we noticed that versican silencing seemed to decrease the total number of spheroids formed in culture. Thus, we decided to verify this observation by culturing the spheroids in a P60 dish divided into a grid as outlined in the methods section. We found that versican downregulation did in fact have a negative effect on the total number of spheroids formed. This was not an unexpected result based on our previous results that versican effects size, and that versican is a binding partner of beta 1-integrin.[150] Treatment of Skov-3 cells with VCAN siRNA and VCAN shRNA correlated to a 10-15% decrease in the total number of spheroids formed. We observed that treatment of DOV13, OVCA-429, and OVCA-433 cells with VCAN siRNA were found to decrease spheroid formation by 20%, 12%, and 10% respectively.

a)

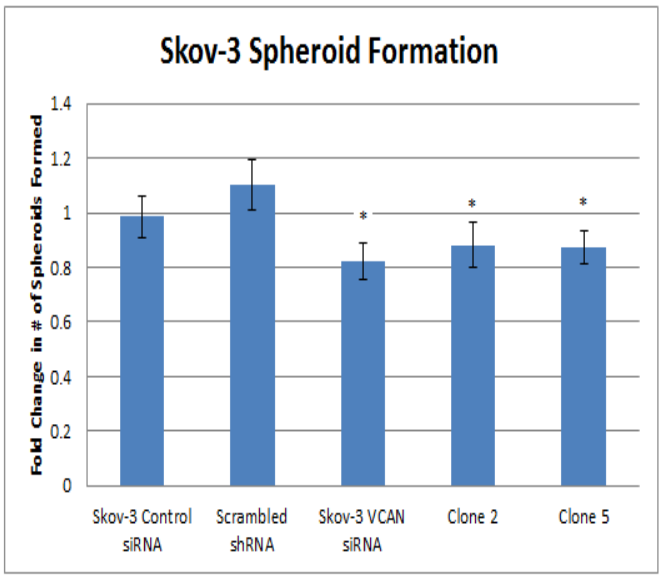

b)

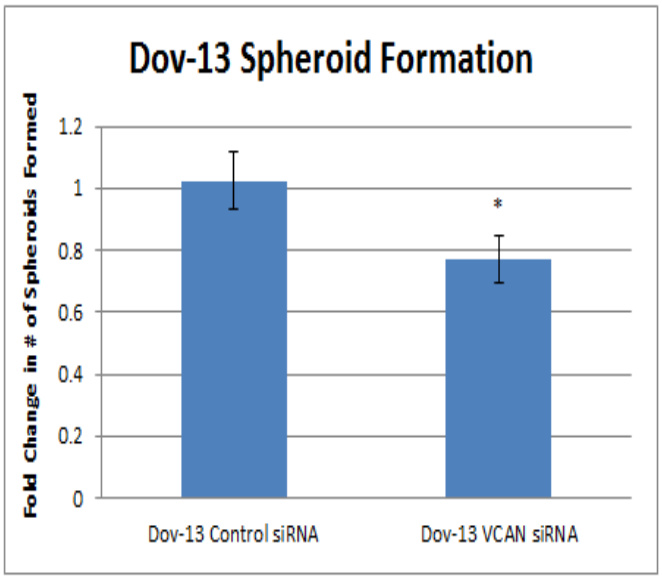

c)

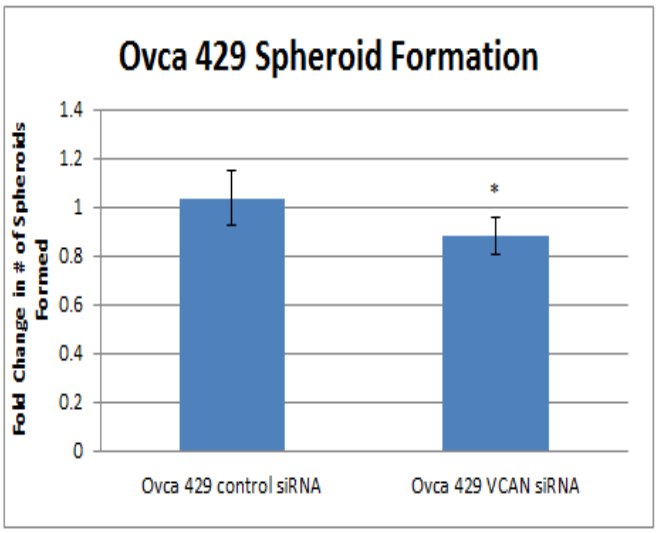

d)

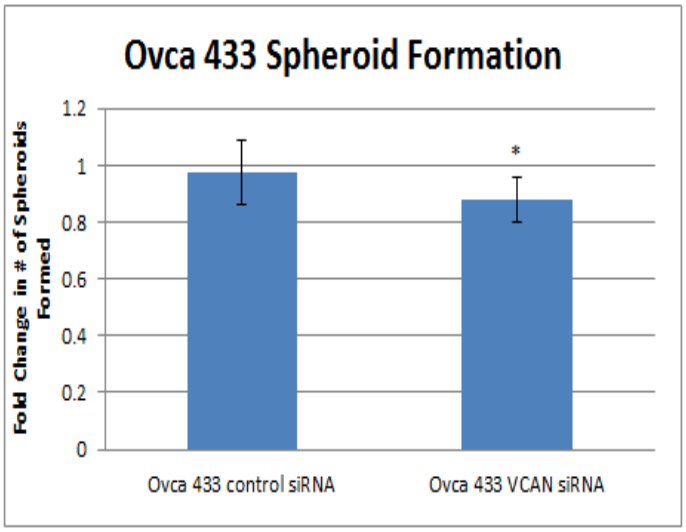

Figure 23. Effect of versican on the formation of spheroids was investigated. We observed that downregulation of versican corresponded to a decrease in the average number of spheroids formed. The data is represented as fold change in the number of spheroids formed, which is calculated by manually counting the number of spheroids and comparing it to the average number of spheroids formed in the control group. (a) Loss of versican in Skov-3 spheroids corresponded to a 12-17% decrease in the number of spheroids. (b) Treatment of cells with VCAN siRNA caused 20% fewer DOV-13 spheroids as compared to control spheroids. (c) There were 12% fewer OVCA-429 spheroids for cells treated VCAN siRNA. (d) OVCA-433 spheroids with downregulated versican

a) Skov-3 Control Spheroids

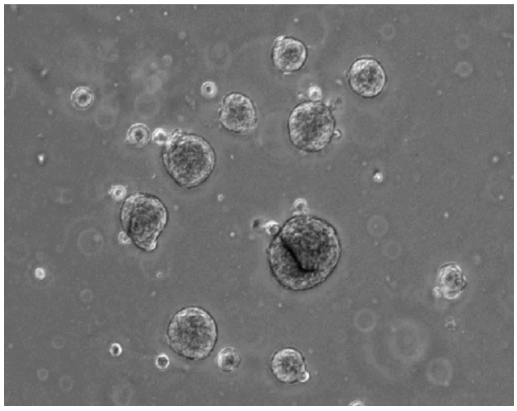

b) Skov-3 scrambled shRNA Spheroids

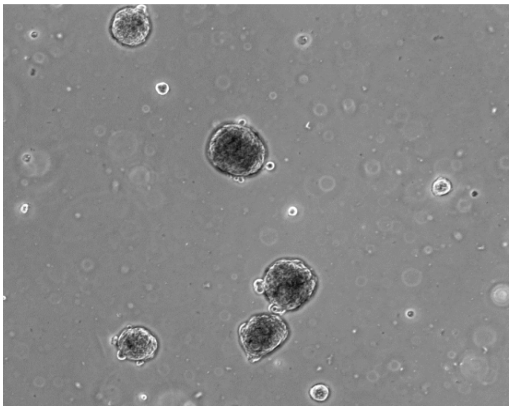

c) Skov-3 VCAN siRNA spheroids

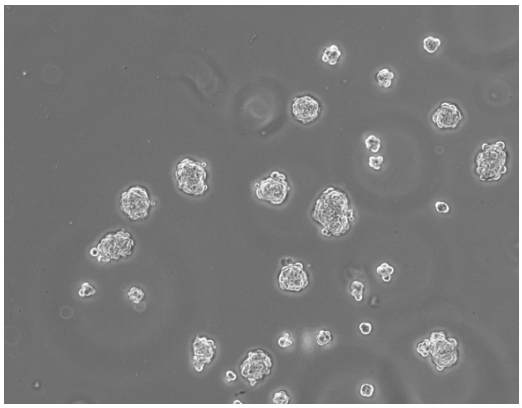

d) Skov-3 VCAN shRNA Clone 2 spheroids

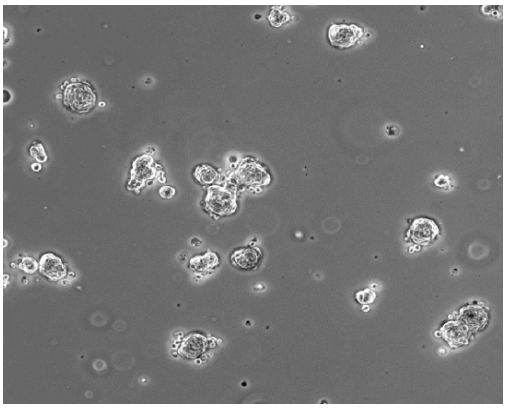

Figure 24. Formation of spheroids was accomplished by transferring 250,000 cells to a 6-well culture platecoated with agarose. After 48-72 hours the spheroids were digitally photographed (a-d). As can be seen in images (c) and (d) the spheroids with downregulated versican expression were noticeably smaller in diameter, and do not appear to undergo the same degree of compaction as spheroids expressing versican (a-b).

Spheroid Size		
Cell Line	**Diamter (µm)**	**Student T-test**
Skov-3	110.5 ± 15.8	
Skov-3 Ctrl siRNA	106.9 ± 14.6	
Skov-3 Scrambled shRNA	113.1 ± 16.4	
Skov-3 VCAN siRNA	86.1 ± 10.9	P < 0.01
Skov-3 Clone 2	95.2 ± 12.7	P < 0.01
Skov-3 Clone 5	93.8 ± 13.8	P < 0.01
Skov-3 Clone 6	88.1 ± 11.1	P < 0.01
Dov-13 Control	97.9 ± 10.8	
Dov-13 Control siRNA	96.2 ± 10.1	
Dov-13 VCAN siRNA	85.0 ± 9.2	P < 0.05
Ovca 429 control	91.5 ± 11.8	
Ovca 429 control siRNA	96.7 ± 14.5	
Ovca 429 VCAN siRNA	87.6 ± 12.4	P > 0.05
Ovca 433 control	93.6 ± 13.6	
Ovca 433 control siRNA	87.9 ± 12.7	
Ovca 433 VCAN siRNA	83.5 ± 15.4	P > 0.05

Table 2. Spheroids were allowed to form for a duration of 48-72 hours using the agarose overlay technique. The 6-well plates were divided into grids and the spheroids were counted under a light microscope. Spheroids smaller than 30µm or larger than 275µm were not used for statistical analysis. The loss of versican expression in Skov-3 spheroids corresponded to a 16-21% decrease in diameter size, while the altered versican expression in Dov-13 spheroids caused roughly a 12% smaller spheroid diameter. Changes in OVCA-429 and OVCA-433 spheroid diameter size were calculated not be of statistical significance according to the student t-test.

3.4 Role of Versican in Spheroid Adhesion and Disaggregation

For years, researchers thought spheroids represented a population of cells that were non-adherent and thus had no significance in ovarian carcinoma.[152-157] However, this proved to be untrue as Burleson and et al showed that spheroids adhere and disaggregate readily on extracellular matrix components.[158] Now spheroid adhesion and disaggregation represent an important understudied model in ovarian carcinoma dissemination.

In order to effectively spread, spheroids must be able to adhere to the mesothelial cell layer lining the peritoneal cavity. The integrin receptor family, which was shown previously to be vital in formation of spheroids, appears to be similarly important in mediating adhesion to the mesothelial cells as mAbs against those integrins decrease adhesion dramatically.[151] Having observed the effects of versican on adhesion in single cells and spheroid formation, we investigated whether altered versican expression may modulate spheroid adhesion to extracellular matrix components and ultimately to mesothelial cells.

To assess spheroid adhesion we cultured Skov-3, Dov-13, OVCA-429, and OVCA-433 spheroids for 48-72 hours and then transferred 50-75 isolated spheroids to P60 plates coated in either collagen (25µg/mL), matrigel (1:100), or left untreated. For quantification of adhesion, the spheroids were allowed to adhere to the plates for 1, 2, 5, and 24 hours. Non-adherent spheroids were removed by gently rinsing with PBS. Spheroids were manually counted at one hour to establish the number of seeded spheroids and then were counted under a light microscope following the PBS rinse. The data is represented Figures (25-32) as percent adhesion, and calculated as outlined in the methods section**.** Overall, we saw a decrease in spheroid adhesion when we downregulated the expression of versican. Adhesion to collagen type I and to the untreated tissue culture plate was nearly identical for the spheroids tested. As in the single cell

adhesion assays we observed the largest effect on adhesion at the 5 hour time point. The various VCAN shRNA clones exhibited insignificant differences in adhesion, which we hypothesized may be a consequence of differences in degrees of versican downregulation. At 5 hours we saw roughly a 25% decrease in spheroid adhesion to the 3 tissue culture coatings (collagen, matrigel, and no treatment) in the Skov-3 spheroids treated with VCAN siRNA as compared to the Skov-3 control spheroids. For the Dov-13 spheroids there was a 20-30% decrease in adhesion at 5 hours for the VCAN siRNA treated cells. There was a 12-20% decrease in adhesion after 5 hours of seeding for the OVCA-429 on the 3 different plate coatings, with the lowest decrease on matrigel. Results for VCAN siRNA OVCA-433 were similar to VCAN siRNA OVCA-429, with a 10-24% decrease in adhesion at 5 hours as compared to the control group.

The peritoneal cavity represents a significantly different environment than the testing done on extracellular matrix components. The mesothelial cells secrete a variety of factors, in addition to expressing a number of cell surface receptors that can regulate adhesion and migration. Thus we proceeded to examine spheroid adhesion on the mesothelial cells LP-3. Prior to culturing spheroids, we incubated the cells with Vybrant DiO, so the spheroids would be easily discernible under a fluorescent microscope. At 5 hours there was an overall decrease in spheroid adhesion of 21%, 17%, 27%, and 20% for the VCAN siRNA OVCA-429, OVCA-433, Skov-3, and Dov-13 cells respectively. To more accurately simulate the environment encountered in vivo, we added hyaluronan to the LP-3 monolayer that would have been removed by the PBS rinse. We observed that the hyaluronan slightly increased adhesion for all cell lines and groups. The increases in adhesion were 3%, 6%, 4%, and 5% for OVCA-429, OVCA-433, Skov-3, and Dov-13 control groups respectively. In the siRNA treated OVCA-429, OVCA-433, Skov-3, and Dov-13 spheroids we saw increases in adhesion of 2%, 5%, 1-2%, and 0.5-1%.

Initially we used 20 µg/mL of hyaluronan and then repeated the assay using 40 µg/mL to assess whether there would be an additional increase in adhesion with a higher concentration. We found that the higher hyaluronan content resulted in decreased adhesion because it was acidic enough that over the duration of the experiment it actually caused cell death.

For inhibition assays, we used a monoclonal antibody against CD44 to help determine mechanisms responsible for spheroid adhesion in the Dov-13 and Skov-3 cell lines. We expected a greater inhibition of adhesion upon administration of CD44 antibody, but only noticed a marginal decrease of 1-4% in both cells lines in the VCAN siRNA treated cells as well as the control cells.

One study has shown that blocking disaggregation of spheroids inhibits the spread of tumor sites in the peritoneal cavity.[149] It has been previously observed by other labs, that cells compact tightly into spheroids actually have an enhanced ability to dissociate.[36] A proposed explanation for this phenomenon is that aggregation and dissociation rely on similar active processes, so cells that can aggregate tightly have the ability to dissociate extensively.[36] This hypothesis coincides with our observations that versican expressing cells appear to form a more compact spheroid, which led us to explore how spheroid disaggregation is altered when versican expression is downregulated.

For quantification of spheroid disaggregation, we isolated the spheroids after culturing and transferred roughly 25 spheroids to each well of the six well plates and allowed them to adhere for 24 hours. The spheroids were allowed to adhere for 1 hour before being digitally photographed, and the area of the spheroid was calculated by the Axiovision software after the spheroids were outlined. Then after the 24 hour period, the area occupied by the spheroid and its dispersed cells were outlined and calculated by the microscope's software. Our results are

summarized in figures 33-35, and the change in disaggregation is represented as fold change in area, which was derived by taking the area at 1 hour divided by the area at 24 hours. Across the cell lines the degree of disaggregation varied on the ECM components, for instance Dov-13 spheroids and Skov-3 spheroids exhibited the highest degree of dissociation on matrigel coated plates while OVCA-429 and OVCA-433 spheroids dissociated more readily on collage (type I) coated plates. As expected from our single cell adhesion assays, we found that VCAN siRNA treated spheroids exhibited lower disaggregation especially the siRNA treated Skov-3 spheroids. The Skov-3 control spheroids increased their area 8.5 fold on matrigel as compared to the VCAN altered spheroids, whose area only increased roughly 6.1 fold. When compared to the control Skov-3 spheroids the treated spheroids displayed a 30% decrease in overall area on matrigel after the 24 hour duration. It should be noted, that the vast majority of untreated spheroids fully disaggregated, while larger spheroids that were comprised of VCAN siRNA treated cells did not fully dissociate over the 24 hour period. OVCA-429 and OVCA-433 disaggregated considerably less than the spheroids of the other cell lines, which can skew the statistics as a result of a small increase or decrease in total area can have a much larger effect on the fold change in area. Another observation that came out of this study was that spheroid size did not seem to affect the spheroid's ability to disaggregate. OVCA-429 spheroids whose diameter is only 80% of Skov-3 spheroids were only able to disaggregate to an area equal to 30% of that observed in the more compact Skov-3 spheroids.

Disaggregation on the mesothelial monolayer LP-3, is more complex then dissociation on the ECM components in the sense that now that spheroids must be more invasive in order to break down multiple ECM components and invade the LP-3 cells in order to successfully colonize the site. As a result of this more hostile environment, spheroids were much less

successful in fully disaggregating on the LP-3 monolayer as compared to the ECM components. The addition of hyaluronan to the LP-3 monolayer failed to dramatically increase adhesion in all of the cell lines. Based upon previous literature we had expected the addition of hyaluronan to have a more profound effect on spheroid adhesion. The loss of versican in Skov-3 spheroid caused a 39% reduction in occupied area, with some variability between clones. Dov-13 spheroids expressing versican saw a 23% decrease in area compared to those with silenced versican expression. For OVCA-429 and OVCA-433 spheroids the reduced adhesiveness correlated with the downregulation of versican expression was calculated to be 10-15%. The addition of hyaluronan to the LP-3 monolayer corresponded to an increase in spheroid adhesion, but this effect was significantly smaller in spheroids with reduced versican levels. For inhibition assays, we incubated Dov-13 and Skov-3 spheroids briefly for 30 minutes with a monoclonal antibody against CD44 prior to being added to the LP-3 monolayer. We received variable results, with the mAb causing increased adhesion in the Dov-13 cell line and decreased adhesion in the Skov-3 cell line. Increased concentration of the CD44 antibody appeared to have no increased effect not seen at the lower concentration of mAb. Digital images were taken of the spheroids at time 0 hours and at 24 hours, and Figures 36-38 represent Skov-3 spheroid disaggregation.

a)

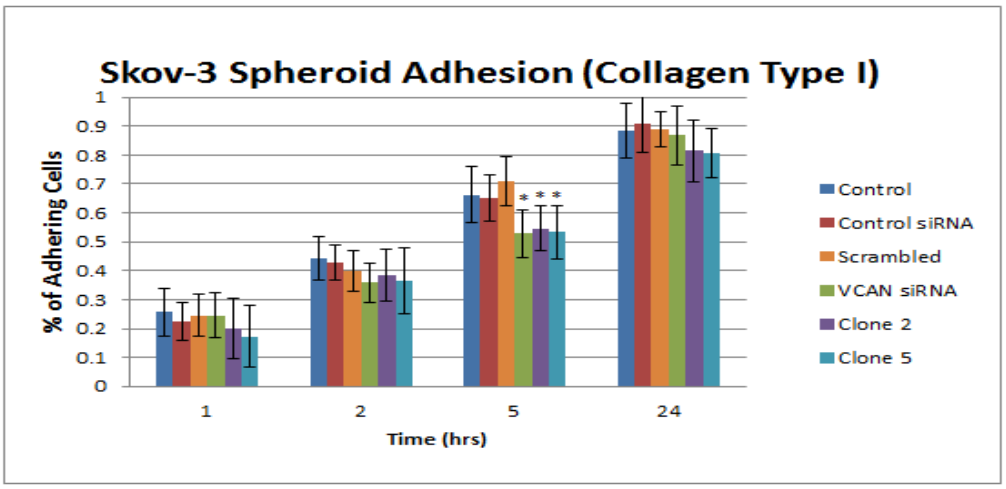

b)

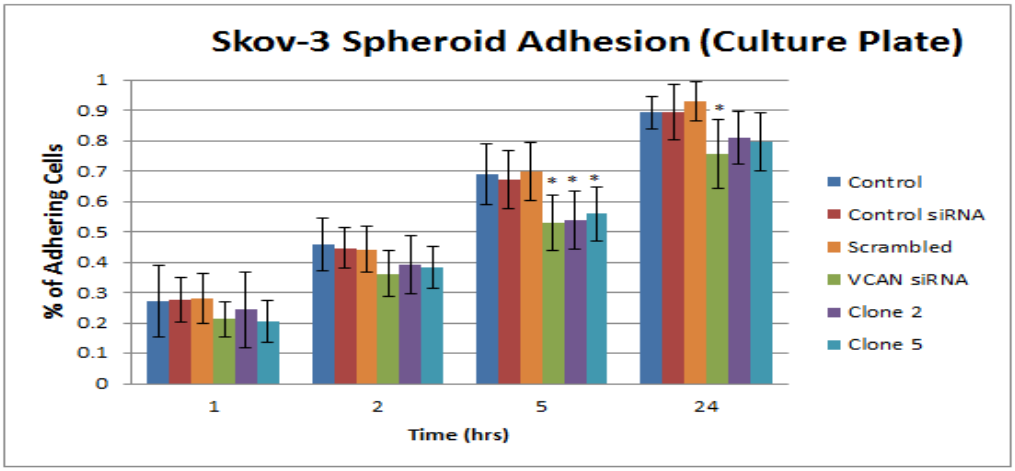

c)

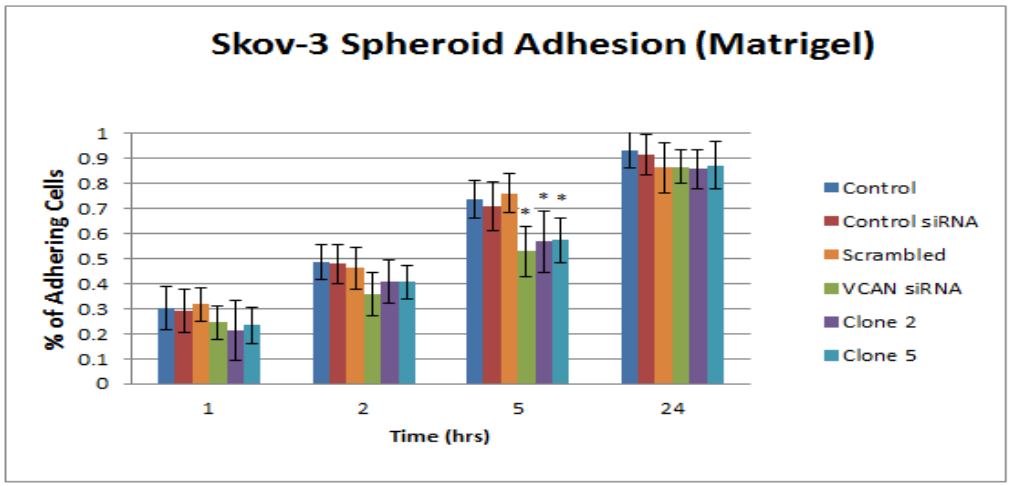

Figure 25. 35-70 isolated spheroids were allowed to adhere to a culture plate, collagen type I, and matrigel. Adhesion was assessed at 1, 2, 5, and 24 hours by manual counting under a light microscope. Non-adherent spheroids were removed by a PBS risne. The data is represented as % of adhering spheroids, which was calculated by dividing the number of adhering spheroids at 24 hours by the total number of starting spheroids. At 5 hours there was roughly a 30% decrease in the number of adherent spheroids on matrigel when versican expression was silenced. On collagen there was a 21% decrease in the number of adherent spheroids when VCAN expression was silenced.

a

*, $p < 0.01$
**, $p < 0.005$

a)

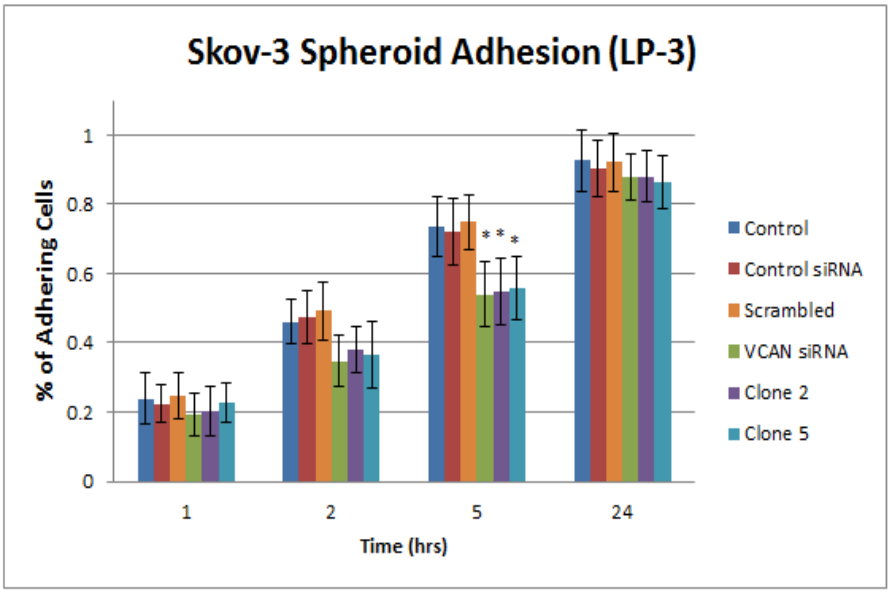

b)

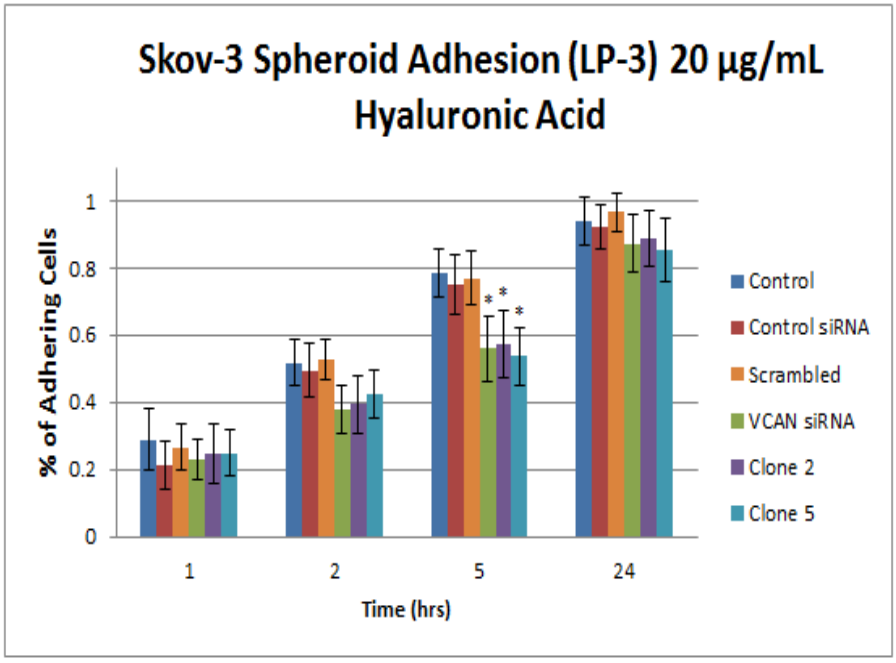

Figure 26. Skov-3 spheroids ability to adhere to a LP-3 monolayer was assessed, and then repeated in the presence of hyaluronic acid and a CD44 mAb. (a) VCAN siRNA and VCAN shRNA transfected spheroids had roughly 26% fewer adherent spheroids after 5 hours as compared to control cells. (b) Supplementation of the media with hyaluronic acid resulted in only a marginal increase in spheroid adhesion.

*, $p < 0.01$
**, $p < 0.005$

a)

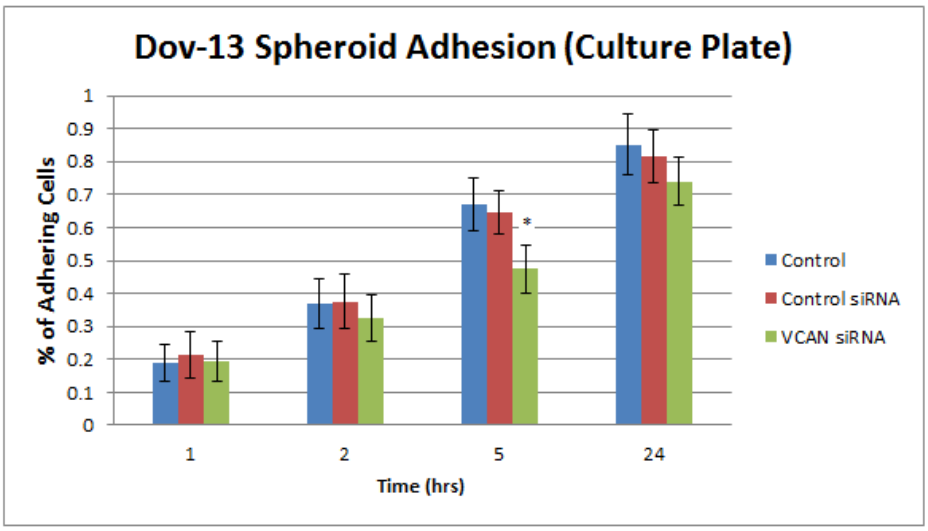

b)

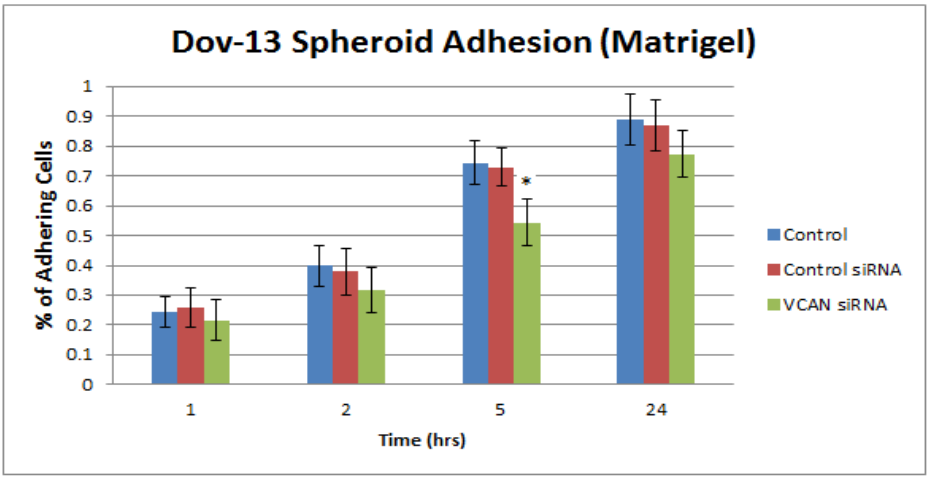

c)

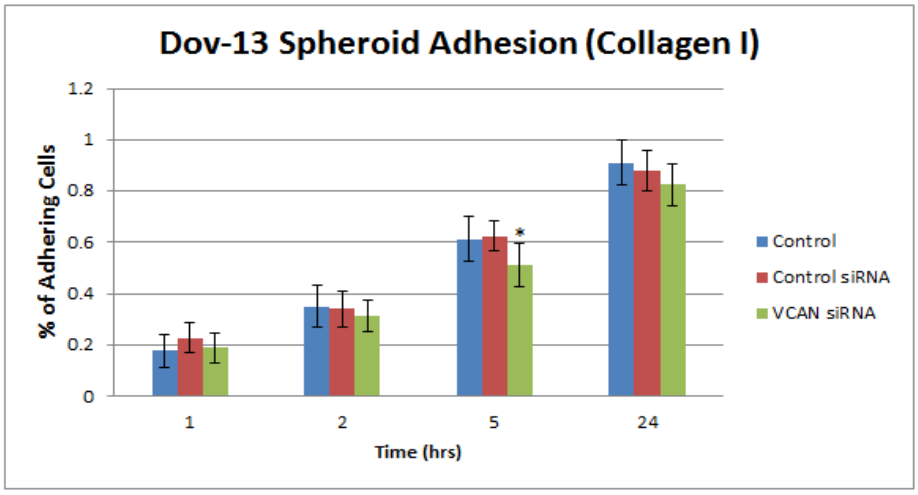

Figure 27. Examination of the role of versican on spheroid adhesion on the 3 surfaces revealed that loss of versican negatively affected adhesion. (a) There were 26% fewer adherent Dov-13 VCAN siRNA after 5 hours when compared to the control groups. (b) On matrgiel there were 25% more adherent spheroids after 5 hours in the control cells then in the treatment group. (c) The number of adhering spheroids on collagen following 5 hours was 16% less in the VCAN siRNA spheroids.

*, $p < 0.01$
**, $p < 0.005$

a)

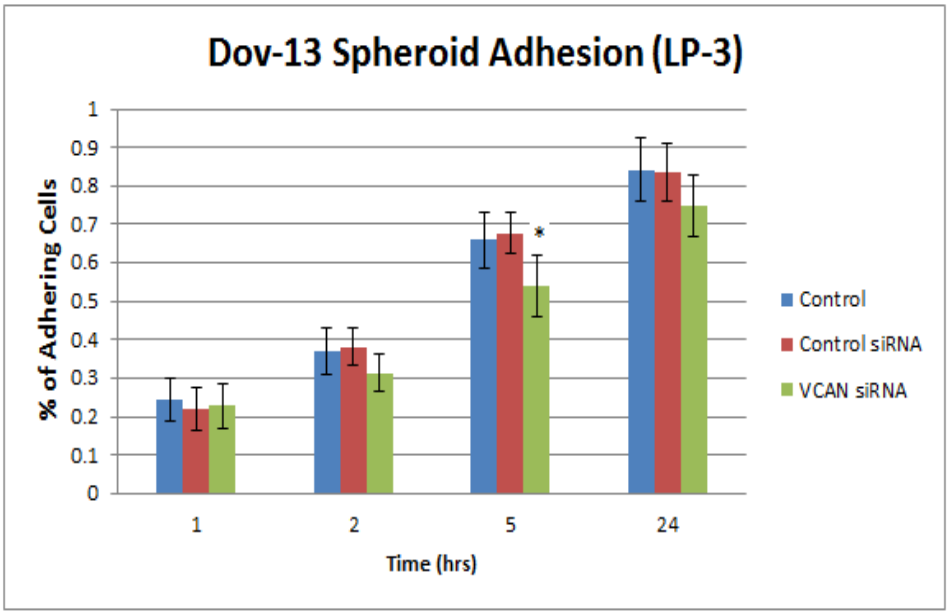

b)

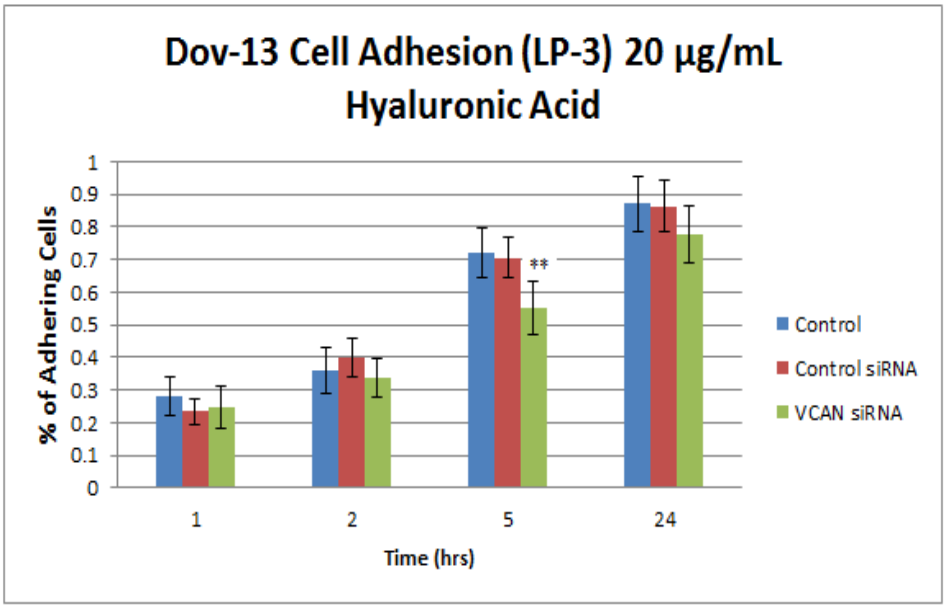

Figure 28. Dov-13 spheroid adhesion was observed on the mesothelial cell line LP-3. (a) Decrease in spheroid adhesion on LP-3 from loss of versican was determined to be 19%. (b) Adhesion remained essentially unchanged with modest increases of 2-4%.

*, $p < 0.01$
**, $p < 0.005$

a)

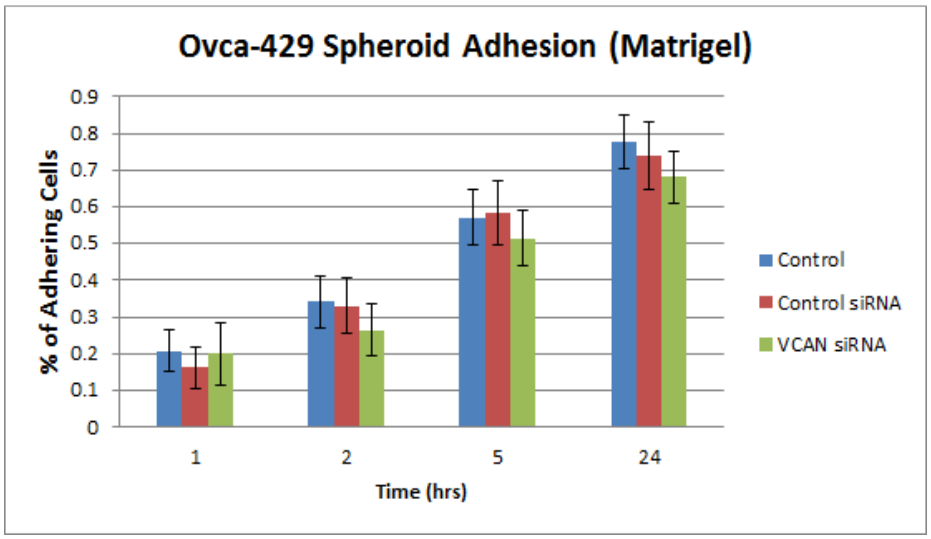

b)

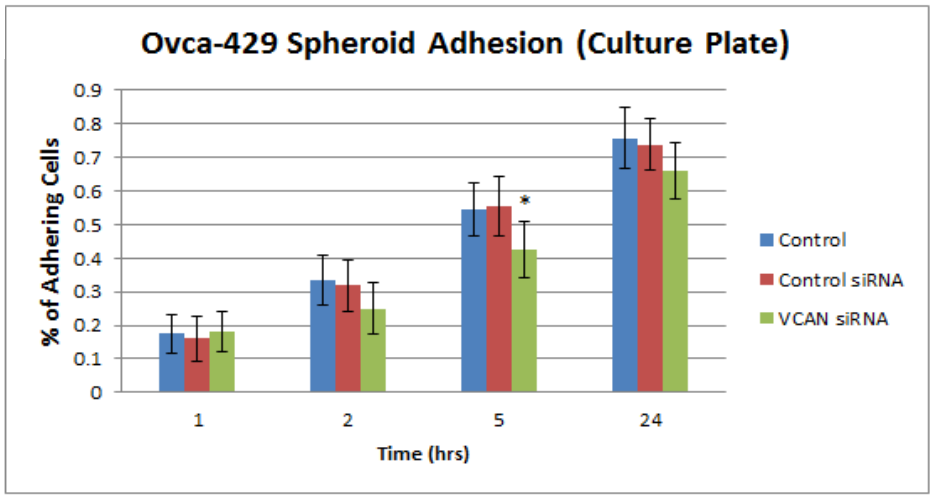

c)

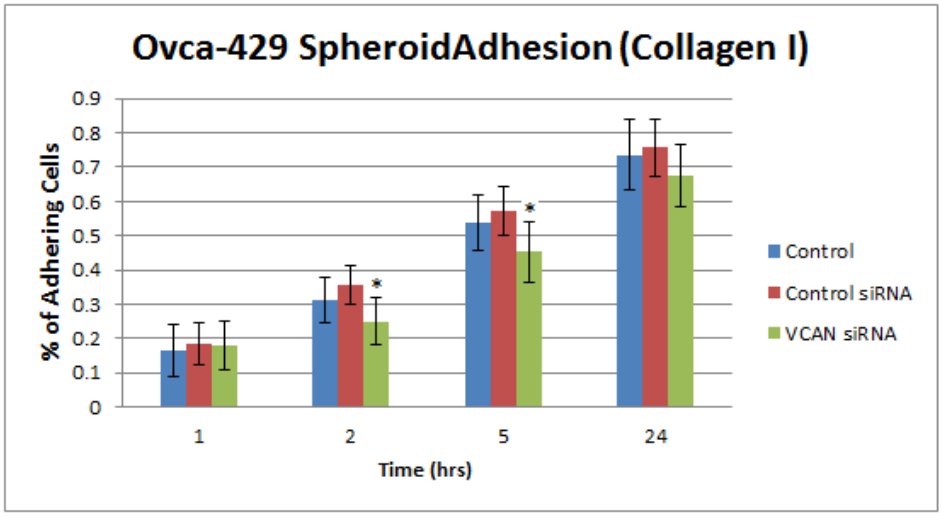

Figure 29. OVCA-429 spheroids displayed lower adhesion than Dov-13 and Skov-3 spheroids. The difference in adhesion after 5 hours between control spheroids and VCAN siRNA spheroids on matrigel, culture plate, and collagen were 11%, 23%, and 17% respectively.

*, $p < 0.05$

a)

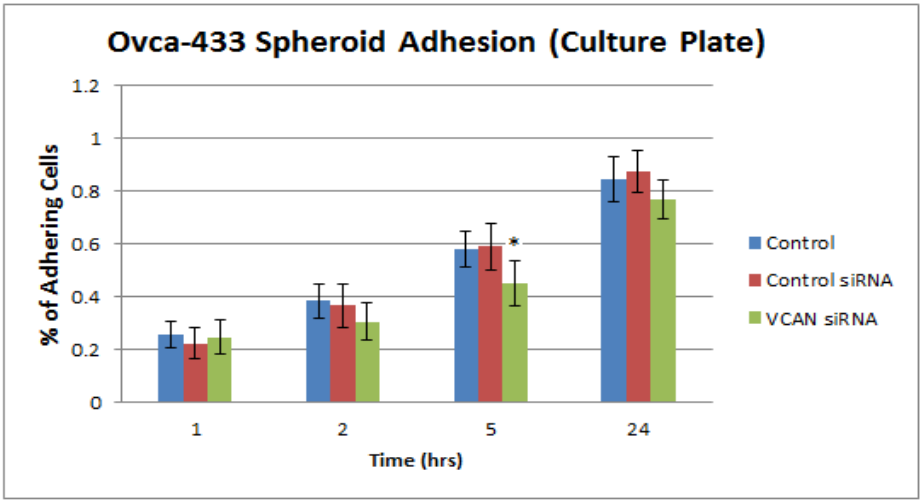

b)

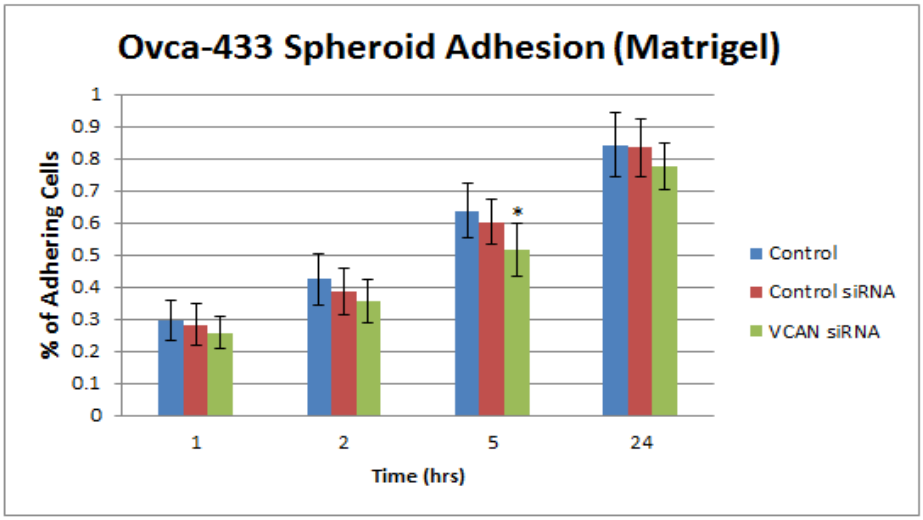

c)

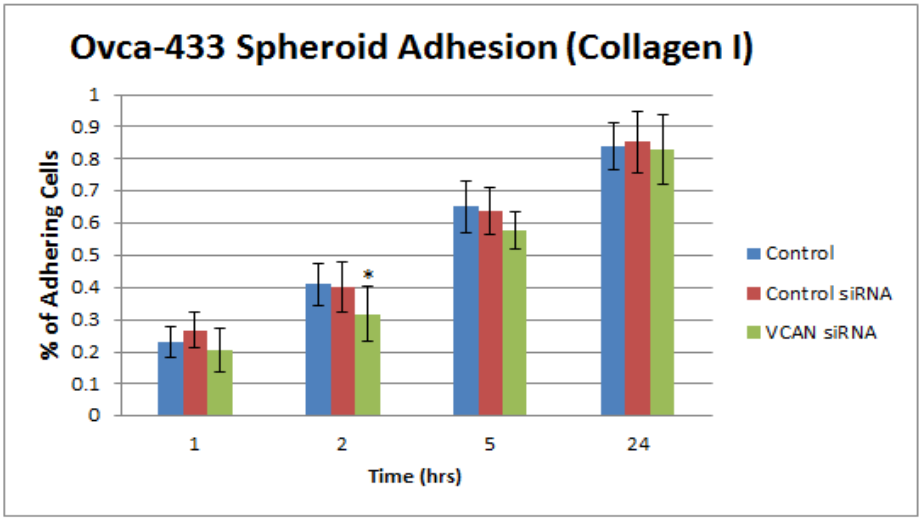

Figure 30. Investigation of OVCA-433 spheroid adhesion revealed that versican albeit expressed in low amounts directly affects adhesion. Rates of adhesion on the 3 surfaces of the OVCA-433 spheroids were similar to those observed previously for OVCA-429 aggregates. Treatment of cells with VCAN siRNA resulted in 24%, 15%, and 10% decreases in adhesions on culture plate, matrigel, and collagen type I respectively.

*, $p < 0.05$

a)

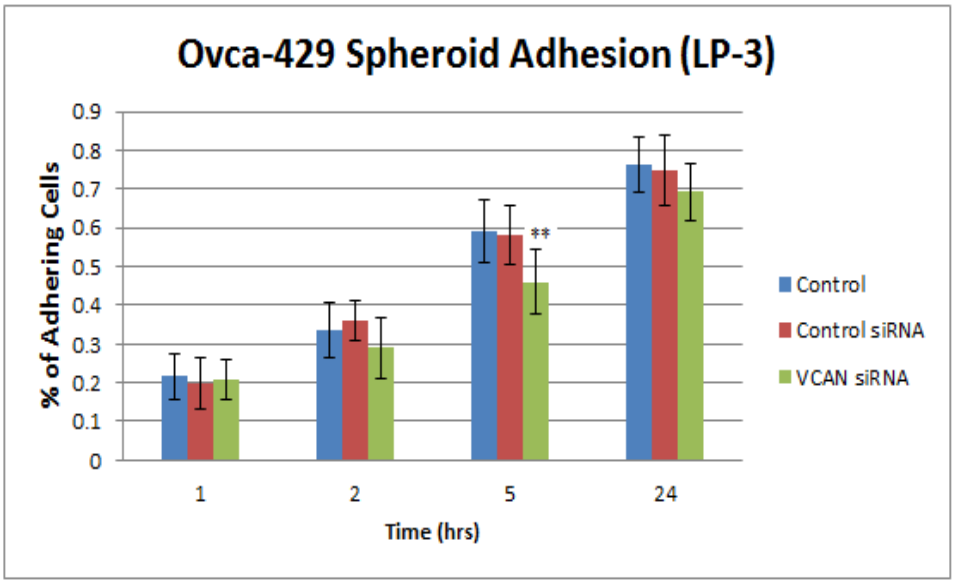

b)

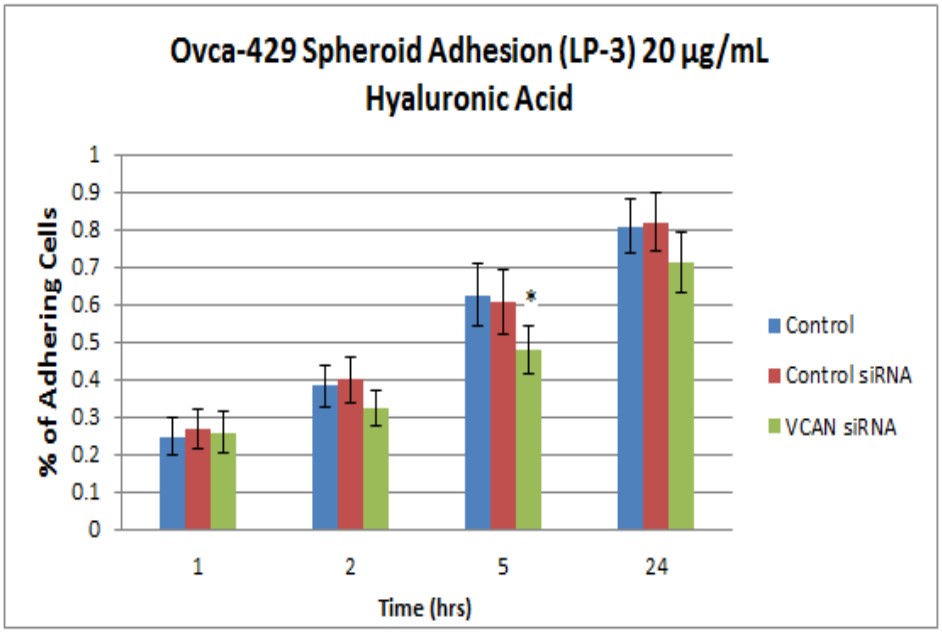

Figure 31. Versican's role in mediating OVCA-429 spheroid adhesion on a LP-3 monolayer was assessed by fluorescently labeling the cells prior to spheroid formation. The fluorescence allowed us to quicker count the spheroids and differentiate easily between the two types of cells. (a) On the LP-3 monolayer we found that the loss of versican was the main driving force in a 23% reduction in the number of adherent spheroids after 5 hours. (b) The effect of adding hyaluronan to the mesothelial cells had a muted effect on adhesion as represented in (b).

*, $p < 0.05$
**, $p < 0.01$

a)

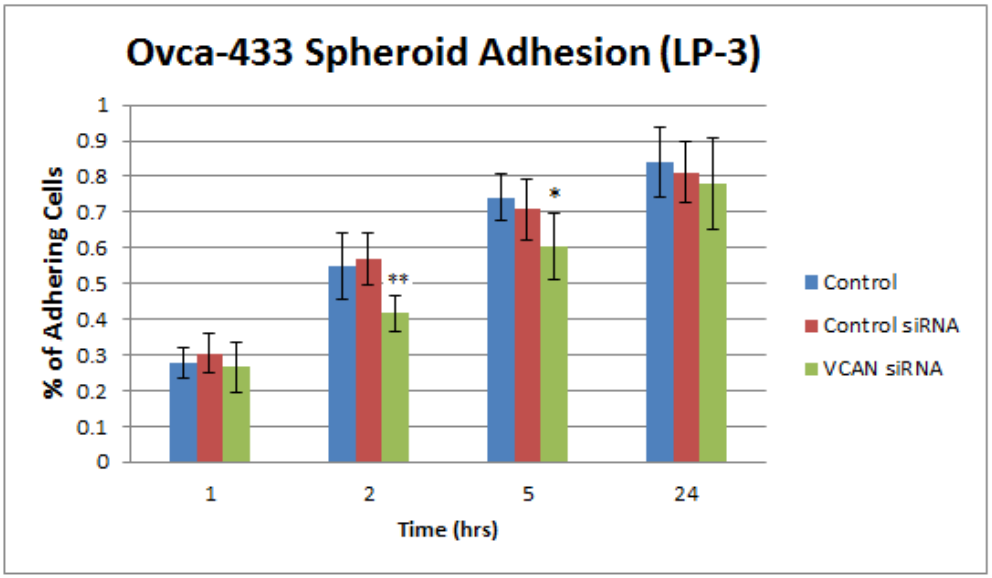

b)

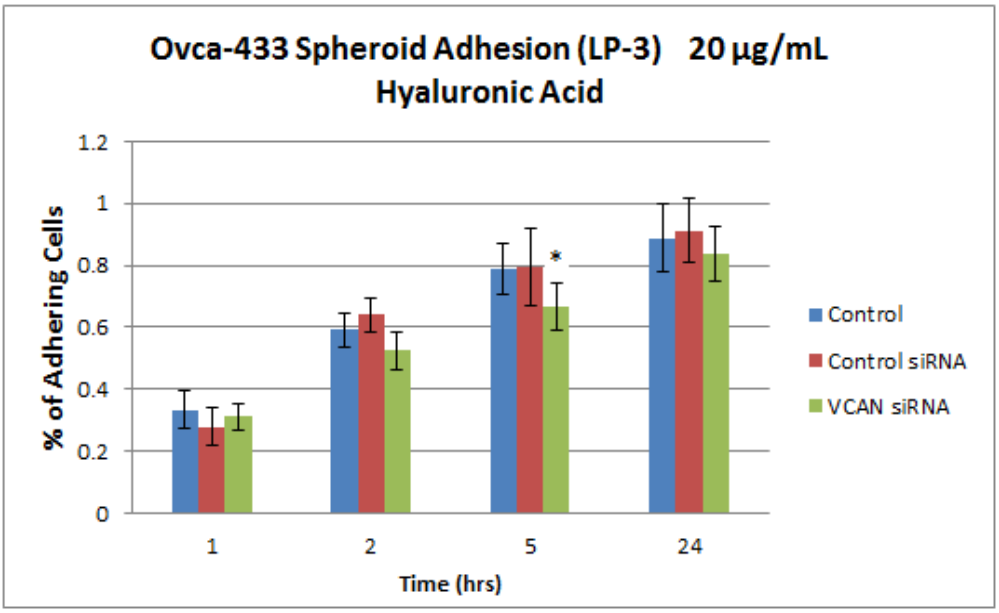

Figure 32. Cells were fluorescently labeled prior to spheroid formation for ease of quantification on a LP-3 monolayer under a microscope. (a) At 2 hours and 5 hours the silencing of versican caused a 24% and 19% decrease in the number of adhering spheroids. (b) Spheroid adhesion after 5 hours was increased by 7% for control cells and 10% VCAN siRNA treated cells in the presence of hyaluronan.

*, $p < 0.05$
**, $p < 0.01$

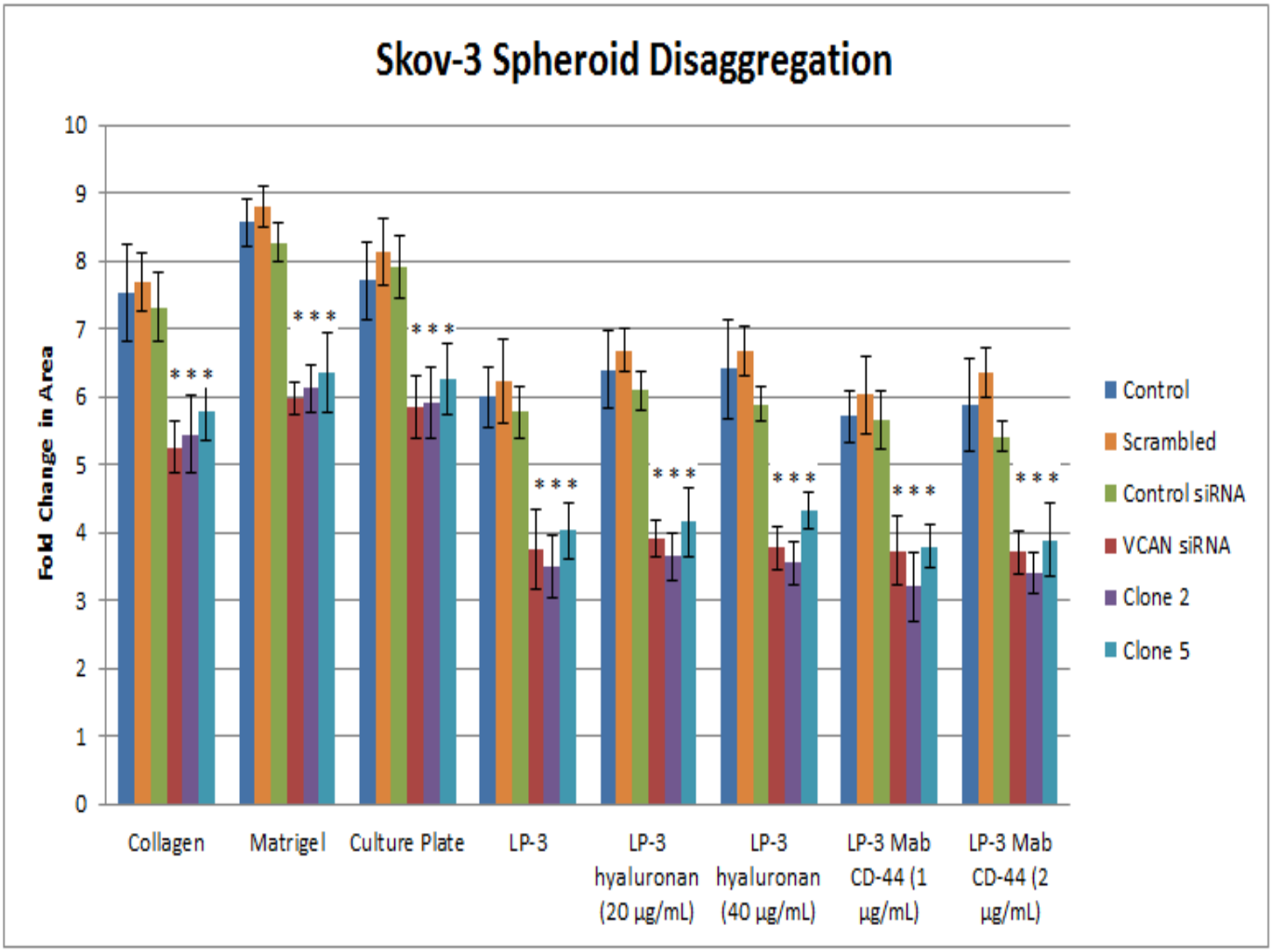

Figure 33. Spheroid disaggregation was assessed by allowing spheroids to adhere and dissociate on their respective matrix over a 24 hour period. The data above represent fold change in area of spheroid at 24 hours divided by the area occupied by the spheroid at time 0. Skov-3 spheroids demonstrate variable disaggregation on the ECM components as well as on the mesothelial monolayer, LP-3. It can be deducted from the figure that loss of versican reduction correlated to a decrease in the area occupied by the spheroids after 24 hours. Addition of hyaluronan resulted in a non-significant fold change in area of 6% for control spheroids, and roughly a 4% increase for spheroids formed from transfected cells. Disaggregation on LP-3 cells was significantly lower as spheroids had to invade the mesothelial, and form a foci before successfully spreading. VCAN siRNA and VCAN shRNA spheroids had a more difficult time disaggregating on LP-3 cells compared to the control cells. Administration of CD44 mAb to the spheroids prior to being added to the LP-3 cells had only a very slight impact on inhibiting spheroid adhesion in any of thecontrol or treatement groups.

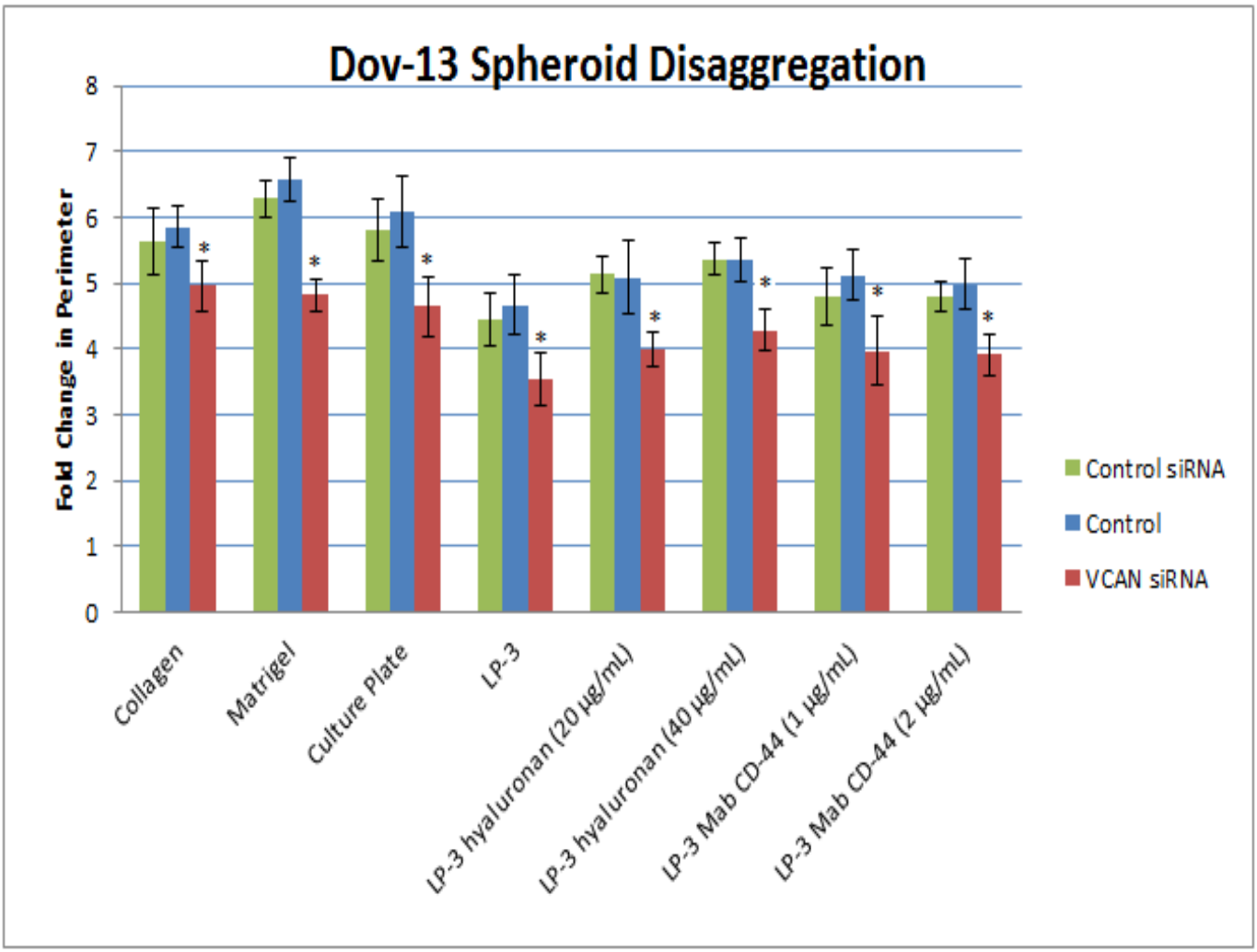

Figure 34. Spheroids were allowed to disaggregate on collagen type I (25 µg/mL), matrigel, culture plate, and LP-3. To assess whether hyaluronan increases disaggregation mediated by versican binding we added hyaluronan to the spheroids prior to addition to the six well plates. For inhibition assays, we used the mAb against the CD44 receptor protein, which is proposed to bind to hyaluronan causing adhesion. However, we observed that the CD44 mAb actually caused an increase in the area of the dissociated spheroids. As in Skov-3 spheroids, it was observed that reduction of versican expression corresponded to decreased fold change in area occupied by the spheroid and its constituent cells. Addition of hyaluronan was found to increase disaggregation, as a result of its ability to increase adhesion allowing for disaggregation.

*, $p < 0.05$

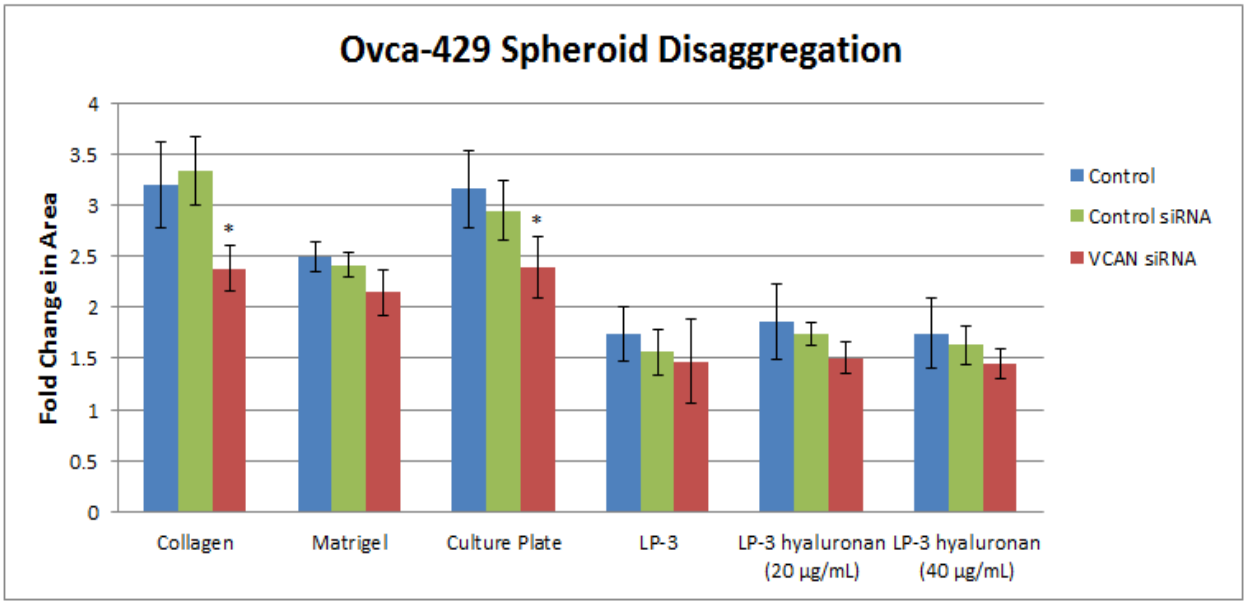

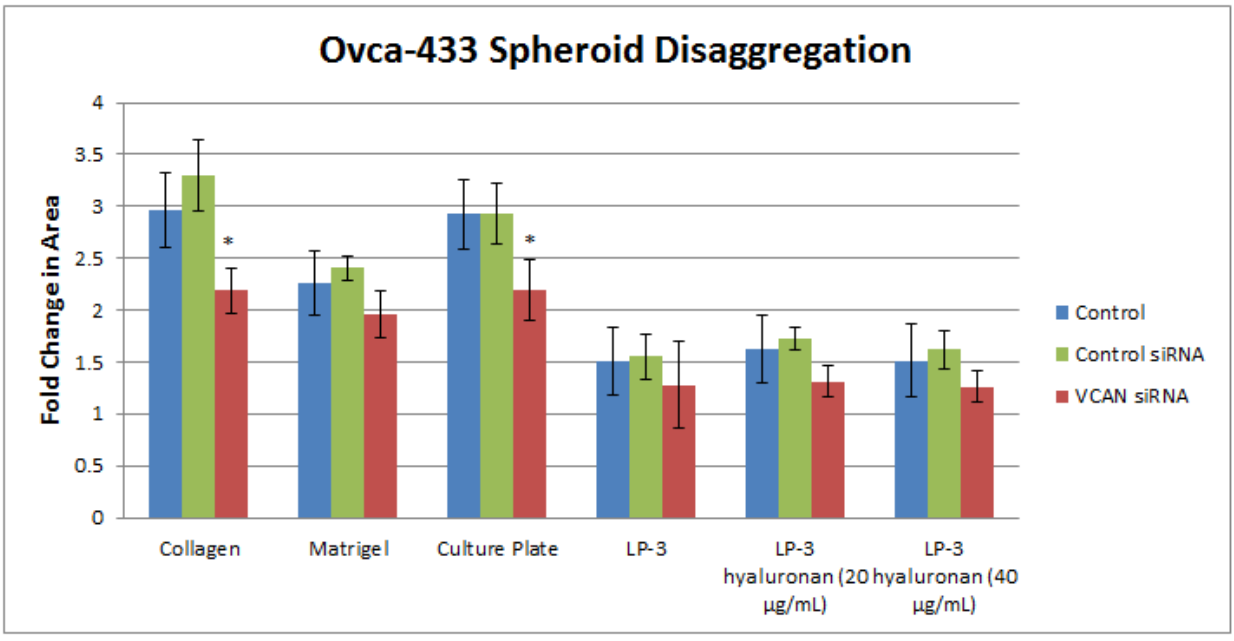

Figure 35. Disaggregation of OVCA-429 and OVCA-433 cells on ECM components was limited compared to Skov-3 and Dov-13 spheroids. These two cell lines express low levels of versican and thus we expected for there only to be a minimal difference between control spheroids and VCAN siRNA treated spheroids. In both cell lines the disaggregation between control spheroids and transfected spheroids was only noticeably different on collagen and on the culture plate.

*, $p < 0.05$

Skov-3 VCAN shRNA clone 2 Spheroids on Culture Plate

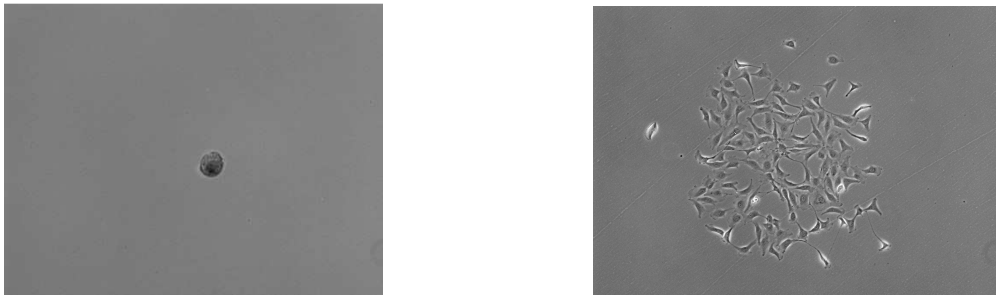

O hours 24 hours

Skov-3 VCAN shRNA clone 2 Spheroids on Collagen

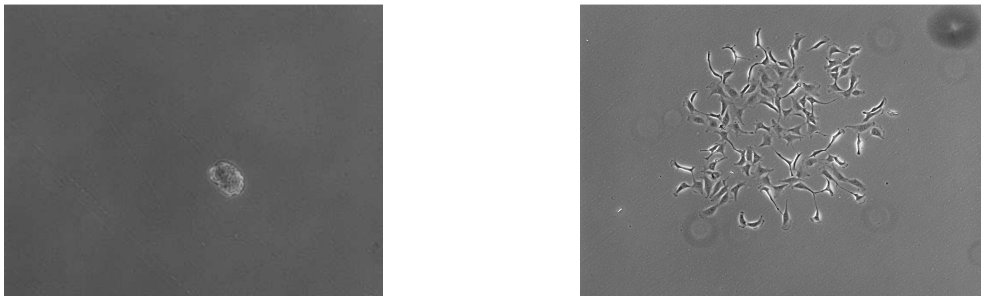

O hours 24 hours

Skov-3 VCAN shRNA clone 2 Spheroids on Matrigel

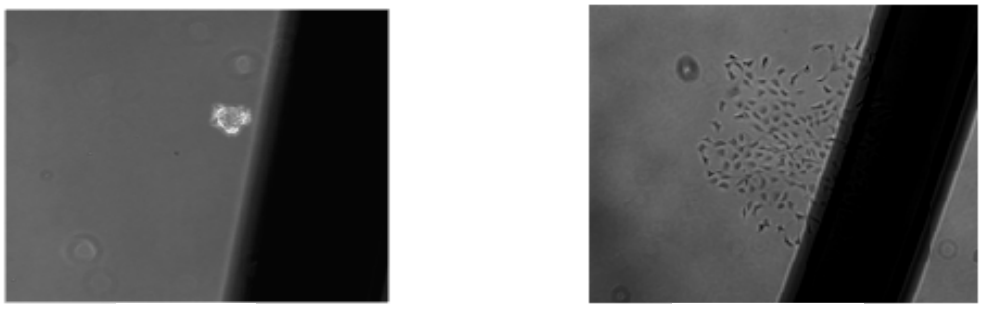

O hours 24 hours

Skov-3 VCAN shRNA clone 2 Spheroids on LP-3

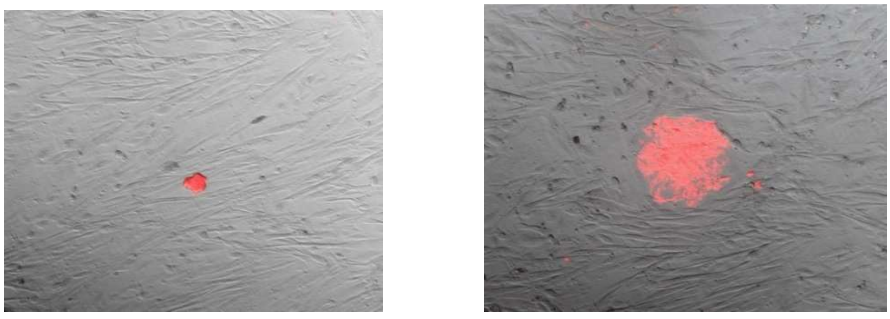

O hours 24 hours

Figure 36. Skov-3 VCAN shRNA clone 2 spheroids were digitally photographed on culture plate, matrigel, collagen, and LP-3. Cells used for spheroid formation for disaggregation on LP-3 were incubated with Vybrant DiO.

Skov-3 Spheroids on Culture Plate

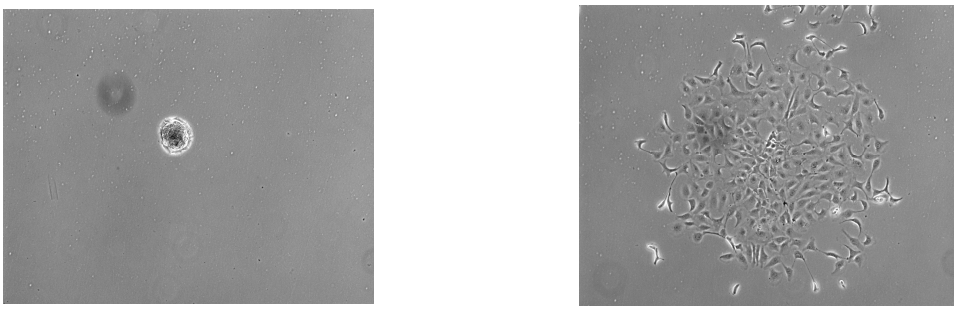

O hours 24 hours

Skov-3 Spheroids on Collagen

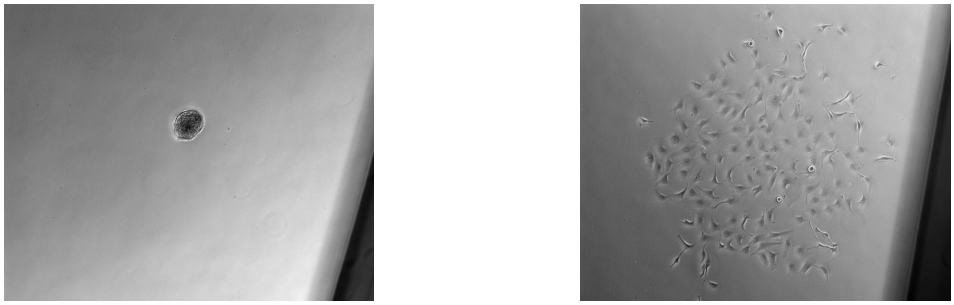

O hours 24 hours

Skov-3 Spheroids on Matrigel

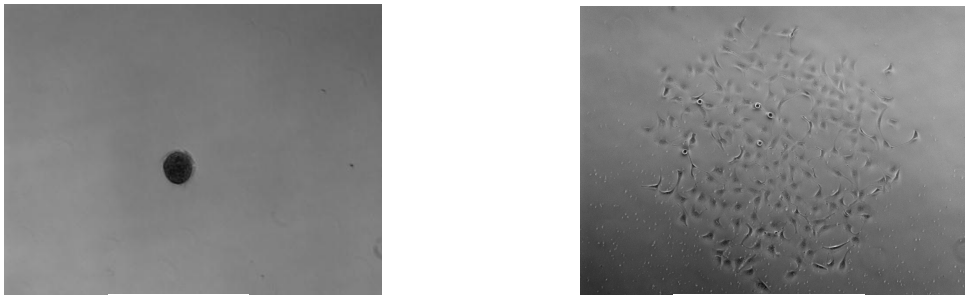

O hours 24 hours

Skov-3 Spheroids on LP-3

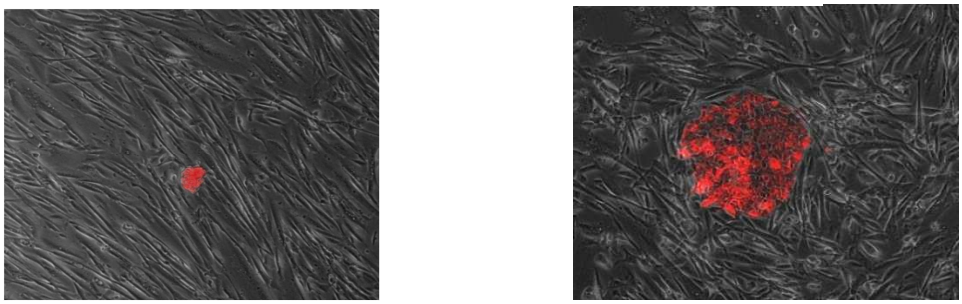

O hours 24 hours

Figure 37. Skov-3 spheroids were digitally photographed on culture plate, matrigel, collagen, and LP-3. Cells used for spheroid formation for disaggregation on LP-3 were incubated with Vybrant DiO.

Skov-3 scrambled shRNA Spheroids on Culture Plate

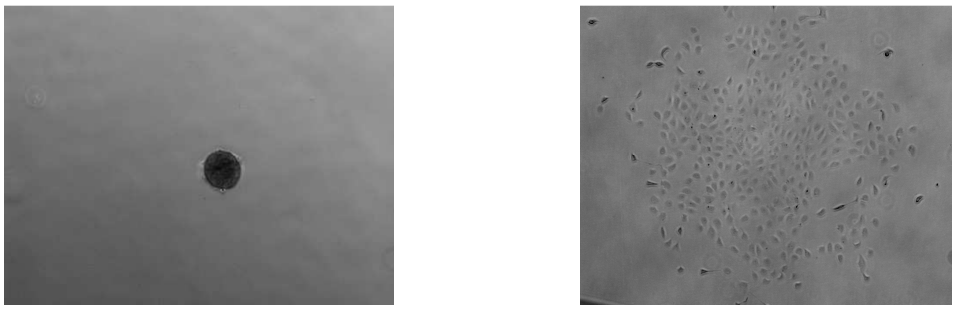

O hours 24 hours

Skov-3 scrambled shRNA Spheroids on Matrigel

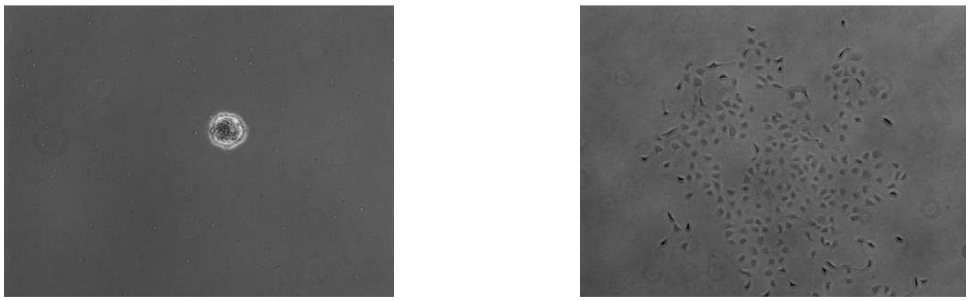

O hours 24 hours

Skov-3 scrambled shRNA Spheroids on Collagen

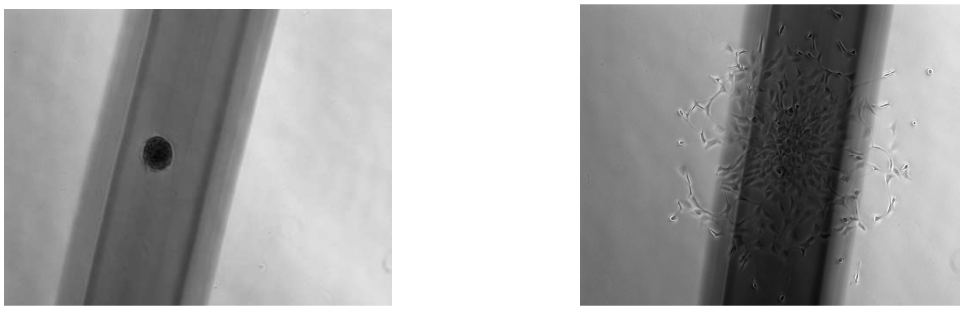

O hours 24 hours

Skov-3 scrambled shRNA Spheroids on LP-3

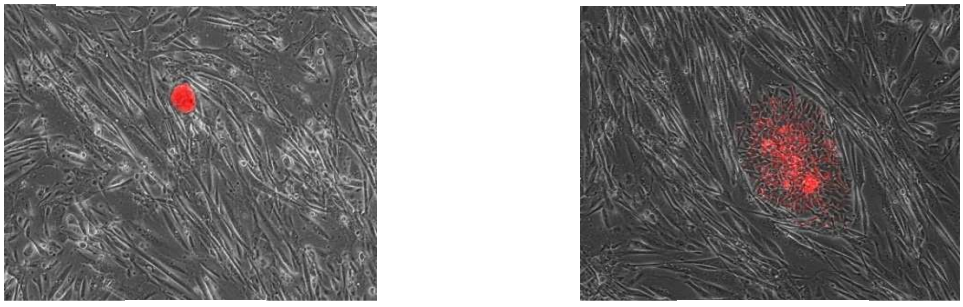

O hours 24 hours

Figure 38. Skov-3 scrambled shRNA spheroids were digitally photographed on culture plate, matrigel, collagen, and LP-3. Cells used for spheroid formation for disaggregation on LP-3 were incubated with Vybrant DiO.

3.5 Quantification of Versican Expression using qRT-PCR

To date there have been relatively few studies examining the levels of each isoform of versican in ovarian carcinoma cells. This lack of knowledge regarding the quantification of versican isoforms not only in ovarian tissues but other tissues as well has probably contributed to conflicting results regarding the roles of versican in proliferation, migration, adhesion, and apoptic resistance. Thus we set out to examine the levels of gene expression of each isoform using quantitative real-time polymerase chain reaction. The primer sequences and protocol used in quantification of mRNA expression is described in the methods section. We attempted to detect a fifth versican isoform V4, which had been recently detected in breast tissue but we were unsuccessful perhaps as a result of the isoform being sparingly expressed in ovarian tissue. Additionally, we decided to measure real-time the levels of versican under different conditions, such as cells in monolayer and in spheroids. Furthermore, upon the completion of the previously mentioned functional assays we measured the levels of versican to ensure that we were in fact silencing the expression of versican. Real-time PCR was repeated at least three times for statistical analysis (Table 3). The data is represented as fold change in gene expression, and was calculated using the PFAFFL method which is an adaptation of the 2 ^(-) delta delta ct method. Efficiency values for each primer were calculated using a standard serial dilution method. When cells treated with VCAN siRNA were analyzed for residual expression of versican, we detected no quantifiable levels of gene expression with Ct values near 40 indicating no detectable expression. Furthermore, the isoform V2 was virtually undetectable in any of the samples withaverage Ct values near 40 . We noticed that in all the cell lines examined that the versican isoforms V0, V1, and V3 were upregulated in spheroids as compared to single cells from a monolayer. Additionally, the detection of versican isoforms became detectable in IGROV-1 cells when they were allowed to form spheroids.

Table 3: QRT-PCR Data for Versican Isoforms					
Cell Line	**V0 expression (Δct)**	**V1 expression (Δct)**	**V2 expression (Δct)**	**V3 expression (Δct)**	**EE**
OVCA-429 monolayer	34.9	33.8	44.7	44.3	21.6
OVCA-429 monolayer	35.4	36.2	42.5	40.8	19.5
OVCA-429 monolayer	36.1	35.8	41.3	42.5	20.9
OVCA-429 VCAN siRNA	42.7	46.11	-	47.2	21.4
OVCA-429 VCAN siRNA	41.1	43.5	46.9	45.2	20.2
OVCA-429 VCAN siRNA	43.8	42.6	-	-	19.3
OVCA-429 Spheroids	34.8	33.9	45.2	42.1	20.08
OVCA-429 Spheroids	33.5	34.3	38.9	37.4	21.4
OVCA-429 Spheroids	33.9	32.7	37.1	36.6	21.1
OVCA-433 monolayer	37.8	34.86	47.4	40.57	20.2
OVCA-433 monolayer	36.7	34.1	40.6	36.2	22.9
OVCA-433 monolayer	35.6	34.5	42.3	38.9	21.6
OVCA-433 Spheroids	38.6	35.71	-	39.82	21.7
OVCA-433 Spheroids	35.2	33.02	39.7	38.3	22.3
OVCA-433 Spheroids	34.9	32.6	39.8	37.4	22.6
OVCA-433 VCAN siRNA	39.7	38.2	-	43.9	19.2
OVCA-433 VCAN siRNA	41.1	39.2	-	44.6	20
OVCA-433 VCAN siRNA	43.5	43.8	-	-	19.5
IGROV-1 VCAN siRNA	37.5	35.8	41.6	39.8	18.3
IGROV-1 VCAN siRNA	42.6	37.5	-	42.4	20.6
IGROV-1 VCAN siRNA	41.1	40.4	43.4	40.3	19.1
IGROV-1 Monolayer	32.27	29.1	37.88	34.16	19.03
IGROV-1 Monolayer	29.4	27.2	38	33.3	17.6
IGROV-1 Monolayer	31.2	28.5	39.2	33.9	18.4
IGROV-1 Aggregates	34.8	34.6	-	36.08	23.5
IGROV-1 Aggregates	33.6	32.7	-	36.1	23.7
IGROV-1 Aggregates	32.3	31.2	37.3	34.1	22.8

Table 3. QRT-PCR data for Versican Isoforms There was no expression detected for versican isoform V4.

Table 4: QRT-PCR Data for Versican Isoforms					
Cell Line	**V0 expression (Δct)**	**V1 expression (Δct)**	**V2 expression (Δct)**	**V3 expression (Δct)**	**EE**
Dov-13 VCAN siRNA	36.4	38.1	-	39.6	18.9
Dov-13 VCAN siRNA	39.2	39.3	41.6	41.5	21.7
Dov-13 VCAN siRNA	37.9	40.5	43.3	42.7	20.2
Dov-13 Monolayer	27.1	24.8	35.6	30.8	18.2
Dov-13 Monolayer	29.7	27.3	37.5	33	22.3
Dov-13 Monolayer	30.3	26.7	36.8	32.4	21.5
Dov-13 Spheroids	27.5	23.5	37	28.8	18.4
Dov-13 Spheroids	28.14	25.8	36.77	31.23	21.6
Dov-13 Spheroids	29.8	24.6	35.9	30.1	20.4
Skov-3 Monolayer	29.2	32.2	37.3	34.8	18.5
Skov-3 Monolayer	26.8	24.3	35.4	30.1	16.7
Skov-3 Monolayer	30.1	27.23	36.8	34.9	19.32
Skov-3 VCAN siRNA	40.9	38.4	-	42.7	21.9
Skov-3 VCAN siRNA	43.6	40.8	-	44.2	20.8
Skov-3 VCAN siRNA	38.5	37.1	40.2	41.3	19.4
Skov-3 Scrambled shRNA	29.8	29.4	-	31.2	19.5
Skov-3 Scrambled shRNA	27.9	27.5	37.9	32.7	17.2
Skov-3 Scrambled shRNA	33.5	31.8	36.1	33.8	20.8
Skov-3 spheroids	28.8	31.1	-	33.2	19
Skov-3 spheroids	25.8	25.5	35.2	32.4	20.2
Skov-3 spheroids	28.6	27.3	-	33.6	20.6
Clone 1	39.02	42.43	-	42.37	21.42
Clone 1	38.19	40.28	44.26	40.99	16.17
Clone 1	40.3	43.7	-	44.1	17.9
Clone 2	37.11	44.72	46.89	38.44	22.43
Clone 2	42.58	39.21	-	40.32	18.78
Clone 2	43.66	41.02	-	41.61	19.33
Clone 5	41.71	42.08	-	39.65	18.29
Clone 5	40.36	43.53	46.19	38.17	16.27
clone 5	42.95	41.66	-	39.48	18.54
Clone 6	44.66	41.67	-	42.14	17.06
clone 6	47.91	44.9	-	45.3	18.5
Clone 6	45.82	43.38	-	40.25	16.61

Table 4: QRT-PCR data for Versican Isoforms There was no expression detected for versican isoform V4.

4. DISCUSSION AND CONCLUSION

Cell migration and adhesion, are normal cell processes that when deregulated can lead to the progression of cancer. In order to successfully migrate and form secondary metastatic sites, carcinoma cells must be able to dissociate from the extracellular matrix. This detachment from the extracellular matrix is typically accompanied by a decrease in cellular adhesion through changes in expression of cellular adhesion molecules (CAMs), integrins, and extracellular matrix proteins. Once free the cells must be able to migrate and adhere to a secondary site, and then proliferate to continue the progression of the cancer. Metastatic progression of epithelial ovarian cancer differs from other cancer forms in that epithelial ovarian cancer spreads locally in the peritoneal cavity and rarely through the bloodstream.[29,30] Additionally, dissemination of cancer cells from the ovary surface is unique in that the cells can dissociate as single cells or as multicellular aggregates referred to as spheroids.[29]

Formation of spheroids in epithelial ovarian cancer dissemination has presented researchers and clinicians with a number of challenges stemming from their resistance to common chemotherapeutic agents as well as radiation therapy.[37-50] There are a few mechanisms that appear to be responsible for spheroids enhanced ability to resist therapy. One proposed mechanism is that spheroids secrete larger quantities of extracellular matrix components that may facilitate closer cell-cell contact decreasing the penetration of chemotherapeutic agents. This increased cellular contact is believed to be a driving force that decreases the spheroids response to apoptotic signals.[42,44] Spheroids cells in one study were found to have a higher expression of bcl-(X)L proteins when exposed to paclitaxel compared to cells grown in monolayers.[157-159] Cells in spheroids are in a virtual quiescent state, and as a result drugs targeting proliferating cells have a diminished ability to kill these slow dividing cells. Resistance

to radiation therapy is hypothesized to come from increased levels of proteins responsible for oxidation repair, as well as from decreased presence of apoptosis proteins.[42,44]

The extracellular matrix (ECM) is composed of numerous constituents that are important in the regulation of migration, proliferation, and adhesion. Due to their vast interaction with growth factors, signaling molecules, chemokines, and structural matrices it is no surprise that the ECM has become implicated in the formation of cancer. A major component of the ECM are a class of proteins called proteoglycans, one of which is Versican, and has been discussed in detail in the aforementioned sections. Versican in functional assays have been shown to be involved in the regulation of proliferation, migration, and adhesion in prostate, breast, skin, and ovarian tissue.[79-82] Despite the studies assessing the function of versican, there have been conflicting results and conclusions. Some studies have found that versican can increase adhesion, while others have observed it actually decreases adhesion as a result of its negatively charged GAG chains. Based upon our results and our own observations we believe that the function of versican is more than likely tissue specific, which could explain the contradictory functions of versican. A further complication in assessing the role of versican is that it is spliced into at least 4 isoforms with different functions. To complicate matter furthers in the in vivo environment there are matrix proteases such as ADAMTS capable of cleaving versican into cleaved products, which could represent another pathway in regulation of migration, proliferation, and adhesion.[107]

From our studies assessing versican's effect on migration in epithelial ovarian cancer cells, we observed that cells treated with VCAN siRNA had a decreased percent wound closure compared to the control cells. The increased wound closure percentage we observed could be a result of the anti-adhesive effect of the V0 and V1 isoforms as a direct result of their highly negatively charged GAG chains that repel each other in the ECM.[161] This anti-adhesive effect of the V0 and V1 are believed to reside in the G1 domain, and when deleted has been shown to

increase adhesion and decrease proliferation.[162] Our qRT-PCR data which indicates V0 and V1 are the predominant isoforms corroborates previous observations that these two isoforms increase migration and proliferation which explains our wound healing results. Although these observations are complicated due to fact that data in endothelial cells supports the concept that expression of the isoforms are dynamic. The researchers observed that V0 and V1 are initially upregulated during the wound healing process, followed by a transition to expression of V2 and V3. Transition to V2 and V3 result in remodeling of the cell-substratum interactions that increase adhesion to the substrate, which is required for successful wound healing.[163]

Due to the involvement of extracellular matrix components in the formation of spheroids, and the contribution of spheroids to chemotherapeutic resistance led us to investigate the effect of versican on EOC spheroids. The first hypothesized step of spheroid formation is cell aggregation, of which is believed to be initiated by beta 1-integrin clustering.[150,151] Versican happens to be a binding partner of beta 1-integrin, so we hypothesized that downregulation of versican expression may inhibit the degree of cell aggregation required for spheroid formation. We found that silencing of versican did not significantly inhibit the formation of spheroids, however we did notice that VCAN siRNA did result in an overall reduction in spheroid size (Table 2). The reduction in diameter of the spheroids may be significant, due to the fact that smaller spheroids have been shown to be less resistant to radiation therapy and chemotherapy compared to enlarged spheroids.[56] Despite the inability to block spheroid formation, targeting versican expression in spheroids could represent a potential target as the reduction in spheroid diameter could lead to less resistant EOC. In addition to the decrease in spheroid diameter, we noticed that loss of versican expression corresponded to formation of fewer spheroids. Fewer spheroids could potentially result in the formation of less secondary metastatic sites, however this hypothesis would need to be investigated more fully to validate this theory. Additionally,

when we looked at how versican expression impacted disaggregation on ECM components as well as on a LP-3 monolayers we saw a reduction in the area occupied by spheroid cells that had downregulated versican expression. The importance of the extracellular matrix in disaggregation has been shown in studies, where it is the interaction between the matrices that induces dissociation as multivalent cell-matrix contacts replace cell-cell adhesive interactions. Thus, we concluded that the smaller area of dissociation is a result of a loss of migratory abilities from low V0 and V1 expression combined with a decreased ability to adhere from decreased V3 expression.

Our results also showed that versican has a positive effect on ovarian carcinoma cell adhesion, which is contradictory to previous studies indicating that versican should function as an anti-adhesive molecule. It appears that cleavage products of versican, could represent the observations for conflicting actions, since it appears the G3 domain enhances adhesion. Activation of focal adhesion kinase (FAK) by the binding of versican to beta 1- integrin, is one of the mechanisms responsible for changes in cellular adhesion.[164] Additionally, there is evidence that versican expression correlates to higher levels of integrins, which could also help to explain increased adhesion. A lot of the work elucidating the functions of the versican has been done using domains rather than intact isoforms, paving the way for potential misleading information. Isoform V3 when overexpressed has been shown to cause an elevation in the number of adhering cells.[165] It is speculated that V3 unlike the other 3 isoforms is void of any GAG chains, and when expressed can outcompete other isoforms for binding resulting in pro-adhesive effects. For the formation of spheroids there is a requirement for increased cell-cell adhesion to allow compaction, and in our qRT-PCR data we calculated that V3 expression in spheroids was elevated when compared to monolayers. Thus, we propose that the driving force for the increased adhesion observed in epithelial ovarian carcinoma cells is the expression of V3.

One mechanism of action for V3 involves interfering with the ERK1/2 and p38 MAPK pathways which are responsible for regulating proliferation, migration, and adhesion.[166] To be clear we are not dismissing the role that cleavage products may play in these events, but are suggesting that they play a supporting role. This conclusion is based on our in vitro assays data, where we saw increased adhesion without the presence of the mesothelial monolayer which is proposed to be a source of secretion for the enzymes responsible for cleavage of versican.

In addition to the mounting evidence that versican is important in the formation and promotion of a variety of cancer including breast, prostate, melanomas,etc.[79-82, 166] Recently, in the past few years versican expression in epithelial ovarian carcinoma tissue has been examined, and authors of these studies have detected strong versican staining in ovarian stromal tissue as well as in epithelial ovarian cancer cells.[115] A further observation has been that there are elevated levels of versican expression in secondary ovarian cancer metastatic sites as compared to primary cancer sites.[167] This result has been corroborated by other researchers who found that overexpression of the versican isoform V3, correlated with a greater number of metastatic sites in mouse model for melanoma.[91, 165] Based on our lab's observation that silencing of versican results in a phenotypic change in the cells morphology, see figure 39**.** The loss of versican causes the cells to undergo a process similar to a mesenchymal state with a structure resembling that of a fibroblast. However, the gain of versican expression results in reversion back to a epithelial state where the predominant cadherin is e-cadherin.[168] This transition to a epithelial like state mimics the mesenchymal-to-epithelial transtion (MET), which in epithelial ovarian carcinoma is hypothesized to be vital to the survival of EOC cells at secondary sites.[34,169-171] In our preliminary data we observed using immunohistochemistry that silencing of versican resulting in very low detectable levels of e-cadherin under a fluorescent microscope. Based upon this information, it is no surprise that versican is found in greater quantities in metastatic sites, as

its upregulation could initiate MET which is required for colonization of EOC cells at secondary sites as well as survival.[168]

In conclusion, we have shown that versican is important in the regulation of such cell physiologic functions as migration, and adhesion. The loss of which in our functional assays resulted in decreased adhesion, migration, spheroid disaggregation, and spheroid diameter. To date versican has not been directly studied as a drug target in epithelial ovarian cancer, but the synthesis of versican in vascular smooth muscle cells has been inhibited by genistein, a tyrosine kinase inhibitor.[172] A major hurdle in targeting versican in EOC is that there is plenty of evidence suggesting that proteases such as ADAMTS and MMPs are present in the tumor microenvironment and are capable of cleaving versican isoforms into active domains.[107] These domains as previously stated have been investigated in numerous studies in other cell lines and have been shown to have properties mimicking those of full length versican isoforms.[107] Thus, to effectively target versican one would also need to inhibit these proteases or abrogate expression of versican. An alternative mechanism has been applied to attempt to block the effects of versican indirectly by the administration of HA oligomers. The oligomers did in fact inhibit the growth of ovarian cancer xenografts in vivo, and the result is expected to be derived from their ability to block the formation of a HA-rich cell associated matrix that is strengthened by versican.[116]

a)

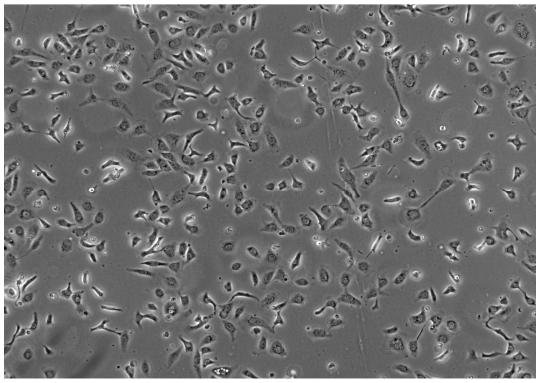

b)

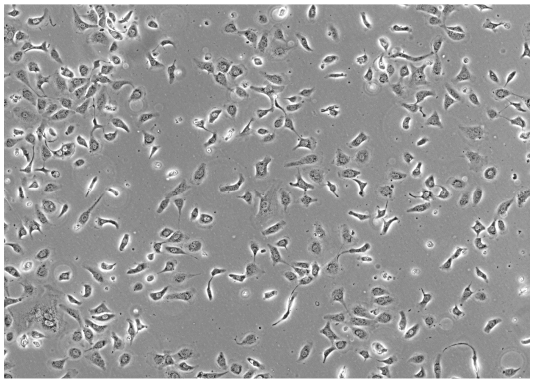

c)

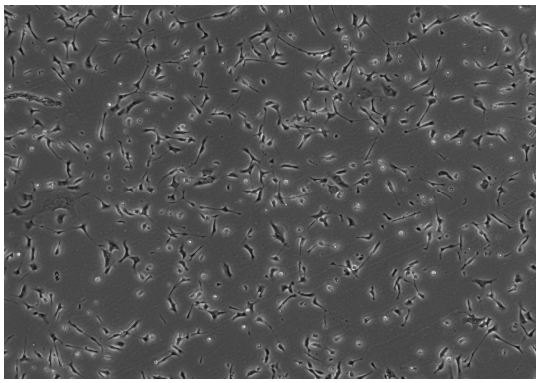

d)

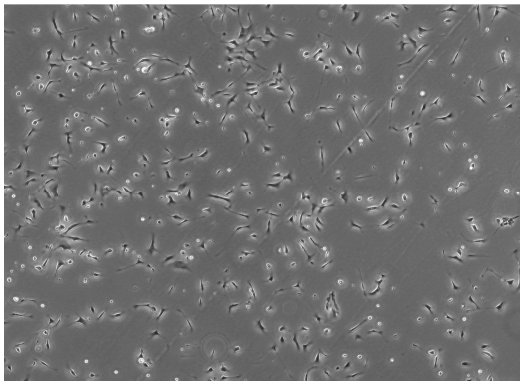

Figure 39. Exogenous expression of versican leads to a more epithelial like morphology. (A) Control Skov-3 cells were examined under a light microscope, and a epithelial cell type is observed. (B) HuSH shRNA scrambled vector Skov-3 transfected cells also reveal a epithelial nature. (C) siRNA treated Skov-3 cells undergo a morphology change similar to a mesenchymal state. (D) HuSH VCAN shRNA Skov-3 transfected cells underwent a similar transition to a mesenchymal state seen in the siRNA treated cells. This EMT transition is a result of a transition from e-cadherin expression to N-cadherin expression due to the silencing of versican in EOC cells.

References

1 U.S. Cancer Statistics Working Group. *United States Cancer Statistics: 1999–2007 Incidence and Mortality Web-based Report.* Atlanta (GA): Department of Health and Human Services, Centers for Disease Control and Prevention, and National Cancer Institute; 2010. Available at: http://www.cdc.gov/uscs.

2 *Sherman ME, Mink PJ, Curtis R, et al. Survival among women with borderline ovarian tumors and ovarian carcinoma: a population-based analysis. Cancer 2004; 100:1045 –1052.*

3 Howlader N, Noone AM, Krapcho M, Neyman N, Aminou R, Waldron W, Altekruse SF, Kosary CL, Ruhl J, Tatalovich Z, Cho H, Mariotto A, Eisner MP, Lewis DR, Chen HS, Feuer EJ, Cronin KA, Edwards BK (eds). *SEER Cancer Statistics Review, 1975-2008*, National Cancer Institute.

4 Lister-Sharp D, McDonagh MS, Khan KS, Kleijnen J (2000) A rapid and systematic review of the effectiveness and cost-effectiveness of the taxanes used in the treatment of advanced breast and ovarian cancer. *Health Technol Assess* **4**: 1–113.

5 *Bookman MA, McGuire WP III, Kilpatrick D et al. Carboplatin and paclitaxel in ovarian carcinoma: a phase I study of the Gynecologic Oncology Group. J Clin Oncol 1996;14:1895-1902.*

6 Bast Jr RC, Klug TL, St John E, Jenison E, Niloff JM, Lazarus H,et al. A radioimmunoassay using a monoclonal antibody to monitor the course of epithelial ovarian cancer. N Engl J Med1983, 309(15), 883–887.

7 Jacobs IJ, Skates SJ, MacDonald N, Menon U, Rosenthal AN,Davies AP, et al. Screening for ovarian cancer: a pilot randomized controlled trial. Lancet 1999, 353(9160), 1207–1210.

8 Jelovac, Danijela, and Deborah K. Armstrong. "Recent Progress in the Diagnosis and Treatment of Ovarian Cancer." *CA: A Cancer Journal for Clinicians* 61.3 (2011): 183-203.

9 Scully RE. Ovarian tumors. A review. Am J Pathol. 1997;87:686–720.

10 Parazzini F, Chatenoud L, Chiantera V, Benzi G, Surace M, La Vecchia C. Population attributable risk for ovarian cancer. Eur J Cancer 2000;36:520–4.

11 La Vecchia C, Decarli A, Negri E, et al. Dietary factors and the risk of epithelial ovarian cancer. J Natl Cancer Inst 1987;79:663–9.

12 Risk Factors for Ovarian Cancer: An Overview with Emphasis on Hormonal FactorsFariba Salehi, Lesley Dunfield, Karen P. Phillips, Daniel Krewski, Barbara C. Vanderhyden Journal of Toxicology and Environmental Health, Part B Vol. 11, Iss. 3-4, 2008.

13 Bjersing L, Cajander S: Ovulation and the mechanism of follicle rupture. V. Ultrastructure of tunica albuginea and theca externa of rabbit graafian follicles prior to induced ovulation. Cell Tissue Res 1974, 153:15-30.

14 Ackerman RC, Murdoch WJ: Prostaglandin-induced apoptosis of ovarian surface epithelial cells. Prostaglandins 1993, 45:475-485.

15 P.C. Leung, J.H. Choi, Endocrine signaling in ovarian surface epithelium and cancer, Hum. Reprod. Update 13 (2007) 143–162.

16 American Cancer Society.: Cancer Facts and Figures 2011. Atlanta, Ga: American Cancer Society, 2011 www.cancer.orgBhoola, S. and W. J. Hoskins (2006). Diagnosis and management of epithelial ovarian cancer. Obstet Gynecol 107(6): 1399-410.

17 http://www.cancer.org/Cancer/OvarianCancer/DetailedGuide/ovarian-cancer-key-statistics.

18 PDQ® Cancer Information Summary. National Cancer Institute; Bethesda, MD. Genetics of Breast and Ovarian Cancer (PDQ®) - Health Professional. Date last modified 04/24/2009. Available at: http://www.cancer.gov/cancertopics/pdq/genetics/breast-and-ovarian/healthprofessional. Accessed Jan. 5th 2012.

19 Kotsopoulos J, Lubinski J, Neuhausen SL, et al. Hormone replacement therapy and the risk of ovarian cancer in BRCA1 and BRCA2 mutation carriers. *Gynecologic Oncology* 2006; 100(1):83–88.

20 John Hopkins Pathology. Ovarian Cancer. http://ovariancancer.jhmi.edu/hereditary.cfm Accessed Jan. 12 2012.

21 Markman M. Intraperitoneal antineoplastic drug delivery: rationale and results. Lancet Oncol 2003;4:277–283.

22 Alberts DS, Liu PY, Hannigan EV, et al. Intraperitoneal cisplatin plus intravenous cyclophosphamide versus intravenous cisplatin plus intravenous cyclophosphamide for stage III ovarian cancer. N Engl J Med 1996;335:1950–1955.

23 Gadducci A, Carnino F, Chiara S, et al. Intraperitoneal versus intravenous cisplatin in combination with intravenous cyclophosphamide and epidoxorubicin in optimally cytoreduced advanced epithelial ovarian cancer: a randomized trial of the Gruppo Oncologico Nord-Ovest. Gynecol Oncol 2000;76:157–162.

24 Kirmani S, Braly PS, McClay EF, et al. A comparison of intravenous versus intraperitoneal chemotherapy for the initial treatment of ovarian cancer. Gynecol Oncol 1994;54:338–344.

25 Markman M, Bundy BN, Alberts DS, et al. Phase III trial of standard dose intravenous cisplatin plus paclitaxel versus moderately high-dose carboplatin followed by intravenous paclitaxel and intraperitoneal cisplatin in small-volume stage III ovarian carcinoma: an intergroup study of the Gynecologic Oncology Group, Southwestern Oncology Group, and Eastern Cooperative Oncology Group. J Clin Oncol 2001; 19:1001–1007.

26 Polyzos A, Tsavaris N, Kosmas C, et al. A comparative study of intraperitoneal carboplatin versus intravenous carboplatin with intravenous cyclophosphamide in both arms as initial chemotherapy for stage III ovarian cancer. Oncology 1999;56:291–296.

27 Yin BW, Lloyd KO. Molecular cloning of the CA125 ovarian cancer antigen: identification as a new mucin, MUC16. J Biol Chem 2001; 276:27371–27375.

28 Wagner U, Kohler S, Reinartz S, et al. Immunological consolidation of ovarian carcinoma recurrences with monoclonal anti-idiotype antibody ACA125: immune responses and survival in palliative treatment. Clin Cancer Res 2001;7:1154–1162.

29 Multicellular spheroids in ovarian cancer metastases: Biology and pathology. Kristy Shield, M. Leigh Ackland, Nuzhat Ahmed, Gregory E. Rice Gynecol Oncol. 2009 April; 113(1): 143–148.

30 Ahmed N, Thompson EW, Quinn MA. Epithelial–mesenchymal interconversions in normal ovarian surface epithelium and ovarian carcinomas: an exception to the norm. J Cell Physiol 2007;213(3):581–8.

31 Lengyel E. Ovarian cancer development and metastasis. *Am J Pathol.* 2010;177:1053–1064.

32 Naora H, Montell DJ. Ovarian cancer metastasis: integrating insights from disparate model organisms. Nat Rev, Cancer 2005;5(5):355–66.

32 Allen HJ, Porter C, Gamarra M, Piver MS, Johnson EA. Isolation and morphologic characterization of human ovarian carcinoma cell clusters present in effusions. ExpCell Biol 1987;55(4):194–208.

33 Waleh NS, Gallo J, Grant TD, Murphy BJ, Kramer RH, Sutherland RM. Selective down-regulation of integrin receptors in spheroids of squamous cell carcinoma. Cancer Res 1994;54(3):838–43.

34 Hudson, L.G., Zeineldin, R., and Stack, M.S. "Phenotypic Plasticity of Neoplastic Ovarian Epithelium: Unique Cadherin Profiles in Tumor Progression." *Clin. Exp. Metastasis* 2008; 25: 643-655.

35 Moss N.M., Barbolina M.V., Liu Y., Sun L., Munshi H.G., and Stack, M.S. "Ovarian Carcinoma Cell Detachment and Multi-cellular Aggregate Formation are Regulated by MT1-MMP: A Potential Role in Intra-Peritoneal Metastatic Dissemination." *Cancer Research* 2009; 69: 7121-9.

36 Sodek, Katharine L., Maurice J. Ringuette, and Theodore J. Brown. "Compact Spheroid Formation by Ovarian Cancer Cells is Associated with Contractile Behavior and an Invasive Phenotype." *International Journal of Cancer* 124.9 (2009): 2060-70.

37 Y.J. Kim, C. Sauer, K. Testa, J.K. Wahl, R.A. Svoboda, K.R. Johnson *et al.* Modulating the strength of cadherin adhesion: evidence for a novel adhesion complex. J. Cell. Sci., 118 (Pt 17) (2005), pp. 3883–3894.

38 Sutherland RM. Cell and environment interactions in tumor microregions: the multicell spheroid model. *Science.* 1988;240:177–84.[PubMed]

39 Green SK, Francia G, Isidoro C, Kerbel RS. Anti-adhesive antibodies targeting E-cadherin sensitize multicellular tumor spheroids to chemotherapy in vitro. *Mol Cancer Ther.* 2004;3:149–59.[PubMed]

40 Desoize B, Jardillier J. Multicellular resistance: a paradigm for clinical resistance? *Crit Rev Oncol Hematol.* 2000;36:193–207.[PubMed]

41 Bates RC, Edwards NS, Yates JD. Spheroids and cell survival. *Crit Rev Oncol Hematol.* 2000;36:61–74.[PubMed]

42 Minchinton AI, Tannock IF. Drug penetration in solid tumors. *Nat Rev Cancer.* 2006;6:583–92.

43 Sutherland RM, McCredie JA, Inch WR. Growth of multicell spheroids in tissue culture as a model of nodular carcinomas. J Natl Cancer Inst 1971;46(1):113–20.

44 Sutherland RM, Durand RE. Radiation response of multicell spheroids—an in vitro tumour model. Curr Top Radiat Res Q 1976;11(1):87–139.

45 Zhang S, Balch C, Chan MW, Lai HC, Matei D, Schilder JM, et al. Identification and characterization of ovarian cancer-initiating cells from primary human tumors. Cancer Res 2008;68(11):4311–20.

46 Bapat SA, Mali AM, Koppikar CB, Kurrey NK. Stem and progenitor-like cells contribute to the aggressive behavior of human epithelial ovarian cancer. Cancer Res 2005;65(8):3025–9.

47 Makhija S, Taylor DD, Gibb RK, Gercel-Taylor C. Taxol-induced bcl-2 phosphorylation in ovarian cancer cell monolayer and spheroids. Int J Oncol 1999;14 (3):515–21.

48 Durand RE: Multicell spheroids as a model for cell kinetics studies. Cell Tissue Kinet 23: 141-159, 1990.

49 Nederman T: Effects of vinblastin and 5-fluorouracil on human glioma and thyroid cancer cell monolayers and spheroids. Cancer Res 44: 254-258, 1984.

50 Sutherland RM: Cell and environment interactions in tumor microregions: the multicell spheroid model. Science 240: 177-184, 1988.

51 Sutherland R. M.,Carlsson J.,Durand R. E., Yuhas J. 1981 Spheroids in cancer research. Cancer Res. 41, 2980–2994.

52 Bertout, J. A., Patel, S. A. and Simon, M. C. (2008) The impact of O2 availability on human cancer. Nat Rev Cancer. 8: 967–975.

53 Harrison, L. B., Chadha, M., Hill, R. J., Hu, K. and Shasha, D. (2002) Impact of tumor hypoxia and anemia on radiation therapy outcomes. Oncologist. 7: 492–508.

54 Moeller, B. J. and Dewhirst, M. W. (2006) HIF-1 and tumour radiosensitivity. Br J Cancer. 95:15.

55 Durand RE, Sutherland RM: Effects of intercellular contact on repair of radiation damage. Exp Cell Res 71: 75-80, 1972.

56 Olive PL, Durand RE. Drug and radiation resistance in spheroids: cell contact and kinetics. Cancer Metastasis Rev. 1994 Jun;13(2):121-38.

57 Liotta LA, Kohn EC (2001) The microenvironment of the tumour-host interface. Nature 411(6835):375–379.

58 Zigrino P, Loffek S, Mauch C (2005) Tumor-stroma interactions: their role in the control of tumor cell invasion. Biochimie 87(3–4):321–328.

59 Ricciardelli C, Rodgers RJ (2006) Extracellular matrix of ovarian tumors. Semin Reprod Med 24(4):270–282.

60 Gardner MJ, Jones LM, Catterall JB et al (1995) Expression of cell adhesion molecules on ovarian tumour cell lines and mesothelialcells, in relation to ovarian cancer metastasis. Cancer Lett 91(2):229–234.

61 Gardner MJ, Catterall JB, Jones LM et al (1996) Human ovarian tumour cells can bind hyaluronic acid via membrane CD44: a possible step in peritoneal metastasis. Clin Exp Metastasis 14(4):325–334.

62 Wilson KE, Bartlett JM, Miller EP et al (1999) Regulation and function of the extracellular matrix protein tenascin-C in ovarian cancer cell lines. Br J Cancer 80(5–6):685–692.

63 Strobel T, Cannistra SA (1999) Beta1-integrins partly mediate binding of ovarian cancer cells to peritoneal mesothelium in vitro. Gynecol Oncol 73(3):362–367.

64 Anttila MA, Tammi RH, Tammi MI et al (2000) High levels of stromal hyaluronan predict poor disease outcome in epithelial ovarian cancer. Cancer Res 60(1):150–155.

65 Voutilainen K, Anttila M, Sillanpaa S et al (2003) Versican in epithelial ovarian cancer: relation to hyaluronan, clinicopathologic factors and prognosis. Int J Cancer 107(3):359–364.

66 Freedman RS, Deavers M, Liu J et al (2004) Peritoneal inflammation a microenvironment for epithelial ovarian cancer (EOC). J Transl Med 2(1):23.

67 Salani R, Neuberger I, Kurman RJ et al (2007) Expression of extracellular matrix proteins in ovarian serous tumors. Int J Gynecol Pathol 26(2):141–146.

68 Kenny HA, Kaur S, Coussens LM et al (2008) The initial steps of ovarian cancer cell metastasis are mediated by MMP-2 cleavage of vitronectin and fibronectin. J Clin Invest 118(4):1367–1379.

69 Heyman L, Kellouche S, Fernandes J et al (2008) Vitronectin and its receptors partly mediate adhesion of ovarian cancer cells to peritoneal mesothelium in vitro. Tumour Biol 29(4):231–244.

70 Ricciardelli, C.; Rodgers, R.J. Extracellular matrix of ovarian tumors. *Semin. Reprod. Med.* **2006**, *24* (4), 270–282.

71 Friedl, P., & Wolf, K. (2008). Tube travel: the role of proteases in individual and collective cancer cell invasion. Cancer Research, 68(18), 7247–7249.

72 Wolf, K., Wu, Y. I., Liu, Y., Geiger, J., Tam, E., Overall, C., et al. (2007). Multi-step pericellular proteolysis controls the transition from individual to collective cancer cell invasion. National Cell Biology, 9(8), 893–904.

73 Yeo, T.K.; Nagy, J.A.; Yeo, K.T.; Dvorak, H.F.; Toole, B.P. Increased hyaluronan at sites of attachment to mesentery by CD44-positive mouse ovarian and breast tumor cells. Am. J. Pathol. 1996, 148 (6), 1733–1740.

74 Jojovic, M.; Delpech, B.; Prehm, P.; Schumacher, U. Expression of hyaluronate and hyaluronate synthase in human primary tumours and their metastases in scid mice. Cancer Lett. 2002, 188 (1–2), 181–189.

75 Tzuman, Y.C.; Sapoznik, S.; Granot, D.; Nevo, N.; Neeman, M. Peritoneal adhesion and angiogenesis in ovarian carcinoma are inversely regulated by hyaluronan: the role of gonadotropins. Neoplasia 2010, 12 (1), 51–60.

76 Toole B. P., Wight T. N.,Tammi M. I. (2002) J. Biol. Chem. 277, 4593–4596.

77 Bourguignon, L.Y.; Zhu, H.; Chu, A.; Iida, N.; Zhang, L.; Hung, M.C. Interaction between the adhesion receptor, CD44, and the oncogene product, p185HER2, promotes human ovarian tumor cell activation. J. Biol. Chem. 1997, 272 (44), 27913–27918.

78 Bourguignon, L.Y.; Zhu, H.; Shao, L.; Chen, Y.W. CD44 interaction with c-Src kinase promotes cortactin-mediated cytoskeleton function and hyaluronic acid-dependent ovarian tumor cell migration. J. Biol. Chem. 2001, 276 (10), 7327–7336.

79 Voutilainen, K.; Anttila, M.; Sillanpaa, S.; Tammi, R.; Tammi, M.; Saarikoski, S.; Kosma, V.M. Versican in epithelial ovarian cancer: Relation to hyaluronan, clinicopathologic factors and prognosis. Int. J. Cancer 2003, 107 (3), 359–364.

80 Casey, R.C.; Oegema, T.R., Jr.; Skubitz, K.M.; Pambuccian, S.E.; Grindle, S.M.; Skubitz, A.P. Cell membrane glycosylation mediates the adhesion, migration, and invasion of ovarian carcinoma cells. Clin. Exp. Metastasis 2003, 20 (2), 143–152.

81 Lancaster, J.M.; Dressman, H.K.; Clarke, J.P.; Sayer, R.A.; Martino, M.A.; Cragun, J.M.; Henriott, A.H.; Gray, J.; Sutphen, R.; Elahi, A.; Whitaker, R.S.; West, M.; Marks, J.R.; Nevins, J.R.; Berchuck, A. Identification of genes associated with ovarian cancer metastasis using microarray expression analysis. Int. J. Gynecol. Cancer 2006, 16 (5), 1733–1745.

82 Zagorianakou, N.; Stefanou, D.; Makrydimas, G.; Zagorianakou, P.; Briasoulis, E.; Karavasilis, B.; Agnantis, N.J. CD44s expression, in benign, borderline and malignant tumors of ovarian surface epithelium. Correlation with p53, steroid receptor status, proliferative indices (PCNA, MIB1) and survival. Anticancer Res. 2004, 24 (3a), 1665–1670.

83 Margolis RU, Margolis RK: Aggrecan–versican–neurocan family proteoglycans. Methods Enzymol 1994, 245:105-126.

84 Zimmermann D: Versican. In Proteoglycans-Structure, Biology and Molecular Interactions. 2000:327-341.

85 Naso, M. F., Zimmermann, D. R., & Iozzo, R. V. (1994). Characterization of the complete genomic structure of the human versican gene and functional analysis of its promoter. Journal of Biological Chemistry, 269(52), 32999–33008.

86 Zimmermann, D. R., & Ruoslahti, E. (1989). Multiple domains of the large fibroblast proteoglycan, versican. The EMBO Journal, 8(10), 2975–2981.

87 LeBaron, R. G. (1996). Versican. Perspectives on Developmental Neurobiology, 3(4), 261–271.

88 Ricciardelli C, Sakko AJ, Ween MP, Russell DL, Horsfall DJ. The biological role and regulation of versican levels in cancer. Cancer Metastasis Rev. 2009 Jun;28(1-2):233-45.

89 Kischel P, Waltregny D, Dumont B, Turtoi A, Greffe Y, Kirsch S, De Pauw E, Castronovo V. Versican overexpression in human breast cancer lesions: known and new isoforms for stromal tumor targeting. Int J Cancer. 2010 Feb 1;126(3):640-50.

90 Arslan, F., Bosserhoff, A. K., Nickl-Jockschat, T., Doerfelt, A., Bogdahn, U., & Hau, P. (2007). The role of versican isoforms V0/V1 in glioma migration mediated by transforming growth factor-beta2. British Journal of Cancer, 96(10), 1560–1568.

91 Miquel-Serra, L., Serra, M., Hernandez, D., Domenzain, C., Docampo, M. J., Rabanal, R. M., et al. (2006). V3 versican isoform expression has a dual role in human melanoma tumor growth and metastasis. Laboratory Investigation, 86(9), 889–901.

92 Ang, L. C., Zhang, Y., Cao, L., Yang, B. L., Young, B., Kiani, C., et al. (1999). Versican enhances locomotion of astrocytoma cells and reduces cell adhesion through its G1 domain. Journal of Neuropathology and Experimental Neurology, 58(6), 597–605.

93 Cattaruzza, S., Schiappacassi, M., Kimata, K., Colombatti, A., Perris, R. (2004). The globular domains of PGM/versican modulate the proliferation-apoptosis equilibrium and invasive capabilities of tumor cells. Journal of The Federation of American Societies for Experimental Biology.

94 Zheng, P. S., Wen, J., Ang, L. C., Sheng, W., Viloria-Petit, A., Wang, Y., et al. (2004). Versican/PG-M G3 domain promotes tumor growth and angiogenesis. Journal of The Federation of American Societies for Experimental Biology.

95 Paris, S., Sesboue, R., Chauzy, C., Maingonnat, C., & Delpech, B. (2006). Hyaluronectin modulation of lung metastasis in nude mice. European Journal of Cancer, 42(18), 3253–3259.

96 Ricciardelli, C., Russell, D. L., Ween, M. P., Mayne, K., Suwiwat, S., Byers, S., et al. (2007). Formation of hyaluronan–and versican–rich pericellular matrix by prostate cancer cells promotes cell motility. Journal of Biological Chemistry, 282(14), 10814–10825.

97 Creighton, C. J., Bromberg-White, J. L., Misek, D. E., Monsma, D. J., Brichory, F., Kuick, R., et al. (2005). Analysis of tumorhost interactions by gene expression profiling of lung adenocarcinoma xenografts identifies genes involved in tumor formation. Molecular Cancer Research, 3(3), 119–129.

98 LaPierre, D. P., Lee, D. Y., Li, S. Z., Xie, Y. Z., Zhong, L., Sheng, W., et al. (2007). The ability of versican to simultaneously cause apoptotic resistance and sensitivity. Cancer Research, 67(10), 4742–4750.

99 Yee, A. J., Akens, M., Yang, B. L., Finkelstein, J., Zheng, P. S., Deng, Z., et al. (2007). The effect of versican G3 domain on local breast cancer invasiveness and bony metastasis. Breast Cancer Research, 9(4), R47.

100 Sheng, W., Wang, G., Wang, Y., Liang, J., Wen, J., Zheng, P. S., et al. (2005). The roles of versican V1 and V2 isoforms in cell proliferation and apoptosis. Molecular Biology of the Cell, 16(3), 1330–1340.

101 Schönherr E, Järveläinen HT, Sandell LJ, Wight TN: Effects of platelet-derived growth factor and transforming growth factorbeta 1 on the synthesis of a large versican-like chondroitin sulfate proteoglycan by arterial smooth muscle cells. J Biol Chem 1991, 266:17640-17647.

102 Evanko SP, Johnson PY, Braun KR, Underhill CB, Dudhia J, Wight TN:Platelet-derived growth factor stimulates the formation of versican-hyaluronan aggregates and pericellular matrix expansion in arterial smooth muscle cells. Arch Biochem Biophys 2001, 394:29-38.

103 LeBaron, R. G., Zimmermann, D. R., & Ruoslahti, E. (1992). Hyaluronate binding properties of versican. Journal of Biological Chemistry, 267(14), 10003–10010.

104 Wight, T. N. (2002). Versican: a versatile extracellular matrix proteoglycan in cell biology. Current Opinions in Cell Biology, 14(5), 617–623.

105 Wu, Y. J., La Pierre, D. P., Wu, J., Yee, A. J., & Yang, B. B. (2005). The interaction of versican with its binding partners. Cell Research, 15(7), 483–494.

106 Maria V. BARBOLINA, Rebecca J. BURKHALTER, and M. Sharon STACK. Diverse mechanisms for activation of Wnt signalling in the ovarian tumour microenvironment. Biochem. J. (2011) 437, 1–12.

107 Jonsson-Rylander, A. C., Nilsson, T., Fritsche-Danielson, R., Hammarstrom, A., Behrendt, M., Andersson, J. O., et al. (2005). Role of ADAMTS-1 in atherosclerosis: remodeling of carotid artery, immunohistochemistry, and proteolysis of versican. Arteriosclerosis, Thrombosis, and Vascular Biology, 25(1), 180–185.

108 Rahmani, M., Wong, B. W., Ang, L., Cheung, C. C., Carthy, J. M., Walinski, H., et al. (2006). Versican: signaling to transcriptional control pathways. Canadian Journal of Physiological Pharmacology, 84(1), 77–92.

109 Ang, L.C., Zhang, Y., Cao, L., Yang, B.L., Young, B., Kiani, C., Lee, V., Allan, K., Yang, B.B., 1999. Versican enhances locomotion of astrocytoma cells and reduces cell adhesion through its G1 domain. J. Neuropathol. Exp. Neurol. 58, 597– 605.

110 Yang BL, Zhang Y, Cao L, Yang BB: Cell adhesion and proliferation mediated through the G1 domain of versican. J Cell Biochem 1999, 72:210-220.

111 Sakko, A. J., Ricciardelli, C., Mayne, K., Suwiwat, S., LeBaron, R. G., Marshall, V. R., et al. (2003). Modulation of Prostate Cancer Cell Attachment to Matrix by Versican. Cancer Research, 63(16), 4786–4791.

112 Paris, S., Sesboue, R., Chauzy, C., Maingonnat, C., & Delpech, B. (2006). Hyaluronectin modulation of lung metastasis in nude mice. European Journal of Cancer, 42(18), 3253–3259.

113 Creighton, C. J., Bromberg-White, J. L., Misek, D. E., Monsma, D. J., Brichory, F., Kuick, R., et al. (2005). Analysis of tumorhost interactions by gene expression profiling of lung adenocarcinoma xenografts identifies genes involved in tumor formation. Molecular Cancer Research, 3(3), 119–129.

114 David P. LaPierre, Daniel Y. Lee, Sen-Zhu Li, et al. The Ability of Versican to Simultaneously Cause Apoptotic Resistance and Sensitivity. Cancer Res 2007;67:4742-4750.

115 Ghosh, Sue, et al. "Up-Regulation of Stromal Versican Expression in Advanced Stage Serous Ovarian Cancer." *Gynecologic oncology* 119.1 (2010): 114-20.

116 Ween, M.P.; Hummitzsch, K.; Rodgers, R.J.; Oehler, M.K.; Ricciardelli, C. Versican induces a pro-metastatic ovarian cancer cell behavior which can be inhibited by small hyaluronan oligosaccharides. Clin. Exp. Metastasis 2010, doi: 10.1007/s10585-010-9363-7.

117 Boyer A, Goff AK, Boerboom D. WNT signaling in ovarian follicle biology and tumorigenesis. Trends Endocrinol Metab. 2010 Jan;21(1):25-32.

118 Gatcliffe TA, Monk BJ, Planutis K, Holcombe RF. Wnt signaling in ovarian tumorigenesis. Int J Gynecol Cancer. 2008 Sep-Oct;18(5):954-62.

119 Huang, H. and He, X. (2008) Wnt/beta-catenin signaling: new (and old) players and new insights. Curr. Opin. Cell. Biol. 20, 119–125

120 Karner, C. et al. (2006) Apical-basal polarity, Wnt signaling and vertebrate organogenesis. Semin. Cell. Dev. Biol. 17, 214–222

121 Reya, T. and Clevers, H. (2005) WNT signalling in stem cells and cancer. Nature 434, 843–850.

122 Lee, H.Y. et al. (2004) Instructive role of WNT/beta-catenin in sensory fate specification in neural crest stem cells. Science 303, 1020–1023.

123 Muroyama, Y. et al. (2004) WNT proteins promote neuronal differentiation in neural stem cell culture. Biochem. Biophys. Res. Commun. 313, 915–921.

124 Clevers, H. (2006) Wnt/beta-catenin signaling in development and disease. Cell 127, 469–480.

125 Bodine, P.V. (2008) Wnt signaling control of bone cell apoptosis. Cell Res. 18, 248–253.

126 Reynolds, A.B. and Roczniak-Ferguson, A. (2004) Emerging roles for p120-catenin in cell adhesion and cancer. Oncogene 23, 7947–7956.

127 Lustig, B. and Behrens, J. (2003) The Wnt signaling pathway and its role in tumor development. J. Cancer. Res. Clin. Oncol. 129, 199–221.

128 Giles, R.H. et al. (2003) Caught up in a Wnt storm: Wnt signaling in cancer. Biochim. Biophys. Acta 1653, 1-24.

129 Alberts B, Johnson A, Lewis J, et al. Molecular Biology of the Cell. 4th edition. New York: Garland Science; 2002. Signaling Pathways That Depend on Regulated Proteolysis.

130 Wu, R., Hendrix-Lucas, N., Kuick, R., Zhai, Y., Schwartz, D. R., Akyol, A., Hanash, S., Misek, D. E., Katabuchi, H., Williams, B. O. et al. (2007) Mouse model of human ovarian endometrioid adenocarcinoma based on somatic defects in the Wnt/β-catenin and PI3K/PTEN signalling pathways. Cancer Cell 11, 321–333.

131 Zhai, Y., Wu, R., Schwartz, D. R., Darrah, D., Reed, H, Kolligs, F. T., Nieman, M. T., Fearon, E. R. and Cho, K. R. (2002) Role of β-catenin-T-cell factor-regulated genes in ovarian endometrioid adenocarcinomas. Am. J. Path. 160, 1229–1238.

132 Gatcliffe, T. A., Monk, B. J., Planutis, K. and Holcombe, R. F. (2008) Wnt signalling in ovarian tumorigenesis. Int. J. Gynecol. Cancer 18, 954–962.

133 Rask, K., Nilsson, A., Brannstrom, M., Carlsson, P., Hellberg, P., Janson, P. O., Hedin, L. and Sundfeldt, K. (2003) Wnt signalling pathway in ovarian epithelial tumors: increased expression of beta-catenin and GSK3β. Br. J. Caner 89, 1298–1304.

134 Lee, C. M., Shvartsman, H., Deavers, M. T., Wang, S. C., Xia, W., Schmandt, R., Bodurka, D. C., Atkinson, E. N., Malpica, A., Gershenson, D. M. et al. (2003) β-Catenin nuclear localization is associated with grade in ovarian serous carcinoma. Gynecol. Oncol. 88, 363–368.

135 Howe, L. R. and Brown, A. M. (2004) Wnt signalling and breast cancer. Cancer Biol. Ther. 3, 36–41.

136 Ishigaki, K., Namba, H., Nakashima, M., Nakayama, T., Mitsutake, N., Hayashi, T., Maeda, S., Ichinose, M., Kanematsu, T. and Yamashita, S. (2002) Aberrant localization of β-catenin correlates with overexpression of its target gene in human papillary thyroid cancer. J. Clin. Endocrinol. Metab. 87, 3433–3440.

137 Mazieres, J., He, B., You, L., Xu, Z. and Jablons, D. M. (2005) Wnt signalling in lung cancer. Cancer Lett. 222, 1–10.

138 Miyake, N., Maeta, H., Horie, S., Kitamura, Y., Nanba, E., Kobayashi, K. and Terada, T. (2001) Absence of mutations in the β-catenin and adenomatous polyposis coli genes in papillary and follicular thyroid carcinomas. Pathol. Int. 51, 680–685.

139 Verras, M. and Sun, Z. (2006) Roles and regulation of Wnt signalling and β-catenin in prostate cancer. Cancer Lett. 237, 22–32.

140 Zeng, G., Germinaro, M., Micsenyi, A., Monga, N. K., Bell, A., Sood, A., Malhotra, V., Sood, N., Midda, V., Monga, D. K. et al. (2006) Aberrant Wnt/β-catenin signalling in pancreatic adenocarcinoma. Neoplasia 8, 279–289.

141 Welt, C. K., Lambert-Messerlian, G., Zheng, W., Crowley, Jr, W. F. and Schneyer, A. L. (1997) Presence of activin, inhibin, and follistatin in epithelial ovarian carcinoma. J. Clin. Endocrinol. Metab. 82, 3720–3727.

142 Watson, J. V., Curling, O. M., Munn, C. F. and Hudson, C. N. (1987) Oncogene expression in ovarian cancer: a pilot study of c-myc oncoprotein in serous papillary ovarian cancer. Gynecol. Oncol. 28, 137–150.

143 Dhar, K. K., Branigan, K., Parkes, J., Howells, R. E., Hand, P., Musgrove, C., Strange, R. C., Fryer, A. A., Redman, C. W. and Hoban, P. R. (1999) Expression and subcellular localization of cyclin D1 protein in epithelial ovarian tumour cells. Br. J. Cancer 81, 1174–1181.

144 Toole BP (2004) Hyaluronan: from extracellular glue to pericellular cue. Nat Rev Cancer 4(7):528–539.

145 Nederman T, Norling B, Glimelius B, Carlsson J, Brunk U. Demonstration of an extracellular matrix in multicellular tumor spheroids. Cancer Res 1984;44:3090–7.

146 Glimelius B, Norling B, Nederman T, Carlsson J. Extracellular matrices in multicellular spheroids of human glioma origin: Increased incorporation of proteoglycans and fibronectin as compared to monolayer cultures. APMIS 1988;96:433–44.

147 Galbraith CG,Yamada KM,Galbraith JA. Polymerizing actin fibers position integrins primed to probe for adhesion sites. Science 2007; 315: 992–5.

148 Whittard JD,Akiyama SK. Activation of beta1 integrins induces cell-cell adhesion. Exp Cell Res 2001; 263: 65–76.

149 Shield K,Riley C,Quinn MA,Rice GE,Ackland ML,Ahmed N. Alpha2beta1 integrin affects metastatic potential of ovarian carcinoma spheroids by supporting disaggregation and proteolysis. J Carcinog 2007; 6: 11.

150 Wu Y, Chen L, Zheng PS, Yang BB. beta 1-Integrin-mediated glioma cell adhesion and free radical-induced apoptosis are regulated by binding to a C-terminal domain of PG-M/versican. J Biol Chem. 2002 Apr 5;277(14):12294-301.

151 Casey RC, Burleson KM, Skubitz KM, Pambuccian SE, Oegema TR Jr, Ruff LE, Skubitz AP. Beta 1-integrins regulate the formation and adhesion of ovarian carcinoma multicellular spheroids.Am J Pathol. 2001 Dec;159(6):2071-80.

152 Bardie` s M, Thedrez P, Gestin J-F et al. Use of multi-cell spheroids of ovarian carcinoma as an intraperitoneal radio-immunotherapy model: Uptake, retention kinetics and dosimetric evaluation. Int J Cancer 1992; 50: 984–91.

153 Becker JL, Prewett TL, Spaulding GF et al. Three-dimensional growth and differentiation of ovarian tumor cell line in high aspect rotating-wall vessel: Morphologic and embryological considerations. J Cell Biochem 1993; 51: 283–9.

154 Filipovich IV, Sorokina NI, Robillard N et al. Radiationinduced apoptosis in human ovarian carcinoma cells growing as a monolayer and as multicell spheroids. Int J Cancer 1997; 72: 851–9.

155 Makhija S, Taylor DD, Gibb RK et al. Taxol-induced Bcl-2 phosphorylation in ovarian cancer cell monolayer and spheroids. Int J Oncol 1999; 14: 515–21.

156 Durand RE, Sutherland RM. Effects of intercellular contact on repair of radiation damage. Exp Cell Res 1972; 71: 75–80.

157 Graham CH, Kobayashi H, Stankiewicz KS et al. Rapid acquisition of multicellular drug resistance after a single exposure of Ovarian carcinoma spheroid invasion 695 mammary tumor cells to antitumor alkylating agents. J Natl Cancer Inst 1994; 86(13): 975–82.

158 Burleson KM, Casey RC, Skubitz KM, Pambuccian SE, Oegema TR Jr, Skubitz AP.Ovarian carcinoma ascites spheroids adhere to extracellular matrix components and mesothelial cell monolayers. Gynecol Oncol. 2004 Apr;93(1):170-81.

159 Maria Teresa Santini, Gabriella Rainaldi, Pietro Luigi Indovina. Apoptosis, cell adhesion and the extracellular matrix in the three-dimensional growth of multicellular tumor spheroids. Critical Reviews in Oncology:Hematology 36 (2000) 75–87.

160 Frankel A, Buckman R, Kerbel RS. Abrogation of taxol-induced G2-M arrest and apoptosis in human ovarian cancer cells grown as multicellular tumor spheroids. Cancer Res. 1997 Jun 15;57(12):2388-93.

161 Wu YJ, La Pierre DP, Wu J, Yee AJ, Yang BB. The interaction of versican with its binding partners. Cell Res. 2005 Jul;15(7):483-94.

162 Hernández D, Miquel-Serra L, Docampo MJ, Marco-Ramell A, Bassols A. Role of versican V0/V1 and CD44 in the regulation of human melanoma cell behavior. Int J Mol Med. 2011 Feb;27(2):269-75.

163 Cattaruzza S, Schiappacassi M, Ljungberg-Rose A, Spessotto P, Perissinotto D, Mörgelin M, Mucignat MT, Colombatti A, Perris R. Distribution of PG-M/versican variants in human tissues and de novo expression of isoform V3 upon endothelial cell activation, migration, and neoangiogenesis in vitro. J Biol Chem. 2002 Dec 6;277(49):47626-35.

164 Du WW, Yang BB, Shatseva TA, Yang BL, Deng Z, et al. (2010) Versican G3 Promotes Mouse Mammary Tumor Cell Growth, Migration, and Metastasis by Influencing EGF Receptor Signaling. PLoS ONE 5(11): e13828. doi:10.1371/journal.pone.0013828.

165 Serra M, Miquel L, Domenzain C, Docampo MJ, Fabra A, Wight TN, Bassols A. V3 versican isoform expression alters the phenotype of melanoma cells and their tumorigenic potential. Int J Cancer. 2005 May 10;114(6):879-86.

166 Daniel Hernández,Laia Miquel-Serra, María-José Docampo, Anna Marco-Ramell, Jennifer Cabrera, Angels Fabra, and Anna Bassols. V3 Versican Isoform Alters the Behavior of Human Melanoma Cells by Interfering with CD44/ErbB-dependent Signaling. J Biol Chem. 2011 January 14; 286(2): 1475–1485.

167 Lancaster, J.M.; Dressman, H.K.; Clarke, J.P.; Sayer, R.A.; Martino, M.A.; Cragun, J.M.; Henriott, A.H.; Gray, J.; Sutphen, R.; Elahi, A.; Whitaker, R.S.; West, M.; Marks, J.R.; Nevins, J.R.; Berchuck, A. Identification of genes associated with ovarian cancer metastasis using microarray expression analysis. Int. J. Gynecol. Cancer 2006, 16 (5), 1733–1745.

168 Wang Sheng, Guizhi Wang, David P. La Pierre, Jianping Wen, Zhaoqun Deng, Chung-Kwun Amy Wong, Daniel Y. Lee, and Burton B. Yang. Versican Mediates Mesenchymal-Epithelial Transition. Mol Biol Cell. 2006 April; 17(4): 2009–2020.

169 Brabletz T, Jung A, Spaderna S, Hlubek F, Kirchner T (2005) Opinion: migrating cancer stem cells—an integrated concept of malignant tumour progression. Nat Rev Cancer 5:744–749.

170 Christiansen JJ, Rajasekaran AK (2006) Reassessing epithelial to mesenchymal transition as a prerequisite for carcinoma invasion and metastasis. Cancer Res 66:8319–8326.

171 Chaffer CL, Thompson EW, Williams ED (2007) Mesenchymal to epithelial transition in development and disease. Cells Tissues Organs 185:7–19.

172 Schönherr E, Kinsella MG, Wight TN. Genistein selectively inhibits platelet-derived growth factor-stimulated versican biosynthesis in monkey arterial smooth muscle cells. Arch Biochem Biophys. 1997 Mar 15;339(2):353-61.

Vita

Education

Doctor of Pharmacy (candidate), University of Minnesota Twin Cities 2015

Masters of Biopharmaceutical Science (in progress), University of Illinois at Chicago 2009-2012

Bachelor of Science in Chemistry, University of Wisconsin River Falls 2002-2006

Professional Experience

Pharmacy Intern (June 2012-Present) Park Nicollet Methodist Hospital Inpatient Pharmacy

- Double check pharmacy technician work
- Cover technician shifts

Teaching Assistant (August 2009 – July 2011) University of Illinois at Chicago. Chicago, Illinois.

- Prepared handouts for courses
- Provided supervision as well as instruction for 1st year PharmD laboratories
- Graded quizzes and homework
- Setup technology for guest lecturers

Staff Scientist (June 2007- June 2009) International Technidyne. Saint Paul, Minnesota.

- Designed routine and non-routine experiments
- Prepared technical documents for company products
- Analyzed data from products under development as well as existing products
- Provided technical support to the manufacturing and engineering departments
- Prepared chemical formulations for electrochemical sensors

Research Experience

Graduate Student (August 2009 – August 2011) University of Illinois at Chicago. Chicago, Illinois.

- Studied epithelial ovarian cancer and more specifically a protein suspected of being involved in tumor progression and metastasis.

Undergraduate Student (Sept. 2004 – December 2006) University of Wisconsin River Falls. River Falls, WI.

- Preparation of Nitroxide-based Unimolecular Initiators: Applications in Characterizing Low-Molecular Weight Polystyrene by 1H-NMR Spectroscopy and Differential Scanning Calorimetry.

VITA (continued)

Presentations

"rDNA Insulin." Presented to University of Minnesota College of Pharmacy First Year Students. April 2012.

"Inhibition of Tumor Growth and Metastasis by a Combination of *Escherichia coli*–mediated Cytolytic Therapy and Radiotherapy." Presented to University of Illinois at Chicago Department of Pharmacy Journal Club. January 2011.

"Therapeutic silencing of microRNA-122 in primates with chronic hepatitis C virus infection." Presented to University of Illinois at Chicago Department of Pharmacy Journal Club. Chicago, Illinois. March 2010.

"Preparation of Nitroxide-based Unimolecular Initiators: Applications in Characterizing Low-Molecular Weight Polystyrene by 1H-NMR Spectroscopy and Differential Scanning Calorimetry." Presented to the University of Wisconsin River Falls Department of Chemistry. December 2006.